Brazil Oil & Gas, tt_nrg and Norway Oil & Gas

EPRASHEED
signature series

2014 – Issue 36

Saudi Arabia oil & gas

www.saudiarabiaoilandgas.com

Inside

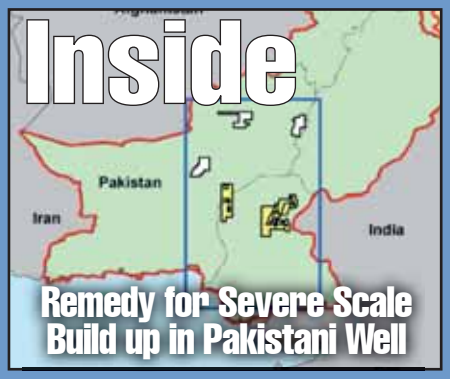

Remedy for Severe Scale Build up in Pakistani Well

Falih at New Tech Center Opening

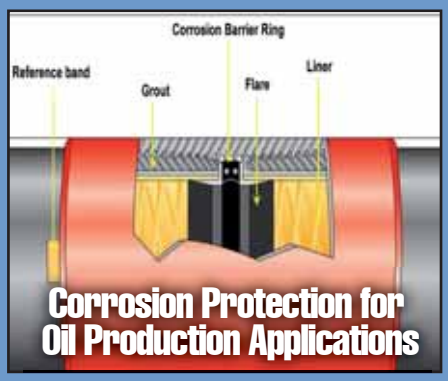

Corrosion Protection for Oil Production Applications

مدينة الملك عبدالعزيز
للعلوم والتقنية KACST

Oil and Gas Research Institute

Hydrocarbon resources (crude oil and gas) are the main source of world energy, and as the international demand increases, the technical challenges increase to meet that demand. Hydrocarbon production optimization at minimum cost and the need to serve the national petroleum industry has been the driving force behind the establishment of the Oil and Gas Research Institute (OGRI) at King Abdulaziz City for Science and Technology (KACST). OGRI is a governmental research and development entity. Its applied research activities concentrate on the upstream sector of the petroleum industry. Fields of interest cover most of the petroleum science and engineering aspects through four main divisions:

- Reservoir Characterization and Numerical Simulation,
- Drilling Engineering,
- Rock Mechanics,
- Production and Enhanced Recovery.

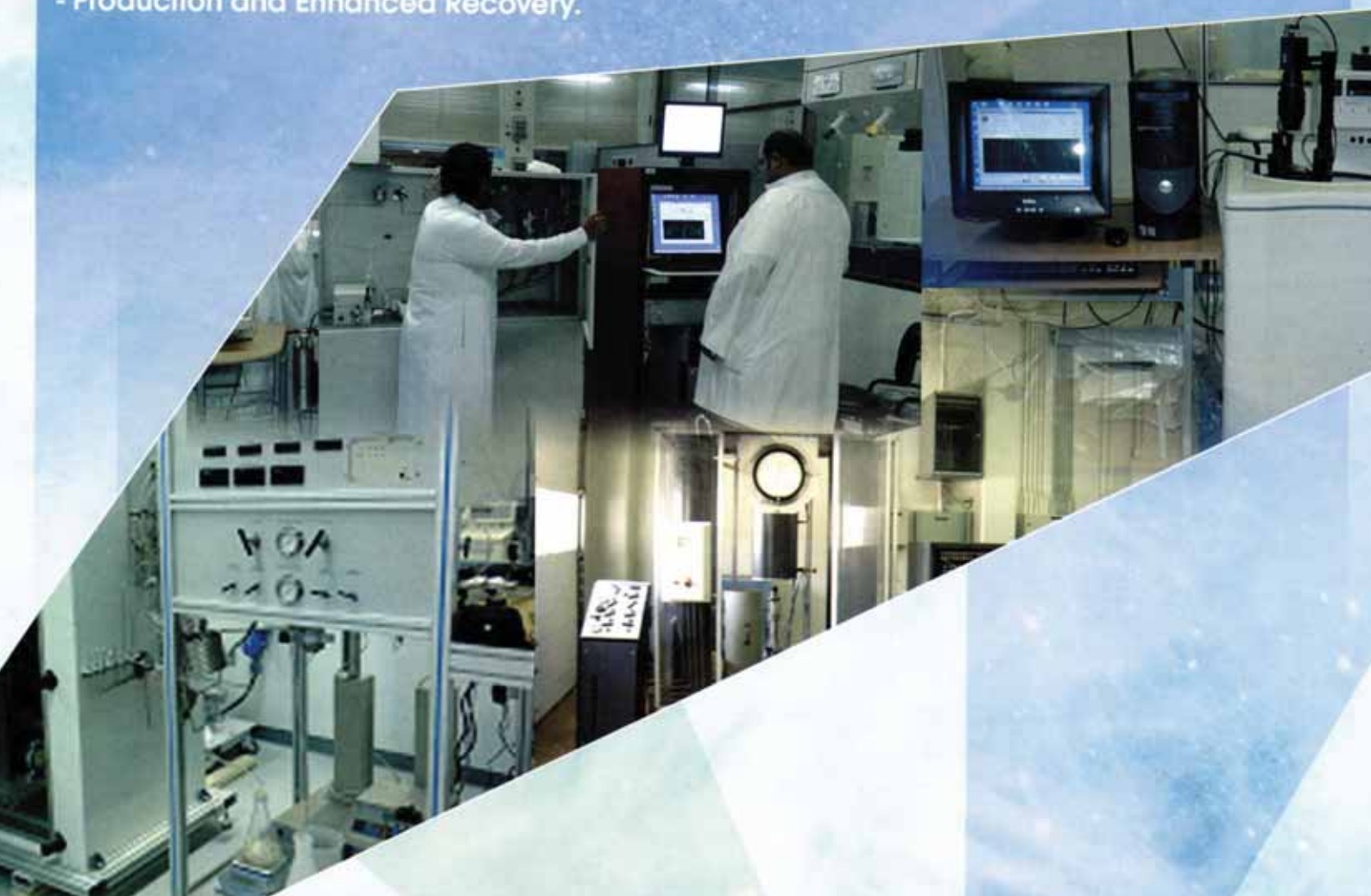

Services Provided

Service	Techniques
CONVENTIONAL CORE ANALYSIS	➤ Helium Porosity (Ambient Conditions) ➤ Gas Permeability & Porosity (Low and Reservoir Overburden Stress) ➤ Klinkenberg Correction ➤ Liquid Permeability (Reservoir Conditions)
SPECIAL CORE ANALYSIS (SCAL)	**CAPILLARY PRESSURE TESTS** ➤ Centrifuge Techniques (Reservoir Conditions) ➤ Low and High Pressure Mercury Injection and Withdrawal Technique ➤ Pore Size Distribution (PSD) **RELATIVE PERMEABILITY MEASUREMENTS** ➤ Unsteady State Flooding Technique (Reservoir Conditions) ➤ Centrifuge Technique (Reservoir Conditions) **WETTABILITY TESTS** ➤ Centrifuge USBM Method ➤ Contact angle Measurement (Ambient and Reservoir Conditions) ➤ Interfacial Tension Measurements **PETROGRAPHIC SERVICES** ➤ Sieve Analysis ➤ Particle Size Analysis ➤ Thin section
RESERVOIR FLUID ANALYSIS	➤ Interfacial & Surface tension ➤ Gas and Gas Condensate Viscosity ➤ Refractive index and pH ➤ Contact angle
ADVANCED RESERVOIR ENGINEERING	➤ Water-Oil /Water-Gas Displacement ➤ Gas Flooding and WAG ➤ Chemical Flooding
PETROLEUM RELATED ROCK MECHANICS	➤ Uniaxial, Triaxial, and Hydrostatic Compressive strength ➤ Stress-Strain Behavior ➤ Failure Envelope ➤ Elastic moduli ➤ Bulk and Pore Compressibility ➤ Fracture Toughness

OGRI - KACST - K.S.A - P.O. Box. 6086 Riyadh 11442
Tel. : +966 1 4813307 Fax : +966 1 4813526

EPRASHEED signature series
2014 – Issue 36
Saudi Arabia oil & gas
Saudi Arabia Oil & Gas (Print) ISSN 2045-6670
www.saudiarabiaoilandgas.com
Saudi Arabia Oil & Gas (Online) ISSN 2045-6689

Contents

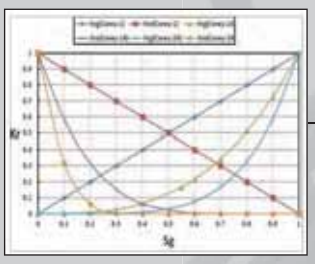

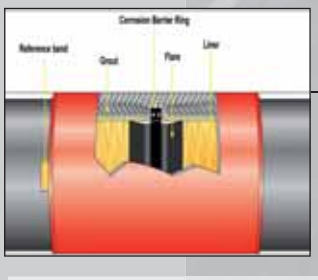

CEO and Founder
EPRasheed
Wajid Rasheed
wajid.rasheed@eprasheed.com

Editors
Majid Rasheed
Mauro Martins

Design
Sue Smith
sue.smith@eprasheed.com

United Kingdom
Head Office
Tel: (44) 207 193 1602

Adam Mehar
adam.mehar@saudiarabiaoilandgas.com
Main: (44) 1753 708872
Fax: (44) 1753 725460
Mobile: (44) 777 2096692

Saudi Arabia
Akram ul Haq
PO BOX 3260, Jeddah 21471
akram.ul.haq@saudiarabiaoilandgas.com
Tel: (966) 557 276 426

Mohanned AlSagri
mohanned.alsagri@saudiarabiaoilandgas.com

Brazil
Ana Felix
afelix@braziloilandgas.com
Tel: (55) 21 9714 8690

Fabio Jones
fabio.jones@braziloilandgas.com
Tel: (55) 21 9392 7821

Roberto S. Zangrando
rzangrando@braziloilandgas.com
Tel: (55) 22 8818 8507

Remarks at Halliburton Technology Center Opening in Dhahran Techno Valley

Dhahran, 8 January 2014

"Your Excellency(ies), Distinguished Guests, Ladies and Gentlemen; it is a pleasure to join you this morning to participate in the opening of the Halliburton Technology Center. I would like to begin by offering congratulations to my good friends His Excellency Khaled Al-Sultan and Dave Lesar, and to all those from Halliburton, KFUPM and the Dhahran Techno Valley who worked tirelessly to bring this remarkable new facility to fruition.

Although we're here to inaugurate a new facility, the relationship behind it has been built on a long history of partnership. As you know, Halliburton's presence in Saudi Arabia dates back to 1938, and so Dave, that means our companies have worked together closely for nearly eight decades. I would like to compliment Halliburton for the important role it has played in the development of the Kingdom's oil and gas industry over this long period. And today, with this technology center, we celebrate the beginning of a fresh new chapter in Halliburton's history in our nation, and as a committed partner in our broad development objectives.

This opening also marks yet another proud step toward realizing the vision of the Dhahran Techno Valley. The building blocks of this vision – namely high-end research; support of education in energy related disciplines; the promotion of entrepreneurship; the commercialization of innovative technologies created

> At Saudi Aramco, we welcome the new Center because it supports our own vision of building on our past successes to create the world's premier energy and chemicals company, while contributing to the Kingdom's quest to develop a vibrant and prosperous knowledge society with a highly competitive local energy sector.

here into successful business ventures; and the creation of knowledge jobs—will each be served by the new Center.

Starting today, Halliburton will assume a prominent place in the Dhahran Techno Valley cluster, which has already attracted a number of world-class firms renowned for their R&D capabilities. The DTV has also brought together some of the best and brightest minds in their fields to become an important and inspirational engine for both advanced research and technology-driven entrepreneurial ventures.

At Saudi Aramco, we welcome the new Center because it supports our own vision of building on our past successes to create the world's premier energy and chemicals company, while contributing to the Kingdom's quest to develop a vibrant and prosperous knowledge society with a highly competitive local energy sector.

Advanced Technology serves as a critical enabler in the achievement of this vision, which is why we have set a goal of turning Saudi Aramco into a research powerhouse and a world leading developer of breakthrough energy technologies by the year 2020.

To this end, we have set some truly challenging goals for ourselves, whose achievement will require the development of game-changing technologies. For example:

We are targeting to increase average recovery rates from our oil reservoirs by 20% which could add 160 billion

barrels of additional reserves. That's more than the current reserves of the United States, Russia, China, the UK and Brazil combined!

Besides increasing recovery, we also want to discover large additional resources of oil and gas from both conventional and unconventional sources.

We want to image 15,000 feet deep into reservoirs with the seismic resolution of 5 feet!

And, we want to drill 50% faster than we do today, cutting costs along the way.

These are indeed ambitious targets and while we will significantly increase our allocated expenditures towards research, I strongly believe that collaboration is the key to achieving these goals that underpin the vision of the company and the Kingdom that I have outlined.

That is why we at Saudi Aramco, are building eight satellite research centers located in the Kingdom, North America, Europe and Asia to benefit from ideas, talent and capabilities available across the world. Five of these centers have already commenced operations with the remaining three expected to be completed this year. These centers will complement our growing in-house R&D capabilities and we are also reaching out to work with our colleagues and counterparts in academia, in the hydrocarbon industry as well as other industrial and commercial sectors and most importantly, in the petroleum services and technology fields.

I am so pleased to hear that this new Center has set an exciting research agenda, encompassing both the productivity enhancement of conventional reservoirs and harnessing unconventional resources, while enabling the transfer of Halliburton's "fit for purpose" productivity practices from North America. I'm confident that the Center's work will help us to achieve our own technology agenda I outlined earlier.

It is exciting to see that the collaboration I'm referring to, is materializing right here in front of us, along the well aligned visions of KFUPM, the Dhahran Techno Valley, the Halliburton Center and Saudi Aramco.

My friends, the Kingdom of Saudi Arabia has long been a major exporter of petroleum and a critical contributor to the wellbeing of the global economy. In the future, we want to see our nation also become a leading exporter of technological solutions, and a valued contributor to the global pool of knowledge and innovation. The opening of this Center represents a significant milestone along that path.

So while I congratulate the many people at Halliburton, the DTV and the King Fahd University for Petroleum & Minerals who are behind the completion of the Center, I also want to congratulate our nation's citizens, for they will be the ultimate beneficiaries of the work that takes place here.

Thank you for your attention, and again let me extend my appreciation to all who have made today's event possible."

Contracts Signed to Help Boost Shaybah Production

Saudi Aramco moved forward on a new project as it signed contracts on Dec. 31, 2014, with two of the world's leading engineering and construction companies for the Shaybah Arabian Extra Light (AXL) Crude Increment Project.

This puts the Shaybah Oil and Power Generation on track to a new production plateau of 1 million barrels per day of Arab Extra Light crude oil.

The Central Processing Facility Expansion contract was awarded to the Korean EPC Contractor Samsung Engineering Co. Ltd.

The scope of work includes expanding the existing facility at Shaybah GOSPs 1, 3 and 4 to increase their total handling capacity by 250,000 barrels of AXL crude. At GOSP 4, three gas oil separators and one wet crude handling train will be added along with the associated charge, disposal and shipping pumps, intermediate and booster gas compressor and all associated utilities. The project will also install additional oil transfer facilities with associated utilities at GOSPs 1 and 3. This expansion to the oil facilities is targeted to be completed by April 2016, which by then will reinforce the company's international role in responding reliably to future oil market demand.

Shandong Electrical Power Construction Co., based in Beijing, China, was selected for the Shaybah Combined Cycle Facility Package. The scope of work in this package includes converting the existing six simple cycle gas generators to two blocks (three each) of combined cycle power generation.

Each block will be coupled with a 120 MW steam turbine generator to produce a total of 240 MW of power from wasted heat. The conversion will include retrofitting the Gas Turbine Generator (GTG) with six once-through steam generators along with an associated cooling and water treatment facility, a new 13.8 KV substation and expansion of the existing 230 KV Gas Insulated Switchgear substation, new process interface building, as well as other auxiliary systems.

The remaining contract for infrastructure facilities is planned to be awarded in January 2014 and will expand the existing Shaybah Residential Industrial Camp capacity and support facilities.

The Shaybah AXL Crude Increment Project is part of the ongoing mega-development of the Shaybah NGL Recovery Program, which includes nine other major contracts that are under way, to be completed by the end of 2014.

Innovation Embraced, Highlighted in Tanajib

TANAJIB, 9 January 2014

Let's Build an Innovative Culture" was the theme of the Third Innovation and Technology Exhibition and Workshop held recently by Northern Area Oil Operations (NAOO) in Tanajib.

More than 500 guests from various Saudi Aramco organizations and companies attended, offering a diverse range of innovative ideas, best practices, technology items and technical presentations related to operations optimization, corrosion and inspection, online analyzers, process control, and water and energy conservation.

Before the opening ceremony, event activities were started by Alexander Blass, president of the Innovation Institute of America, and Christian Majgaard, the top executive at LEGO, who conducted two innovation workshops that provided training to more than 100 employees on overcoming barriers to change toward an "innovation explosion."

Khalid Al-Khalb, manager of the Northern Area Technical Support Department, opened the event by welcoming NAOO management and guests to the innovation and technology roadshow. Nasir K. Al-Naimi, vice president of Northern Area Oil Operations (NAOO), emphasized the major role NAOO plays to promote innovative culture and knowledge sharing among all Saudi Aramco organizations and employees, and he encouraged employees to actively participate in such events.

During the opening ceremony, 30 talented employees from NAOO where rewarded by Al-Naimi and other

> The exhibition offered a variety of technologies that can benefit NAOO facilities in issues related to operations optimization, corrosion and inspection, online analyzers, process control, and water and energy conservation.

members of management for their innovative ideas. Each innovator was given a chance to present his idea in front of management and the audience in an effort to motivate employees to participate in building an innovative culture.

The exhibition offered a variety of technologies that can benefit NAOO facilities in issues related to operations optimization, corrosion and inspection, online analyzers, process control, and water and energy conservation. More than 45 local and international companies, Saudi Aramco organizations and King Fahd University of Petroleum and Minerals participated in the event. As a result, more than 500 employees and guests visited the exhibition, marking a record number of visitors to the NAOO innovation and technology exhibitions since 2010.

The exhibition was also toured by Amin H. Nasser, senior vice president of Upstream, along with vice presidents, executive directors and general managers.

The event provided a chance for Saudi Aramco employees and company representatives to express their technical knowledge and thoughts through technical presentations. With more than 20 presentations, more than 200 participants exchanged knowledge with colleagues in an effective, innovative environment and professional network.

Economy Focus of Visit

JUBAIL, 16 January 2014

HE Ali I. Al-Naimi, the Minister of Petroleum and Mineral Resources, paid a visit to several new economic ventures in the cities of Ras Al-Khair and Jubail in January. The visits provided him an opportunity to assess the progress of a Kingdomwide initiative to create job opportunities and economic diversification.

Al-Naimi visited a new aluminum refinery at Ras Al-Khair, as well as Saudi Aramco's Wasit Gas Plant and the company's two new petrochemical joint ventures – Sadara and SATORP – in Jubail. He was accompanied by HRH Prince Faisal Bin Turki Bin Abdulaziz, adviser to the Ministry of Petroleum and Mineral Resources, and HE Abdulrahman Al-Abdulkarim, the deputy minister for Companies Affairs, as well as Saudi Aramco president and CEO Khalid A. Al-Falih and representatives of the Royal Commission for Jubail and Yanbu.

All of these projects share one thing in common, said Al-Naimi: They are designed to expand the Saudi economy beyond the oil and gas business into new value-added industries in the Kingdom that will spawn economic growth and create jobs for Saudi Arabian youths.

"These mega-projects contribute to economic diversification, the achievement of high returns for shareholders and investors and the transfer and localization of high-skills technical professions," Al-Naimi said.

Later, in a luncheon held at SATORP, Al-Naimi reflected on how the Saudi Arabian economy has developed and strengthened since the mid-1950s, when he joined Saudi Aramco.

"All we had was a few wells producing oil," Al-Naimi said. "Then, we went from oil to gas and then petrochemicals and then mining. But now, the challenge is not the mineral wealth. We know how to develop mineral wealth. But if we succeed in developing man – and by that, I mean males and females – that would be the ultimate development of Saudi Arabia, and we should keep that in mind. Every effort that we can put on this would be very rewarding for every one of us. History will reward us or blame us for this."

The first stop on Al-Naimi's tour was an aluminum smelter built by Ma'aden Mining Co. in the town of Ras Al-Khair. The smelter has a production capacity of

> These mega-projects contribute to economic diversification, the achievement of high returns for shareholders and investors and the transfer and localization of high-skills technical professions

740,000 metric tons of aluminum annually and employs 4,000 people, 70 percent of them Saudi nationals.

Al-Naimi then visited Saudi Aramco's Wasit Gas Plant, which is expected to be one of the largest gas plants ever built by the company. When construction is completed later this year, Wasit will have the capacity to produce 2.5 billion square cubic feet per day of nonassociated gas from Saudi Aramco's offshore fields, Arabiyah and Hasbah.

The Minister's delegation next visited the seamless pipe factory operated by JESCO in the industrial city of Jubail. This factory is in an industrial park, Plaschem Park, which is being developed in Jubail Industrial City by the Royal Commission, adjacent to the Sadara and SATORP refineries. This Seamless Pipes factory is at the leading edge of what the government hopes will be an economic boom for Saudi-owned businesses that supply parts and services to the Saudi energy and petrochemicals industry, and in turn, create thousands of highly skilled jobs for Saudi citizens.

The delegation then visited Sadara Chemical Co., a joint venture between Saudi Aramco and Dow Chemical Co., which, when completed, will be the largest petrochemical complex built in a single phase and represent the largest foreign investment in the Kingdom. The complex is expected to produce more than 3 million metric tons of high value chemical products, generating $10 billion in revenue per year. It is these chemical products that Saudi Aramco believes will create whole new industries within the Kingdom, and create new jobs for Saudi citizens, said Al-Falih. By adding value to the hydrocarbons that Saudi Arabia produces here in the Kingdom, Saudi Arabian businesses will generate new revenue streams and create new highly skilled job opportunities for thousands of Saudi youths.

"The impact of Sadara, as big as it is, is really in the Value Park," Al-Falih said, referring to the industrial park to be developed next to Sadara in Jubail Industrial City. "That is where we see economic growth, new businesses and new high-paying jobs for Saudi youths."

In its final stop, the delegation visited SATORP refining and petrochemical company, a joint venture between Saudi Aramco and Total oil company. The SATORP refinery in Jubail is designed to refine 400,000 barrels of Arabian Heavy crude oil per day into a number of fuels, including diesel, jet fuel, gasoline and LPG, as well as petrochemical products such as aromatic benzene and propylene. SATORP's twin production trains are the first in the Middle East to produce high purity paraxylene, which is used in making bottles. SATORP also operates the first coker in the region and has produced 2 million tons of coke, a highly efficient solid fuel destined for Asian markets.

Remedy for Severe Scale Build

By Syed Saadat Hassan, OMV (Pakistan) GmbH; Tofeeq Ahmad, OMV (Pakistan) Exploration GmbH; and Shoaib Farooqui, Haseeb Mazhar Ali, and Atif Qamar, Weatherford Oil Tools ME Limited Pakistan.

Abstract

With current demand for gas at an historic peak, any decrease in production due to deposits of scale within tubing is most troublesome for any E&P company. Statistically 28% of the time it is scale in the well that hinders producing at optimum rate. "Carbonate" and "Sulfate" scales are the most common mineral scales to form in wells.

Carbonate scales are generally tackled by wellbore cleanout with acid or by using scale inhibitors to slow down the scale deposition process, but none of these solutions solves the problem on a permanent basis. Sulfates scales are generally very hard to remove through acid job and usually chemical chelants are used to control sulfate scales.

The major production enhancement challenge faced in the well was to permanently mitigate a severe scale build up issue in the tubing for optimum production performance. This paper presents how these challenges were faced and overcome by using an electromagnetic device, the ClearWELL unit, resulting in stable and continuous production.

A scale study was conducted by OMV laboratory in Vienna to identify the scale build up mechanism and solutions for its mitigation. The study confirmed that a minor pressure decrease at formation temperature promoted water transfer into the gas phase; if the water rate is low compared to the gas rate, this can result in complete evaporation and formation of precipitate leading to scale build up (mainly calcite). To reinstate production, repeated wellbore cleanouts with coiled tubing using diluted HCl (7.50%) were thought to be the temporary solution in fighting $CaCO_3$ scales.

The unit, an electromagnetic device which continuously generates electronic dipole that induces a randomly varying high frequency electric field throughout the entire piping system, was commissioned at well 'X' xmas tree, which is currently under pilot testing. The electric field generated by the device forces homogeneous crystal formation in suspension rather than on metal surfaces. Scale crystallizes in suspension and is carried away with the gas water mixture.

During the five months of its pilot testing, results achieved were promising. Stable production with no loss of output added reasonable value to the producing asset and saved huge revenue loss to the company.

RESULTS OF CIT (COMPLETION INTEGRITY TEST) PERFORMED ON LOWER INTERVAL:

Perforated interval: 3698.0 – 3705.0 mLD.
Choke: 56/64"; Rate: 1.84 MMscfd; FWHP; 134 psi;
FBHP: 301 psi; WHT: 116 F; BHT: 365 F;
WGR: 13.04 bbls/MMscf.
SIWHP: 4303 psi; SIBHP: 5574 psi.
CH_4 = 85.05%; CO_2 = 14.30%; H_2S = 16ppm;
Chlorides = 1400 ppm.

RESULTS OF CIT PERFORMED ON UPPER AND LOWER INTERVAL BY OPENING SSD (COMMINGLED FLOW):

Perforated interval: 3672.0 – 3686.0 mLD;
3698.0 – 3705.0 mLD.
Choke: 48/64"; Rate: 29.27 MMscfd; FWHP: 2805 psi;
WHT: 227 F; WGR: 12.12 bbls/MMscf.
SIWHP: 4367 psi.
CH_4 = 90.59%; CO_2 = 7.62%; H_2S = 18ppm;
Chlorides = 18000 ppm.

Up in Pakistani Well

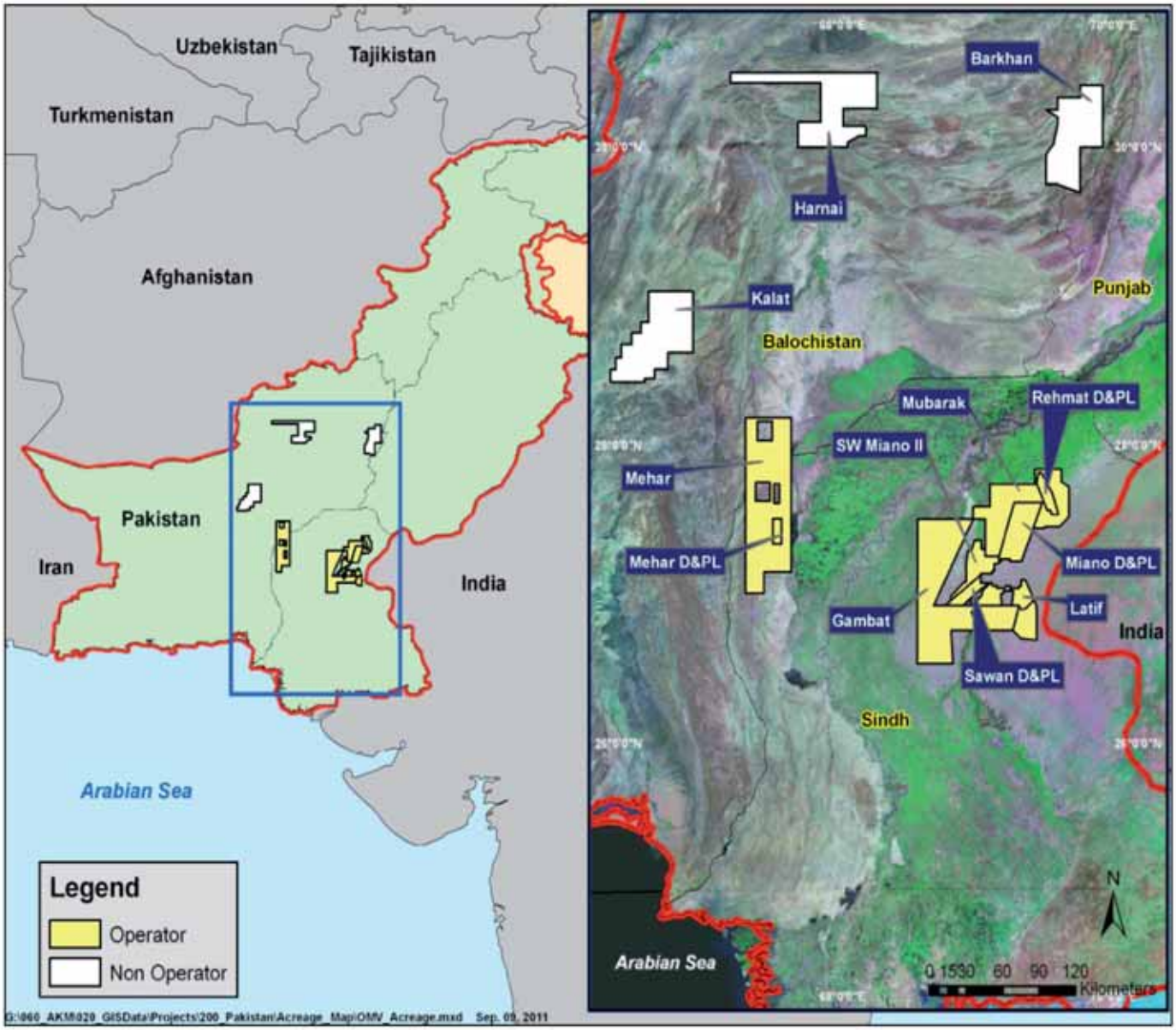

Figure-1: OMV (Pakistan) Concession Area

Introduction

The well was discovered in the OMV (Pakistan) concession area, which is situated in Sindh province, south of Pakistan (Figure 1). It was drilled, tested and suspended as an exploratory well.

Later on it was completed with 4½" CRA tubing using SSD (sliding sleeve door) between two separate zones within B-Sand (Figure 2) as an outcome of MDT and DST results.

Production Profile and Scale Problem

The well was put on stream (Figure 3), since then it has produced at an average gas rate of 30.00 MMscfd (commingled production).

A steeper decline was observed in the gas rate. During the annual bottomhole pressure survey campaign, a restriction was observed at 3662.00 m RKB (SLM) which was on top of perforations. A minor amount of well crystallized sample was collected with sand

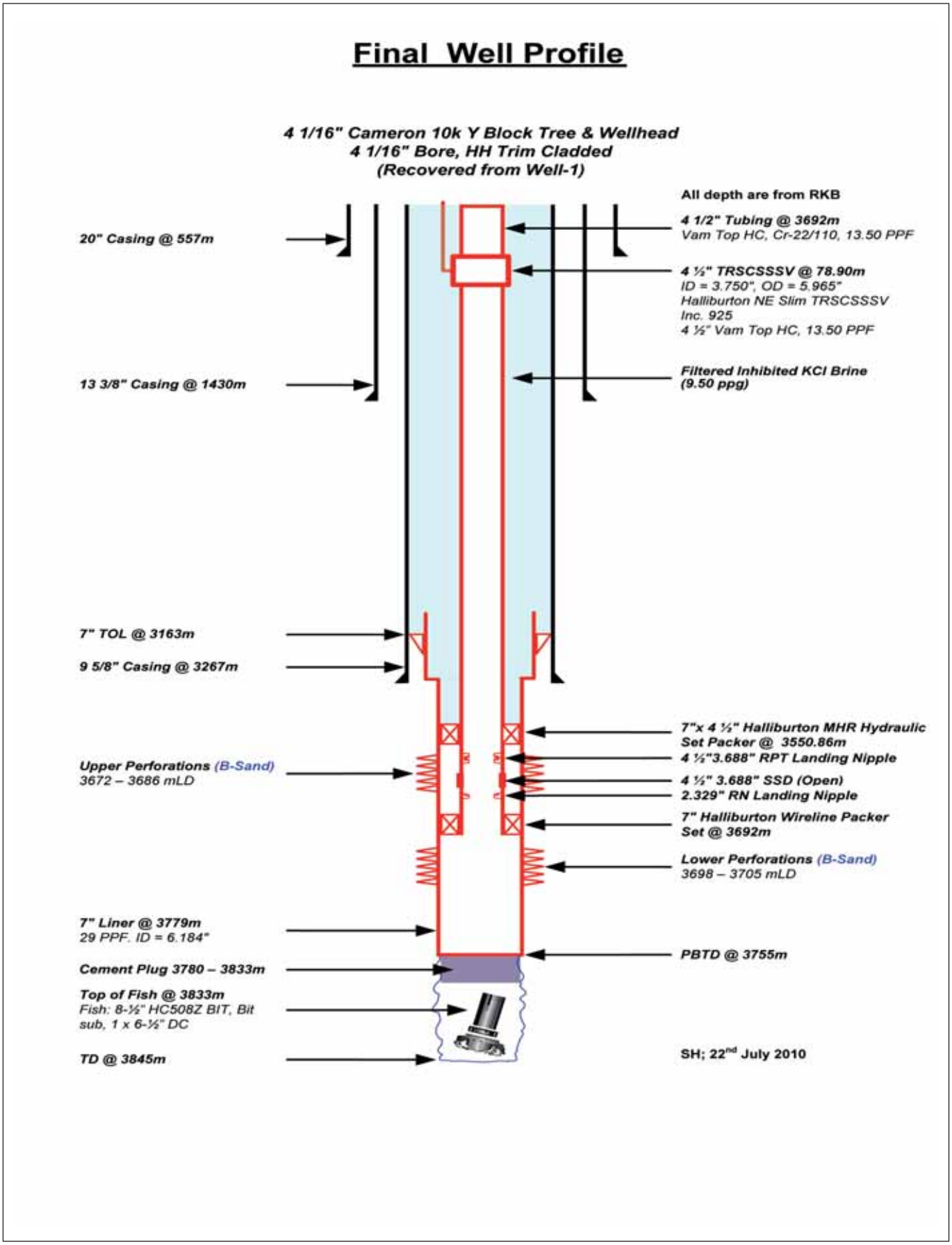

Figure-2: Final Well Profile

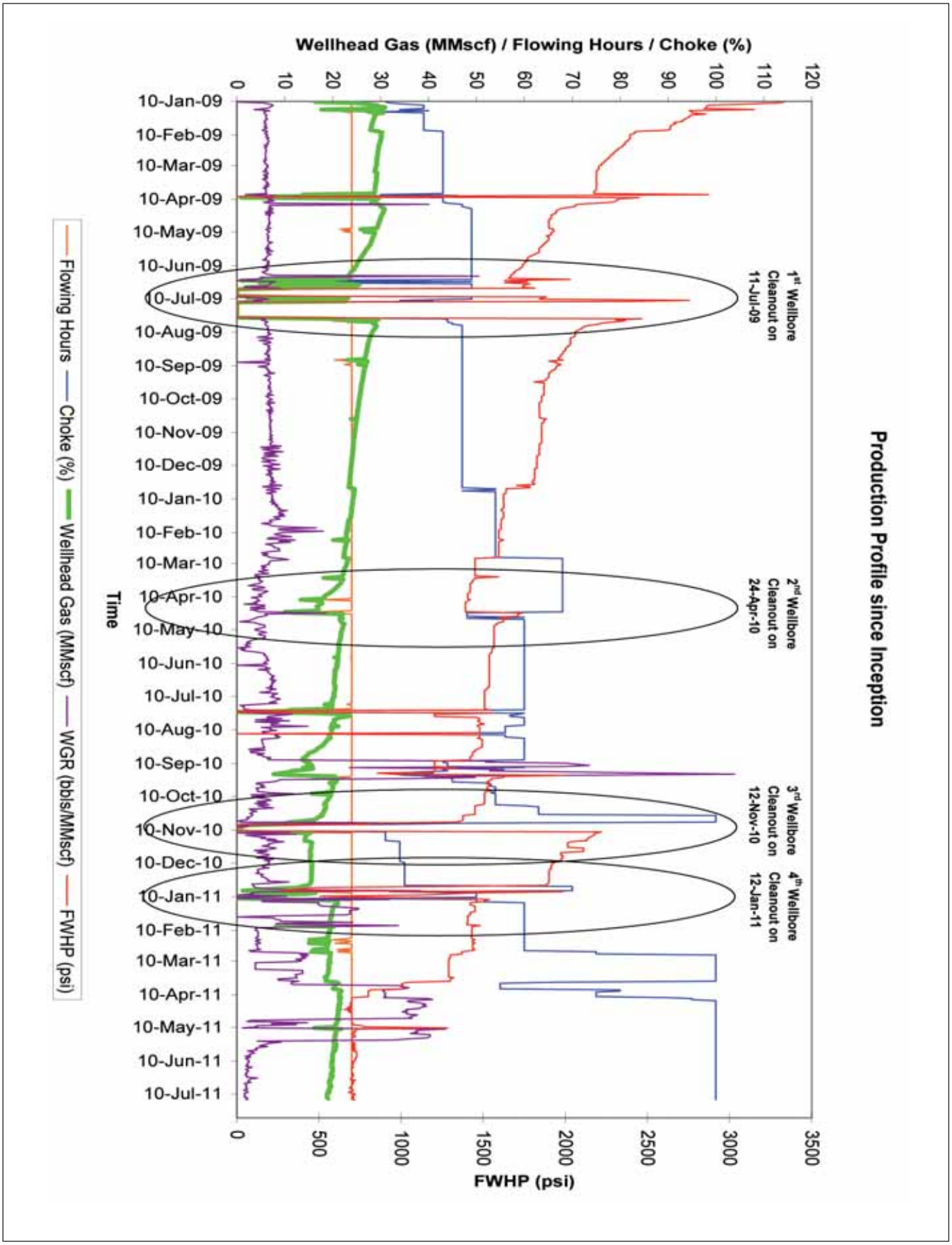

Figure-3: Production Profile since Inception

Figure-4: Scale Sample

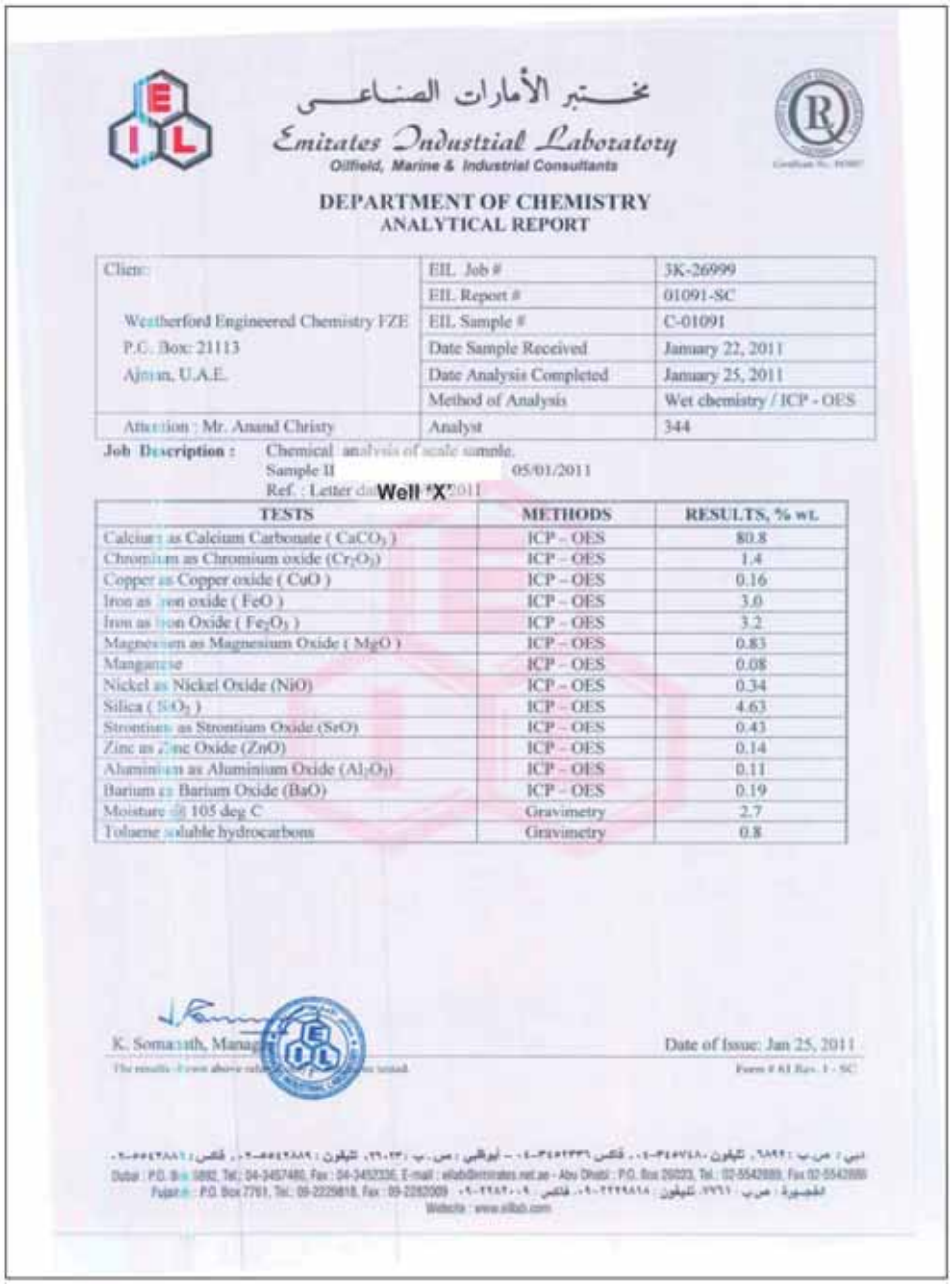

مختبر الأمارات الصناعي

Emirates Industrial Laboratory

Oilfield, Marine & Industrial Consultants

DEPARTMENT OF CHEMISTRY
ANALYTICAL REPORT

Client:	EIL Job #	3K-26999
	EIL Report #	01091-SC
Weatherford Engineered Chemistry FZE	EIL Sample #	C-01091
P.O. Box: 21113	Date Sample Received	January 22, 2011
Ajman, U.A.E.	Date Analysis Completed	January 25, 2011
	Method of Analysis	Wet chemistry / ICP - OES
Attention : Mr. Anand Christy	Analyst	344

Job Description : Chemical analysis of scale sample.
Sample II 05/01/2011
Ref. : Letter dat Well "X" 2011

TESTS	METHODS	RESULTS, % wt.
Calcium as Calcium Carbonate ($CaCO_3$)	ICP – OES	80.8
Chromium as Chromium oxide (Cr_2O_3)	ICP – OES	1.4
Copper as Copper oxide (CuO)	ICP – OES	0.16
Iron as Iron oxide (FeO)	ICP – OES	3.0
Iron as Iron Oxide (Fe_2O_3)	ICP – OES	3.2
Magnesium as Magnesium Oxide (MgO)	ICP – OES	0.83
Manganese	ICP – OES	0.08
Nickel as Nickel Oxide (NiO)	ICP – OES	0.34
Silica (SiO_2)	ICP – OES	4.63
Strontium as Strontium Oxide (SrO)	ICP – OES	0.43
Zinc as Zinc Oxide (ZnO)	ICP – OES	0.14
Aluminium as Aluminium Oxide (Al_2O_3)	ICP – OES	0.11
Barium as Barium Oxide (BaO)	ICP – OES	0.19
Moisture @ 105 deg C	Gravimetry	2.7
Toluene soluble hydrocarbons	Gravimetry	0.8

K. Somanath, Manag

Date of Issue: Jan 25, 2011

Form # 81 Rev. 1 - SC

Website : www.eilab.com

Figure-5: Scale Analysis Report prior to installation of the unit

Figure-6: PC Duracaps SI placed in Rat Hole

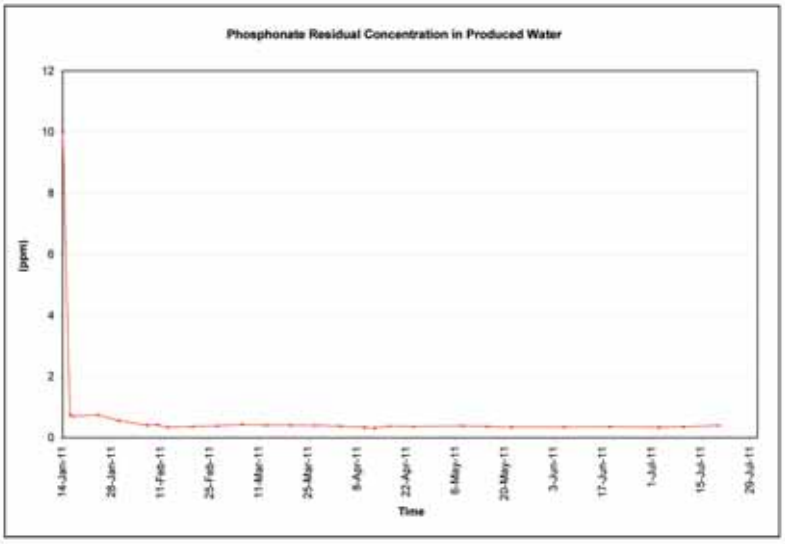

Figure-7: Phosphonate Residual Concentration in Produced Water

bailer, and X-ray analysis revealed it to be almost pure calcite. It was dissolved in HCl and the small residue was found to consist of $BaSO_4$.

Scale Study

To fight scale build up problems a scale study was carried out at OMV Vienna laboratory as summarized below:

- **Scope of Work**
  - Identify the scale formation mechanism.
  - Enable prediction of similar occurrences in other wells.
  - Find possible preventive strategies.

- **Findings**
  - Calculations confirmed that a minor pressure decrease at formation temperature promoted water transfer into the gas phase.
  - If water rate is low compared to gas rate (which was the case in the well), this can result in complete evaporation and formation of precipitate, leading to scale build up.

- **Suggestion**
  - Repeated treatments with diluted hydrochloric acid (HCl) could be thought of as a temporary solution for calcite scale.

Temporary Solution

Four wellbore cleanout jobs (Figure 3) with CT using 7.50% HCl were carried out to reinstate production.

Permanent Remedy

Different options were evaluated and finally two systems were used on an experimental basis at the well.

Production Profile after Installation						
Production Day	Flowing Hours	Wellhead Gas (MMscf)	Choke (%)	FWHP (psi)	FLP (psi)	Remarks
12-Jan-11	12.20	9.163	50	1537	1247	Placement of PC Duracaps SI in Rat Hole on 12-Jan-11 @ 14:30 Hrs
13-Jan-11	24.00	21.084	50	1508	1262	
14-Jan-11	24.00	20.626	50	1500	1262	
15-Jan-11	24.00	20.827	60	1421	1291	
16-Jan-11	24.00	21.042	60	1421	1291	
17-Jan-11	24.00	20.648	60	1421	1291	
18-Jan-11	24.00	20.211	60	1450	1305	Install Weatherford ClearWELL on 18-Jan-11. Switch Off after Function Testing
19-Jan-11	24.00	20.292	60	1450	1305	
20-Jan-11	24.00	20.041	60	1450	1305	
21-Jan-11	24.00	20.042	60	1450	1305	
22-Jan-11	24.00	19.935	60	1450	1305	
23-Jan-11	24.00	19.895	60	1450	1305	
24-Jan-11	24.00	19.841	60	1421	1291	
25-Jan-11	24.00	19.767	60	1421	1291	
26-Jan-11	24.00	19.801	60	1421	1290	
27-Jan-11	24.00	19.781	60	1406	1276	
28-Jan-11	24.00	19.645	60	1406	1276	
29-Jan-11	24.00	19.594	60	1406	1276	
30-Jan-11	24.00	19.520	60	1406	1276	
31-Jan-11	24.00	19.542	60	1406	1276	
01-Feb-11	24.00	19.447	60	1406	1276	
02-Feb-11	24.00	19.380	60	1407	1276	
03-Feb-11	24.00	19.420	60	1400	1276	
04-Feb-11	24.00	19.245	60	1400	1276	
05-Feb-11	15.50	8.265	60	1480	1276	
06-Feb-11	24.00	20.135	60	1430	1276	
07-Feb-11	24.00	19.631	60	1430	1276	
08-Feb-11	24.00	19.457	60	1430	1276	
09-Feb-11	24.00	19.444	60	1430	1276	
10-Feb-11	24.00	19.336	60	1430	1276	
11-Feb-11	24.00	19.256	60	1430	1276	
12-Feb-11	24.00	19.185	60	1430	1276	
13-Feb-11	24.00	19.189	60	1430	1276	
14-Feb-11	24.00	19.080	60	1429	1276	
15-Feb-11	24.00	19.093	60	1429	1276	Power Up Weatherford ClearWELL on 15-Feb-11 @ 10:20 Hrs

Figure-8: Production Table after PC Duracaps SI Job

1. An encapsulated scale inhibitor (SI), Duracaps.
2. Electromagnetic unit.

A scale sample was recovered with Slickline sand bailer (Figure 4), detailed analysis was performed before installation of the unit, showing 81% calcite (Figure 5).

Scale inhibitor (Figure 6) was placed in the well rat hole with the help of CT, and phosphonate residual (Figure 7) was continuously measured in produced water.

In parallel the unit (Figure 9) was also installed at xmas tree/wellhead.

Performance of SI System

The phosphonate residue in produced water was continuously monitored and within a month the residual value (Figure 7) decreased below the threshold value of 0.50 ppm recommended by the vendor. This was also evident from a slight decrease in the production rate (Figure 8) 20.29 MMscfd (FWHP: 1450 psi) to 19.08 MMscfd (FWHP: 1429 psi). The system was found unsatisfactory.

Performance of Electromagnetic Unit

- **Working Mechanism**
  - The device is an electronic dipole generator that induces a randomly varying, high frequency electric field throughout the entire piping system.
  - The electric field generated by the device forces homogeneous crystal formation in suspension rather than on metal surfaces.
  - Scale crystallizes in suspension and is carried away with the gas water mixture.
  - Prevents deposition of both $CaCO_3$, $BaSO_4$ and slowly removes pre-existing $CaCO_3$.
  - Power consumption ~35watts (continuous).
  - AC / generator / solar panels and inverter; source 110 or 220 volts.

- **Commissioning**
  - The unit was powered up.

- **Monitoring**
  - Well ramped up slowly to 100% choke opening and afterwards passed flow through front end compression (FEC) to attain maximum drawdown

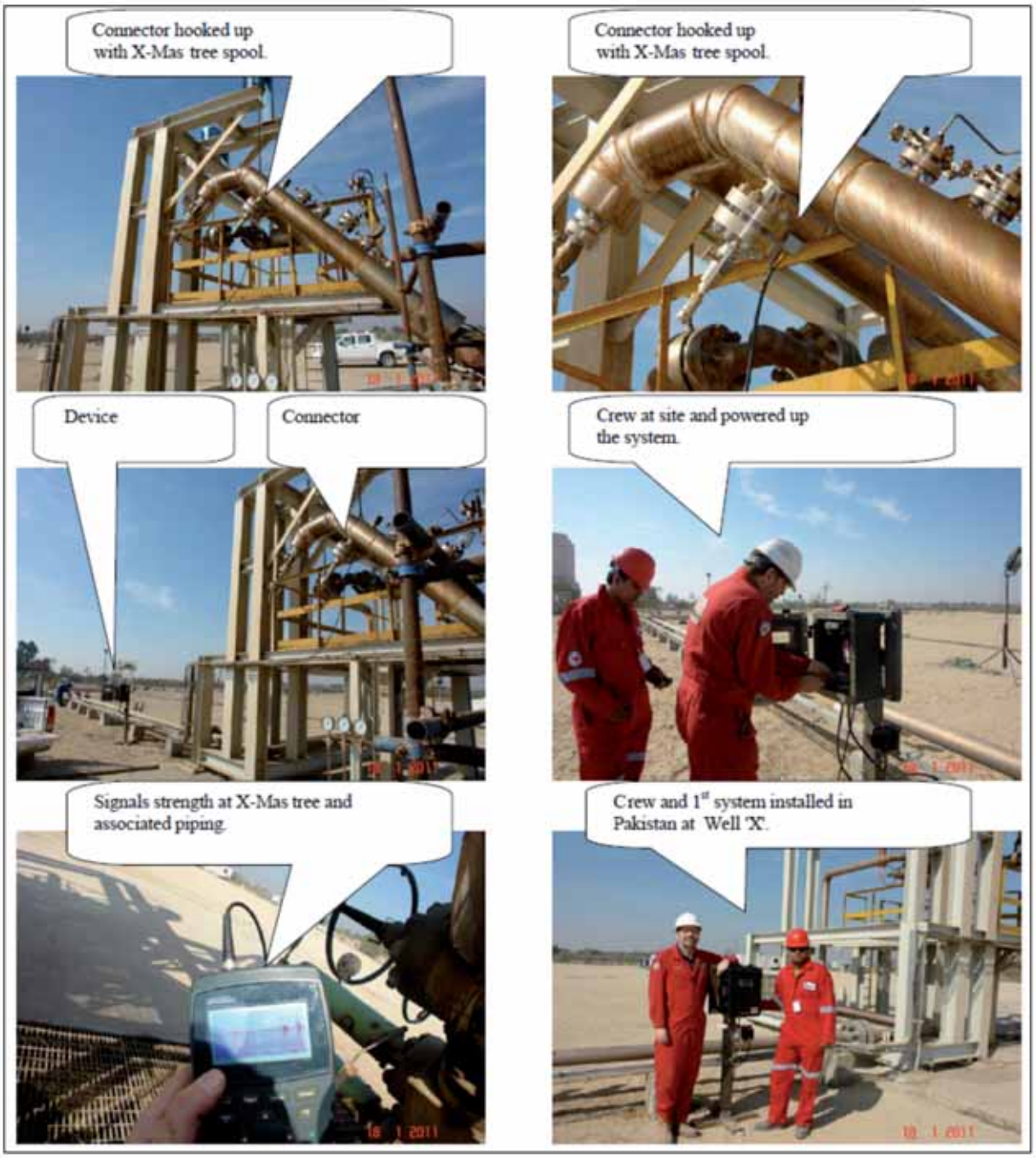

Figure-9: Installation of Unit

[closely monitored wellhead parameters as per unit KPIs (Figure 10)].

- Monthly inspection of the unit by service engineer (Figure 11).
- Continuous monitoring of produced water for chlorides and bicarbonates (Figure 12).

Value Addition to Asset

Electromagnetic device vs. wellbore cleanout and deferred production:

- Wellbore cleanout cost per job = ~230 K USD.
- Extension to life of well due to wellbore cleanout = ~2 Months (60 Days).
- Deferred production (during wellbore cleanout) = ~4 Days (84 MMscf).
- Deferred production (during scale build up) = ~7 MMscfd (420 MMscf).
- Cost = ~95 K USD.
- 95K USD Vs 230K USD and revenue loss of ~504 MMscf (deferred production).

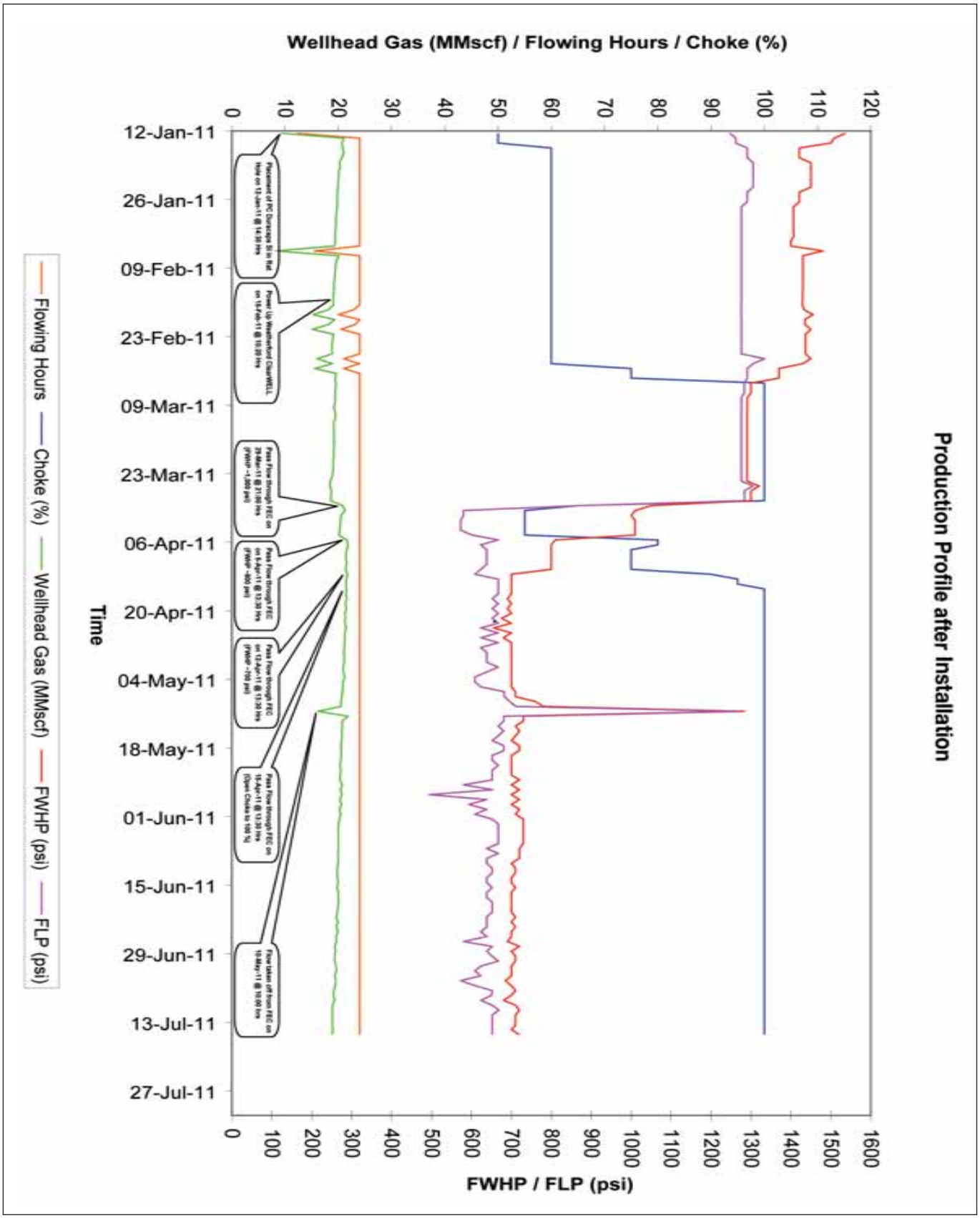

Figure-10: Production Profile after Installation

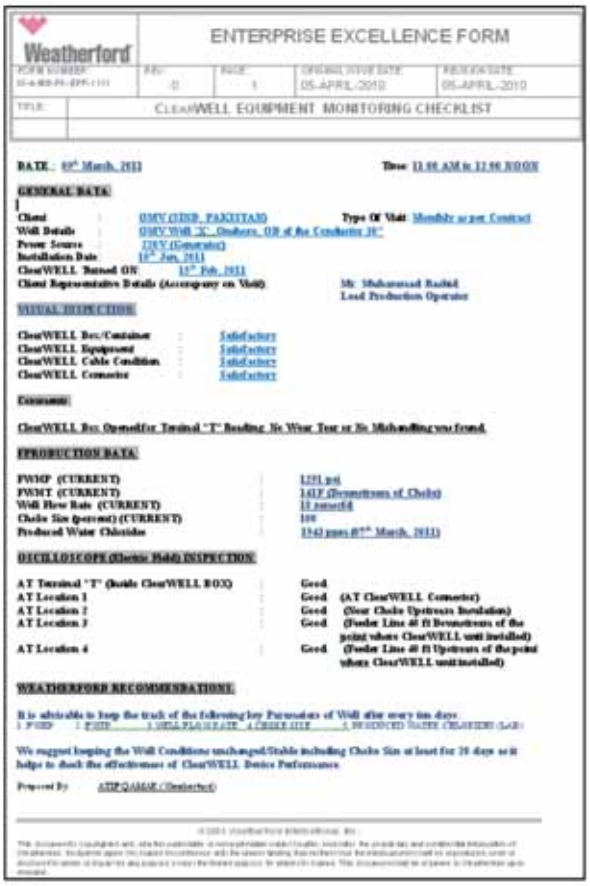
Weatherford

ENTERPRISE EXCELLENCE FORM

CLEARWELL EQUIPMENT MONITORING CHECKLIST

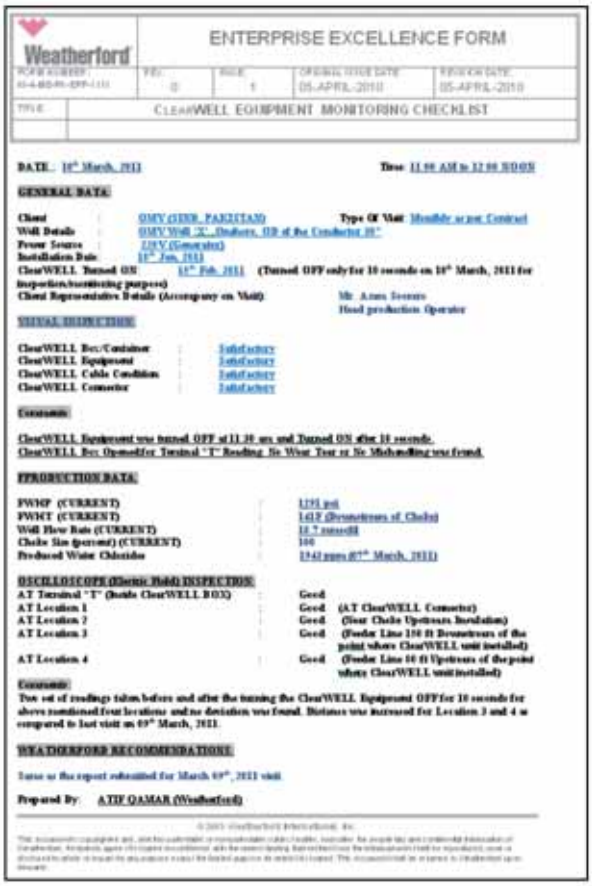
Weatherford

ENTERPRISE EXCELLENCE FORM

CLEARWELL EQUIPMENT MONITORING CHECKLIST

Figure-11: Monthly Inspection Reports by Service Engineer

Results

• Stable production from 5 month period. No lost production.

Conclusions

• The unit is a feasible and economical scale build up remedy for wells having scale build uptendency.

• The unit's performance has been tested as a pilot project for 5 months, however its long term effectiveness is still under evaluation.

Acknowledgements

The authors would like to thank the management of OMV (Pakistan) GmbH for permission to prepare and present this paper. We would also like to thank Weatherford Oil Tools ME Limited Pakistan for their continued support.

References

1. Laboratory for Exploration & Production, Gaenserndorf; July, 2010 "Investigate report on scale problems in OMV (Pak) fields".
2. ClearWELL proposal and brochures.

This paper was prepared for presentation at the SPE/PAPG Annual Technical Conference held in Islamabad, Pakistan, 22–23 November 2011.

OMV (PAKISTAN)

Sawan Laboratory

Produced Water Analysis

Sampling Point		Downstream of Cooler																	
Sampling Date:-		2-Jan-11	7-Jan-11	26-Jan-11	7-Feb-11	13-Mar-11	16-Mar-11	10-Apr-11	13-Apr-11	20-Apr-11	8-May-11	15-May-11	25-May-11	6-Jun-11	10-Jun-11	15-Jun-11	22-Jun-11	13-Jul-11	20-Jul-11
Choke opening (%)		70	50	60	60	60	100	75	95	100	100	100	100	100	100	100	100	100	100
Well Flow Rate (MMscfd)		9.00	17.00	18.50	18.00	18.90	18.10	20.50	20.50	20.30	20.50	19.50	19.40	19.10	19.30	19.00	19.00	17.00	17.50
Flow Line Temperature (^{o} F)		102	176	75	113	143	86	81	104	127	136	136	134	130	108	133	104	104	122
Flow Line Pressure (psi)		498	1247	1142	1334	1153	1146	638	667	623	681	667	595	585	638	482	652	682	609
Sampling Time		08:00	8:00	8:00	8:00	08:00	08:00	08:00	08:00	08:00	08:00	08:00	07:00	17:30		07:00	07:00	12:00	08:00
Tests	Unit																		
Appearance		Light Yellow	Clear	Clear	Clear	Clear	Clear	Clear	Clear	Clear	Clear	Clear	Clear	Clear	Clear	Clear	Clear	Clear	Clear
p H		6.88	7.00	6.08	6.90	6.30	6.31	6.22	7.00	6.39	6.99	6.84	6.3	6.7	6.3	6.31	6.4	6.6	6.3
Conductivity	uS/cm	8590	8100	7270	9220	7190	7020	5250	7400	7120	6820	7200	9800	8300	6340	9551	8190	7940	6890
TDS	ppm	5154	4000	4362	4610	3595	4212	2625	3700	4272	4092	4320	5880	4150	3804	5730	4914	4764	4134
Chloride (Cl)	ppm	2303	2235	1925	2372	2028	1719	1152	1822	1866	1790	1840	2780	2063	1498	2650	2180	2018	1935
Iron (Fe)	ppm	1.23	1.29	9.00	0.93	0.74	0.00	1.0	0.5	0.55	0.48	0.52	0.5	0.52	-	0.4	0.29	0.39	0.42
Hydroxide as $CaCO_3$	ppm	0	0	0	0	0	0	0	0	0	0	0	0	0	-	0	0	0	0
Carbonates as $CaCO_3$	ppm	0	0	0	0	0	0	0	0	0	0	0	0	0	-	0	0	0	0
Bicarbonates as $CaCO_3$	ppm	608	650	584	640	580	600	590	580	620	640	590	456	590	-	460	390	488	600

Sikander

Lab Supervisor

Figure-12: Produced Water Analysis

Biographies

Syed Saadat Hassan is currently Lead Petroleum Engineer with OMV (Pakistan) Exploration GmbH since 2001. He has over 10 years of experience in E&P industry mainly in Production & Operations Engineering, especially in HP/HT completion design. He received B.Sc. Petroleum Engineering from University of Engineering & Technology Lahore Pakistan in year 2000.

Tofeeq Ahmad is currently Production Manager with OMV (Pakistan) Exploration GmbH since June 2009. Previously he worked for BP Pakistan for 8 years. He has over 20 years of experience in E&P industry mainly in Petroleum, Production & Operations Engineering. He received B.Sc. Petroleum Engineering from University of Engineering & Technology Lahore Pakistan in year 1991.

Shoaib Farooqui is serving as "Business Development Manager" in Weatherford Oil Tools M.E. Ltd. Pakistan since 2007. His extensive 10 years experience with the Oil & Gas Industry comprise of Directional Drilling Operations, Development of Concepts of Underbalance Drilling, Effective Utilization of High BTU Gas with early commercialization, Gas Wells Deliquification, Electronic Scale Inhibition in Oil & Gas Wells & Integrated Project Management in Pakistan. Worked as an advisor on Final Year Projects with NED University's Mechanical & Petroleum Engineering Students in 2004, 2007, 2008, 2009, 2010. Business Development & Project Management of Construction & Commissioning of Early Production Facility (NGL, LPG, Condensate) with Weatherford. Involved in the development of Unconventional Reservoir Human Resource pool within Pakistan and at Regional Level. In this paper he worked as a co-author.

Haseeb Mazhar Ali is currently working as Reservoir Stimulation & Thru Tubing Team Leader, Weatherford Pakistan. He holds a bachelors degree in Mechatronics Engineering from NUST. He has 6 years of Oil & Gas experience with Schlumberger and Weatherford. His specializations are Well interventions, Production optimization using Matrix Stimulation & Scale control. In this paper he worked as a co-author.

Atif Qamar is working as a "Lead Engineer – Engineered Chemistry" in Weatherford, Pakistan. He did B.E. Mechanical from NED University of Engineering and Technology (Pakistan) and completed his MS Mechanical degree from University of Oklahoma - Norman, USA. He has more than 06 years experience in Mechanical and Petroleum Industry including 04 years Oil & Gas experience with Weatherford. Currently, he is extensively involved in ClearWELL installation in Middle East Region, Intelligent Pigging activity and Development of Weatherford's Engineered Chemistry and Pipeline Specialty Services in Pakistan. Worked as an advisor for Final Year NED Mechanical Students in 2009-10 for "feasibility study for the cleaning of un-piggable pipelines to achieve optimum production". He is a Certified Lead Auditor and actively participated in API Certification and human resource development of Weatherford Karachi Machine Shop in 2009-10.

A New Method to Predict Performance of Gas Condensate Reservoirs

By Ali M. Al-Shawaf, Dr. Mohan Kelkar and Dr. Mohammed Sharifi.

Reprinted with kind permission from Saudi Aramco Journal of Technology.

Abstract

Gas condensate reservoirs differ from dry gas reservoirs. An understanding of relationships in the phase and fluid flow behavior is essential if we want to make accurate engineering computations for gas condensate systems. That is because condensate dropout occurs in the reservoir as the pressure falls below the dew point, as a result of which gas phase production decreases significantly.

The goal of this study is to understand the multiphase flow behavior in gas condensate reservoirs, in particular focusing on estimating gas condensate well deliverability. Our new method analytically generates inflow performance relationship (IPR) curves for gas condensate wells by incorporating the effect of condensate banking as the pressure near the wellbore drops below the dew point. The only information needed to generate the IPR is the rock relative permeability data and results from the constant composition expansion (CCE) experiment.

We have developed a concept of critical oil saturation near the wellbore by simulating both lean and rich condensate reservoirs, and we have observed that the loss in productivity due to condensate accumulation can be closely tied to critical saturation. We further are able to reasonably estimate re-evaporation of the liquid accumulation by knowing the CCE data.

We validated our new method by comparing our analytical results with fine scale radial simulation model results. We demonstrated that our analytical tool can predict the IPR curve as a function of reservoir pressure. We also developed a method for generating an IPR curve by using field data and demonstrated its application. The method is easy to use and can be implemented quickly.

Introduction

Well productivity is an important issue in the development of most low and medium permeability gas condensate reservoirs. Liquid buildup around the well can cause a significant reduction in productivity, even in lean gas condensate reservoirs where the maximum liquid dropout in the constant composition expansion (CCE) experiment is as low as 1%[1]. Subsequently, accurate forecasts of productivity can be difficult because of the need to understand and account for the complex processes that occur in the near-well region.

The production performance of a gas condensate well is easy to predict as long as the well's flowing bottom-hole pressure (FBHP) is above the fluid dew point pressure (similar to a dry gas well). Once the well's FBHP falls below the dew point, the well performance starts to deviate from that of a dry gas well. Condensate begins to drop out first near the wellbore. Immobile initially, the liquid condensate accumulates until the critical

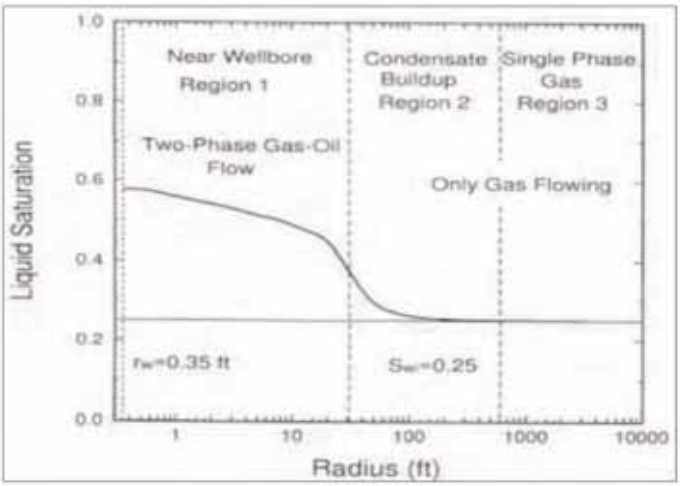

Fig. 1. Three regions of flow behavior in a gas condensate well.

condensate saturation (the minimum condensate saturation for mobility) is reached. This rich liquid zone then grows outward deeper into the reservoir as depletion continues[2].

The loss in productivity due to liquid buildup is mostly influenced by the value of gas relative permeability (krg) near the well when compared with the value of krg in the reservoir further away. The loss in productivity is more sensitive to these relative permeability curves than to fluid pressure-volume-temperature (PVT) properties[3].

The most accurate way to calculate gas condensate well productivity is by fine grid numerical simulation, either in single well models with a fine grid near the well or in full field models using local grid refinement. A large part of the pressure drawdown occurs within 10 ft of the well, so radial models are needed, with the inner grid cell having dimensions of about 1 ft[4, 5].

Several investigators have estimated the productivity of gas condensate reservoirs, but none of these methods is simple to use. Some methods require the use of the modification of a finite difference simulation process, whereas other methods use simplified simulation models[5, 6]. Our objective is to develop a simple yet accurate analytical procedure to estimate the productivity of gas condensate reservoirs without having to run simulations. The only data required by our method is the CCE experiment results and relative permeability curves. As with other simplified methods, our new technique allows well performance to be evaluated quickly without reservoir simulations. A fine grid radial compositional model was built in a commercial flow simulator to validate the results of our analytical approach.

Background

A method has been proposed for modeling the deliverability of gas condensate wells[2]. Well deliverability is calculated using a modified Evinger-Muskat pseudopressure approach[7]. The gas-oil ratio (GOR) needs to be known accurately for each reservoir pressure to use the pseudopressure integral method. Equation 12 is employed to calculate the pseudopressure integral in the pseudo steady-state gas rate equation:

$$q_g = C\int_{P_{wf}}^{P_r} \left[\left(\frac{K_{ro}}{B_o\,\mu_o}\right] R_s + \frac{\mathrm{Krg}}{\mathrm{Bg}\ \mu g}\right) dp \qquad (1)$$

To apply their method, we need to break the pseudopressure integral into three parts corresponding to the three flow regions discussed here:

Region 1: In this inner near-wellbore region, Fig. 1, both condensate and gas are mobile. It is the most important region for calculating condensate well productivity as most of the pressure drop occurs in Region 1. The flowing composition (GOR) within Region 1 is constant throughout and a semi steady-state regime exists. This means that the single-phase gas entering Region 1 has the same composition as the producing well stream mixture. The dew point of the producing well stream mixture equals the reservoir pressure at the outer edge of Region 1.

Region 2: This is the region where the condensate saturation is building up. The condensate is immobile, and only gas is flowing. Condensate saturations in

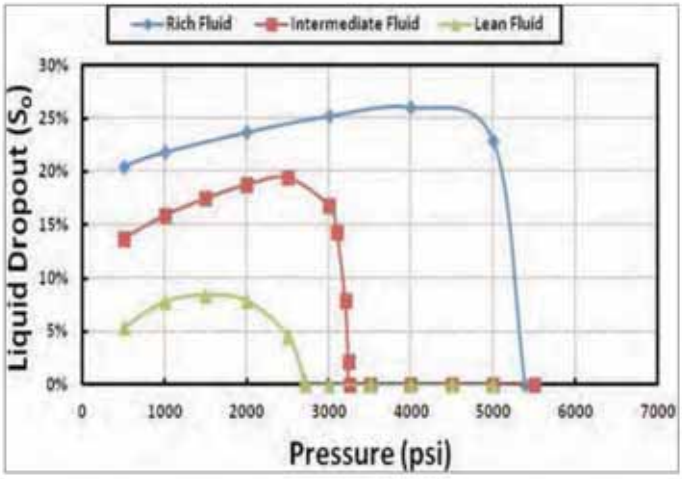

Fig. 2. CCE data for synthetic gas condensate compositions.

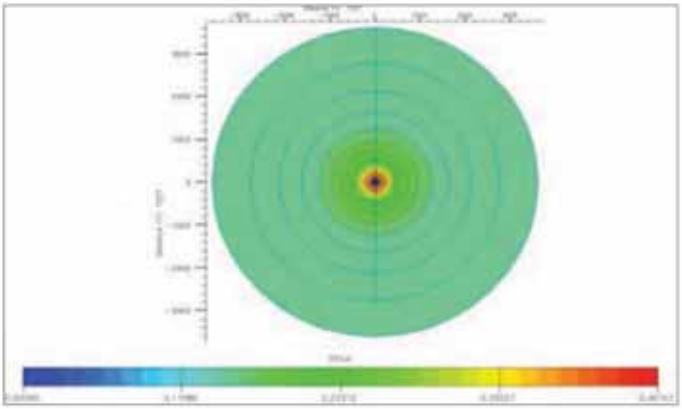

Fig. 3. Fine grid radial model with 36 cells.

Parameters	Rich Gas	Intermediate Gas	Lean Gas
Initial Reservoir Pressure (psia)	7,000	5,500	5,000
Dew Point Pressure (psia)	5,400	3,250	2,715
Reservoir Temperature (°F)	200	260	340
Maximum Liquid Dropout (%)	26	20	8.5

Table 1. Fluid properties of condensate mixtures

Porosity (%)	20
Absolute permeability (md)	10
Reservoir height (ft)	100
Irreducible water saturation (%)	0
Rock compressibility (psi^{-1})	4.0E-06

Table 2. Reservoir properties used in the fine radial model

Region 2 are approximated by the liquid dropout curve from a constant volume depletion (CVD) experiment, corrected for water saturation.

Region 3: This is the region where no condensate phase exists (it is above the dew point). Region 3 only exists in a gas condensate reservoir that is currently in a single phase. It contains a single-phase (original) reservoir gas.

Another major finding[2] is that the primary cause of reduced well deliverability within Region 1 is k_{rg} as a function of relative permeability ratio (k_{rg}/k_{ro}). Fevang and Whitson's approach is applicable for running coarse simulation studies, where the producing GOR is available from a prior time step.

An approach to generate inflow performance relationship (IPR) curves for depleting gas condensate reservoirs without resorting to the use of simulation has been previously presented[6]. The producing GOR (Rp) is calculated with an expression derived from the continuity equations of gas and condensate in Region 1. But his approach requires an iterative scheme by assuming R_p at a given reservoir pressure to generate IPR curves for rich gas condensate, whereas for lean gas condensates, GOR values from the reservoir material balance (MB) model are adequate to achieve good results.

Later, Mott (2003) presented a technique that can be implemented in an Excel™ spreadsheet model for forecasting the performance of gas condensate wells4. The calculation uses a MB model for reservoir depletion and a two-phase pseudo- pressure integral for well inflow performance. Mott's method generates a well's production GOR by modeling the growth of condensate banking without a reservoir simulator.

All these methods do not provide a simple way of generating IPR curves for condensate wells. The IPR curve as a function of reservoir pressure is needed to accurately predict and optimize the performance of the well.

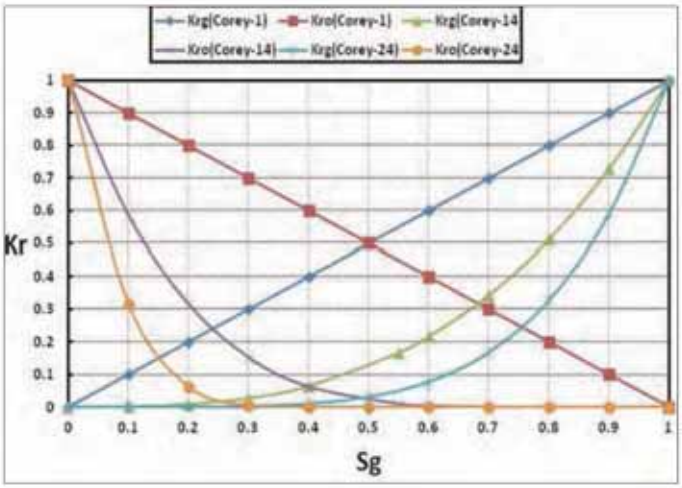

Fig. 4. Different sets of Corey relative permeability curves.

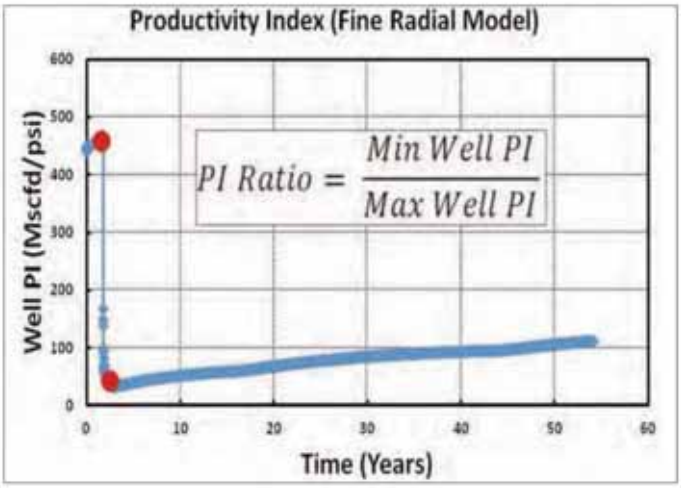

Fig. 5. Well PI as a function of time.

Approach

The pseudo steady-state rate equation for a gas condensate well in field units is given in Eqn. 28:

$$q_{sc} = \frac{(703\text{x}10^{-6})\, kh[m(P_r) - m(P_{wf})]}{T\,[\ln\left(\frac{r_e}{r_w}\right) - 0.75 + S]} \qquad (2)$$

where q_{sc} = gas flow rate in Mscfd; k = permeability in md; h = thickness in ft; m (p) = pseudopressure in (psi^2/cp); T = temperature in (°R), r_e = drainage radius in ft; and r_w = wellbore radius in ft. We can use this equation to estimate the gas production rate as long as the FBHP is above the dew point of the reservoir fluids. This means that this equation is applicable only for single-phase gas flow. As soon as the FBHP drops below the dew point pressure of the reservoir fluid, condensate begins to drop out, first near the wellbore, and the well performance starts to deviate from that of a dry gas well. Liquid condensate accumulates until the critical condensate saturation (the minimum condensate saturation for mobility) is reached. This rich liquid bank/zone grows outward deeper into the reservoir as depletion continues.

Liquid accumulation, or condensate banking, causes a reduction in the gas relative permeability and acts as a partial blockage to gas production, which leads to potentially significant reductions in well productivity. To quantify the impact of gas condensation phenomena, we have developed a method to generate the IPR of gas condensate reservoirs using analytical procedures. The main idea is to combine fluid properties (CCE or CVD data) with rock properties (relative permeability curves) to arrive at an analytical solution that is accurate enough to estimate the IPR curves of gas condensate reservoirs.

Fluid Description

Two different synthetic gas condensate compositions were used to generate the rich, intermediate, and lean fluids represented in Fig. 2. The rich fluid is composed of three components: methane (C1) 89%, butane (C4) 1.55%, and decane (C10) 9.45%. A four-component composition was used to generate the intermediate and lean condensate mixtures at different reservoir temperatures: methane (C1) 60.5%, ethane (C2) 20%, propane (C3) 10%, and decane (C10) 9.5%. The char- acteristics of the condensate mixtures are outlined in Table 1. The Peng-Robinson three parameter equation of state (PR3) was used to simulate phase behavior and laboratory experiments, such as CCE and CVD.

Reservoir Description

The Eclipse 300 compositional simulator was used. A 1D radial compositional model with a single vertical layer and 36 grid cells in the radial direction was used as a test case, Fig. 3. Homogeneous properties were used in the fine scale model as described in Table 2.
A single producer well lies at the center of the reservoir. The model has been refined near the wellbore to accurately observe the gas condensate dropout effect on production. For that purpose, the size of the radial cells were logarithmically distributed with the innermost grid size at 0.25 ft, according to Eqn. 3:

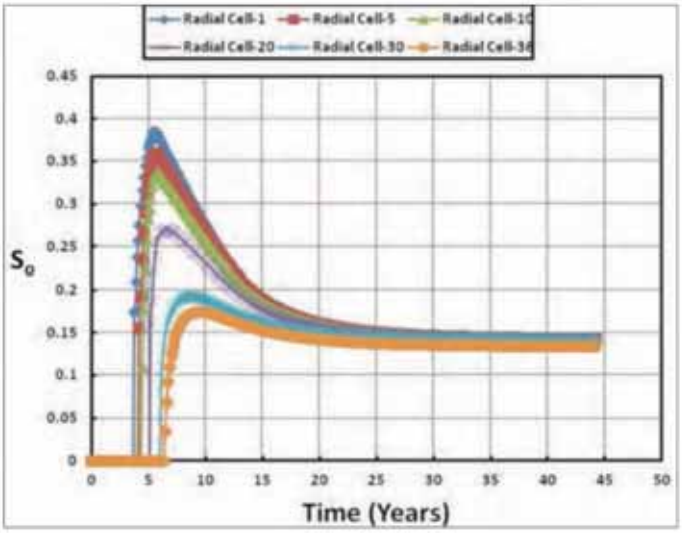

Fig. 6. Oil saturation profiles around the well as a function of time.

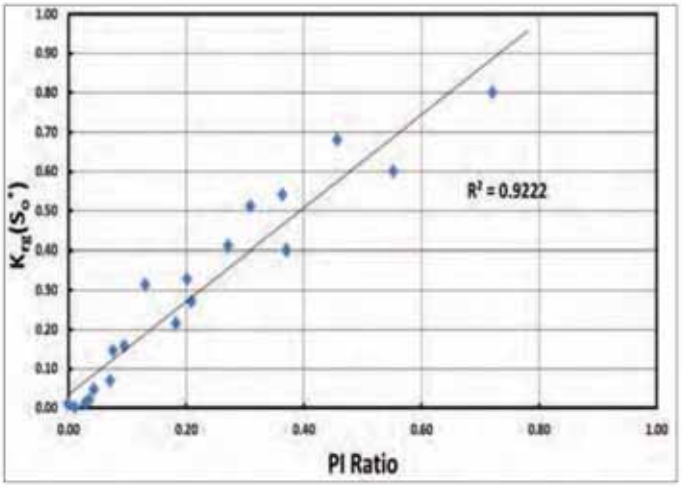

Fig. 7. Krg (So*) vs. PI ratio for rich fluid.

$$\frac{r_{i+1}}{r_i} = \left[\frac{r_e}{r_w}\right]^{\frac{1}{N}} \quad (3)$$

where N is the number of radial cells in the model. In addition to having very small grid blocks around the well, the time steps were refined at initial times, which led to a very smooth saturation profile around the well. The fully implicit method was chosen for all the runs.

Relative Permeability Curves

It has already been noted in the literature that relative permeability curves affect the gas flow significantly in a gas condensate reservoir once the pressure falls below dew point pressure. Accurate knowledge about the relative permeability curves in a gas condensate reservoir therefore would be critical information. Unfortunately, the relative permeability curves are rarely known accurately. It seemed worthwhile to investigate the effect of different relative permeability curves on gas flow and study the uncertainty they bring to the saturation buildup in gas condensate reservoirs.

Different sets of relative permeability curves were used in the study. These curves were generated based on Corey equations, as illustrated in Eqns. 4 and 5:

$$K_{rg} = S_g^{\,n} \quad (4)$$

$$K_{ro} = \left(\frac{1 - S_g - S_{or}}{1 - S_{or}}\right)^m \quad (5)$$

where n is the gas relative permeability exponent, m is the oil relative permeability exponent, and S_{or} is the residual oil saturation. Fractures (X-curves) and intermediate and tight relative permeability curves were generated by changing the n and m exponents from 1 to 5 and changing S_{or} from 0 to 0.60. Figure 4 shows three sets of relative permeability curves. Corey-1 (X-curve) was generated based on n=1, m=1, and S_{or}=0. Corey-14 was generated based on n=3, m=4, and S_{or}=0.20. The third curve, Corey-24, was generated based on n=5, m=4, and S_{or}=0.60.

Sensitivity Study

In this research, we examined a large number of relative permeability curves — over 20 sets of curves. The sensitivity study also examined the effects of fluid richness on gas productivity by using two fluid compositions (lean fluids and rich fluids).

The results of the sensitivity study were checked against simulation results. The simulation runs were done under a constant rate mode of production utilizing the fine compositional radial model. After testing this wide range of relative permeability curves, we found that a very strong correlation exists between the well's productivity index (PI) ratio and k_{rg} (S_o*). The value of S_o* is defined in a later section. Equation 6 defines the well PI ratio:

$$\text{PI Ratio} = \frac{Min\ Well\ PI}{Max\ Well\ PI} \quad (6)$$

Figure 5 shows an example of the well PI as a function of time for a producing well. The abrupt fall of PI

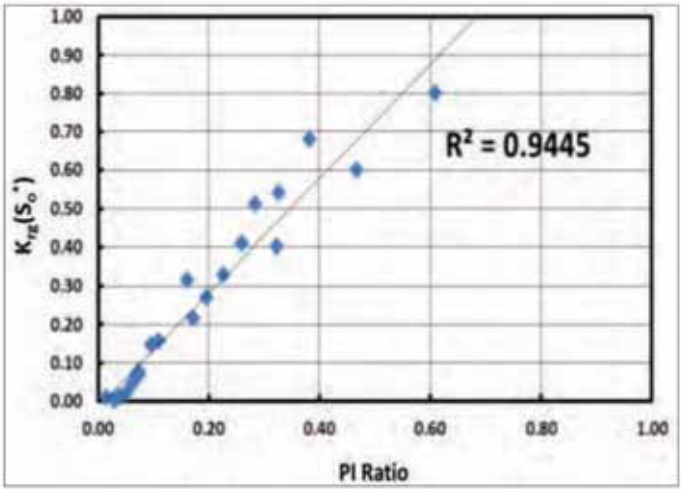

Fig. 8. Krg (So*) vs. PI ratio for lean fluid.

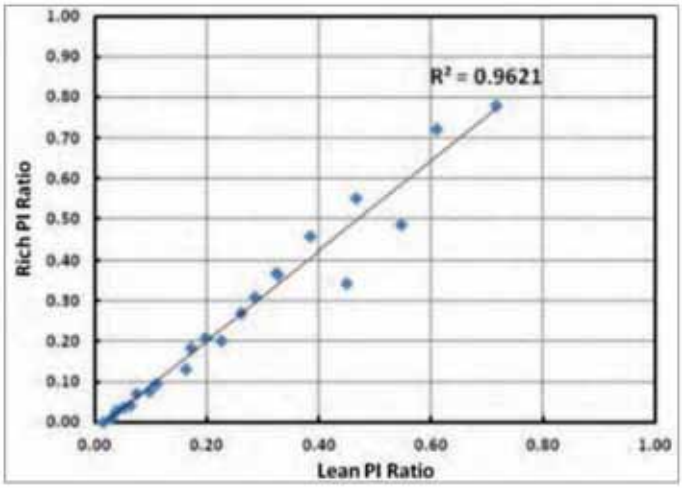

Fig. 10. Rich vs. lean PI ratio.

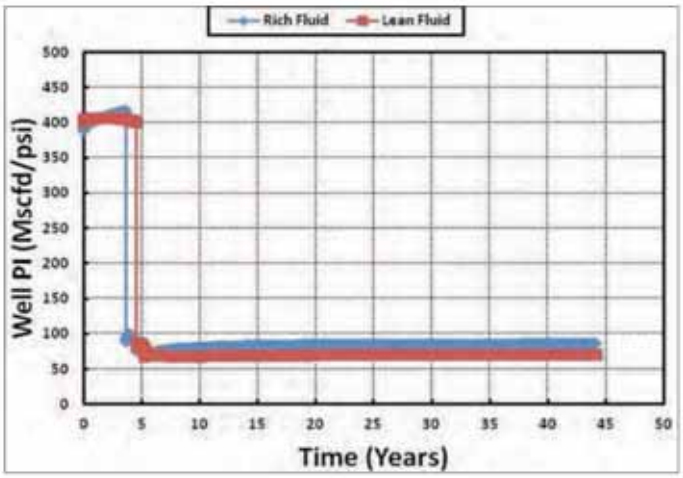

Fig. 9. Well PI vs. time for rich and lean fluids (same relative permeability curves).

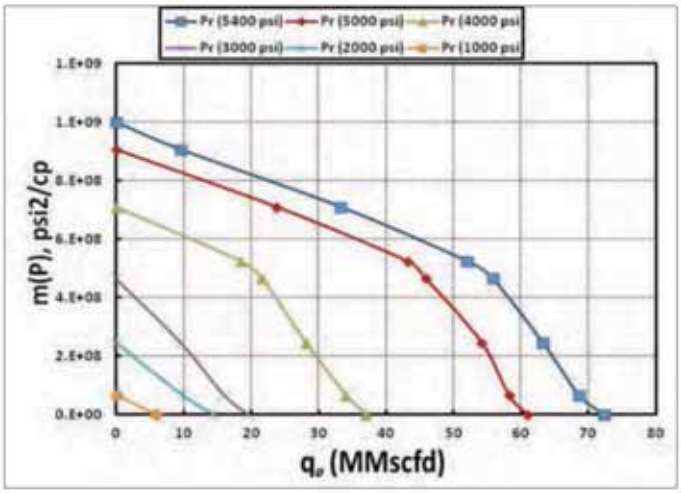

Fig. 11. Pseudo-pressure vs. gas rate plot.

happens immediately after the FBHP falls below the P_d. After analyzing several cases, we found that the PI is very close to krg (S_o*).

As can be seen from Fig. 5, the well PI drops quickly, then eventually increases slightly before stabilizing; the slight increase in PI is due to re-vaporization of oil. This type of PI behavior has been observed in field data where, after the bottom-hole pressure (BHP) drops below the dew point pressure, the PI decreases suddenly before stabilizing.

As we can see from Fig. 6, after oil saturation reaches a maximum value, the S_o drops gradually after a period of pro- duction, which will enhance the gas relative permeability and therefore the gas productivity. Figures 7 and 8 clearly show that for both rich and lean fluids, the relationship between the PI ratio and krg (S_o*) is linear with a strong correlation coefficient.

Another important outcome of this sensitivity analysis is the finding that the loss in productivity is more sensitive to the relative permeability curves than to fluid PVT properties. Figure 9 shows the well PI vs. time for the rich and lean fluids using the same relative permeability set. Figure 9 also demonstrates that the loss in productivity is much more dependent on relative permeability curves than on the fluid composition.

Figure 10 summarizes the results of the sensitivity study done on the rich and lean fluids by using the wide range of relative permeability curves. It appears that the loss is similar for both rich and lean gases so long as the same relative permeability curves are used. The slope is not exactly equal to one, but it is very close to one.

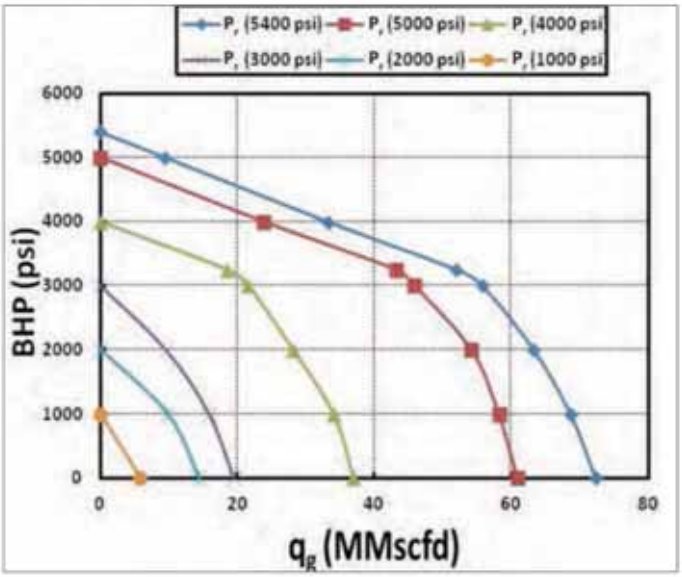

Fig. 12. BHP vs. gas rate (IPR) plot.

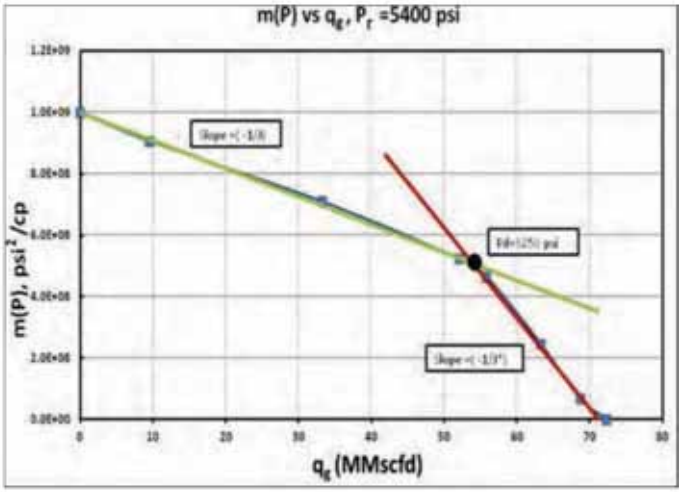

Fig. 13. IPR for Pr of 5,400 psi.

Generation of IPR Curves

IPR curves are very important to predicting the performance of gas or oil wells; however, generating IPR curves using a simulator is not straightforward since the IPR represents the instantaneous response of the reservoir at a given reservoir pressure for a given BHP. This cannot be generated in a single run since, if we change the BHP in a simulation run, depending on how much oil or gas is produced, the average pressure will change.

To generate IPR curves, we had to use a composite method. For different reservoir pressures, we ran a simulator at a fixed BHP. We then varied the BHP from high to low values. We generated rate profiles for a particular BHP and average reservoir pressure as the reservoir pressure was depleted. Using various runs, we picked the rate at a given reservoir pressure and a given BHP and combined them into one curve to generate the IPR curve.

Important Observations from Simulation Study

We wanted to develop simple relationships for generating the IPR curves under field conditions. We used the following important observations from our simulation study to come up with our procedure.

1. As already discussed before, we observed that the relative permeability curves have a bigger impact on the loss of productivity than the type of fluid that is produced.

2. The loss of productivity is significant and instantaneous after the pressure drops below the dew point. After that point, the PI recovers slightly due to re-vaporization of the liquid.

3. The oil saturation profile near the wellbore is a strong function of the average reservoir pressure[9]. Consequently, for a given reservoir pressure, the oil saturation profile does not change significantly for different BHPs, which will be shown in the next section.

New Analytical Approach for Estimating Gas Condensate Well Productivity

When we plotted the IPR curves, as a function of both pressure as well as pseudopressure, we noticed that plotting the pseudo-pressure vs. the gas rate will result in two clear straight lines for every reservoir pressure, Fig. 11. This is consistent with our observation that below the dew point the oil saturation does not change significantly for a given reservoir pressure, while plotting FBHP vs. the gas rate will result in normal IPR curves, Fig. 12.

We also noticed the peculiar behavior of IPR curves when plotted as a function of pseudoreal pressure. The lines are parallel above the dew point, as expected since the productivity does not change. Below the dew point, for different reservoir pressures, the lines are parallel for certain pressure ranges, but as the reservoir pressure depletes, the slope becomes gentler. This is

an indication of improved productivity, a result of the revaporization of the liquid phase as the pressure declines. This type of trend is difficult to capture using the pressure data.

As soon as the reservoir pressure drops below the dew point (P_d), which is 3,250 psi in this example, there will a productivity loss, which is indicated by the straight line below the P_d in the pseudopressure plot, previously shown in Fig. 11. To illustrate our method, we will take P_r = 5,400 psi as an example, Fig. 13.

The pseudopressure plot in Fig. 13 clearly shows that there are two distinct PIs. The first PI (J) is constant for single-phase gas flow (where the FBHP is above P_d), and the second PI (J^*) is for two-phase flow (where the FBHP is below P_d). Refer back to Eqn. 2:

$$q_{sc} = \frac{(703\times10^{-6})\, kh[m(P_r) - m(P_{wf})]}{T\left[\ln\left(\frac{r_e}{r_w}\right) - 0.75 + S\right]} \qquad (2)$$

The PI in terms of pseudopressure is given by:

$$J = \frac{q_{sc}}{[m(P_r) - m(P_{wf})]} \qquad (7)$$

Looking back at Fig. 13, we can define the slopes as:

Slope of the line above $P_d = (-1/J)$ (8)
Slope of the line below $P_d = (-1/J^*)$ (9)

After analyzing several cases, we found that the PI ratio can be determined by dividing the slope above P_d by the slope below P_d as follows:

$$\frac{\text{Slope of the line above } P_d}{\text{Slope of the line below } P_d} = \frac{(-1/J)}{(-1/J^*)} = \frac{J}{J} \cong \text{PI Ratio} \qquad (10)$$

Since the PI (J) for single-phase gas is always higher than the PI (J^*) for two-phase flow, the PI ratio (J^*/J) is always less than one. We found that the PI ratio (J^*/J) is strongly correlated to k_{rg} (S_o^*) for each relative permeability curve used. The application of the proposed method that follows is divided into two cases. The first case is where the initial reservoir pressure is above the P_d, and the second case is where initial reservoir pressure is below the P_d.

General Procedure – Initial Reservoir Pressure is Above the P_d

In this case, where the initial reservoir pressure is above the P_d, the pseudo steady-state gas rate, Eqn. 2, will be used to estimate the gas rate when the FBHP > P_d. When the FBHP drops below the P_d, we need to estimate (J^*) first to be able to calculate the gas rate analytically. Since, in this case, initial reservoir pressure is above the J, we can estimate the PI (J), which will be constant for all BHPs above the P_d.

After estimating (J), we use our knowledge of k_{rg} (S_o^*) as a multiplier to get (J^*) as:

$$\frac{J^*}{J} = \text{PI Ratio} \cong K_{rg}(S_o^*) \qquad (11)$$

After estimating J, which has a constant but higher slope than J, as shown before on the pseudopressure plot, we can use J to estimate the gas rate for all BHP below the P_d. Using the following equation, we assume:

$$y = mx + b \qquad (12)$$

$$m(P_{wf}) = \left(-\frac{1}{J^*}\right)q + b \qquad (13)$$

We can utilize our knowledge of the rate and FBHP at the P_d using the pseudo steady-state gas rate equation above the dew point. Then the intercept b can be calculated as:

$$b = m(P_d) + \frac{q_d}{J^*} \qquad (14)$$

where b in field units is in (psi^2/cp).

Now, our straight line pseudopressure equation is complete and able to estimate the gas rate for any FBHP less than the P_d as:

$$q = [b - m(P_{wf})]\, J^* \qquad (15)$$

where q is in (Mscfd), b and m(P↓wf) are in (psi^2/cp), and J^* is in (Mscfd/psia^2/cp).

General Procedure – Initial Reservoir Pressure is Below the P_d

In this case, the pseudopressure vs. rate plot (IPR) will have only one straight line. Figure 11 shows three examples of IPR lines where the initial reservoir pressure is below the P_d. To be able to generate the IPR curves for these cases, the following procedure should be followed.

Estimate the PI (J)

If an IPR curve is available for the case where reservoir pres- sure is above the P_d, the PI (J) of this case could be used to estimate J^* as a function of pressure using CCE data, as will be explained in the next step. For cases above the P_d where IPR curves are not available, the PI (J) could be estimated using a pseudo steady-state gas rate equation, Eqn. 16:

Case	Cases where P_r above P_d	Cases where P_r below P_d
S_{or} = Max_S_{oCCE}	$J^*/J = K_{rg}(S_{or})$	$\frac{J^*}{J(P_r)} = K_{rg}(S_{oCCE})$
S_{or} < Max_S_{oCCE}	$J^*/J = K_{rg}$ (Max_S_{oCCE})	
S_{or} > Max_S_{oCCE}	$J^*/J = K_{rg}(S_{or})$	

Table 3. General procedure for estimating productivity ratio

Case	Cases where P_r above P_d	Cases where P_r below P_d
S_o^* = Max_S_{oCCE}	$J^*/J = K_{rg}(S_o^*)$	$\frac{J^*}{J(P_r)} = K_{rg}(S^*_{oCCE})$
S_o^* < Max_S_{oCCE}	$J^*/J = K_{rg}$ (Max_S_{oCCE})	
S_o^* > Max_S_{oCCE}	$J^*/J = K_{rg}(S_o^*)$	

Table 4. General procedure for estimating productivity ratio for tight rocks

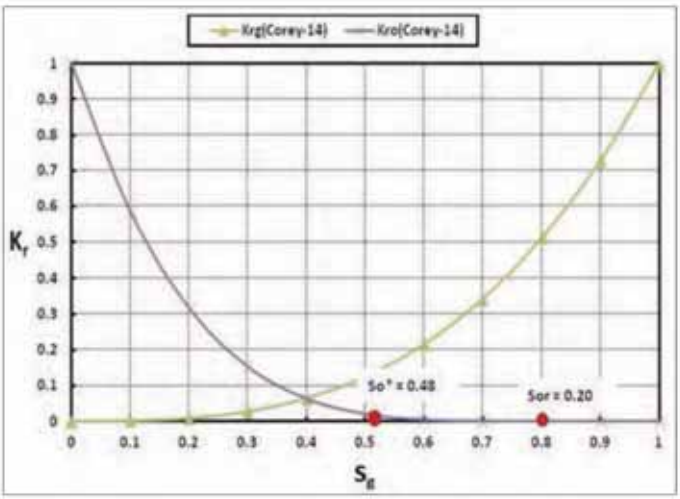

Fig. 14. Illustration of threshold (So*) in tight relative permeability curves.

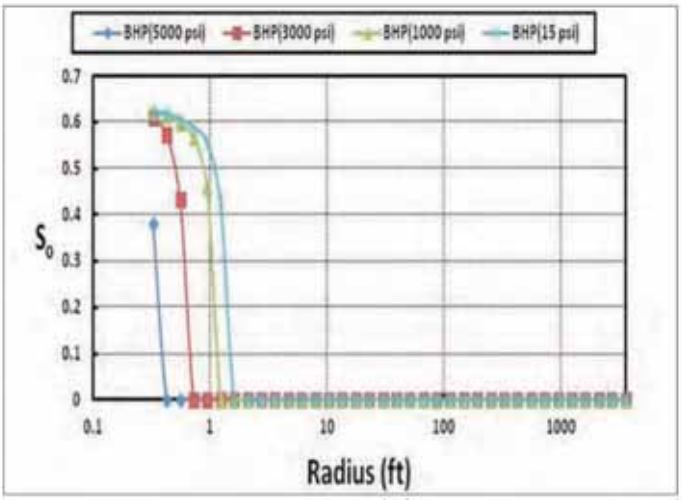

Fig. 15. Oil saturation distribution as a function of BHP for Pr of 6,900 psi.

$$J = \frac{q_{sc}}{[m(P_r) - m(P_{wf})]} = \frac{(703\text{x}10^{-6})\,kh}{T\,[\ln\left(\frac{re}{r_w}\right) - 0.75 + S]} \quad (16)$$

Estimate the PI (J^*)

As we have stated earlier, the PI ratio (J^*/J) is correlated to k_{rg} (S_{or}), but in those cases where initial reservoir pressure is below P_d, liquid re-vaporization plays a very important role in determining the productivity of gas condensate reservoirs. By examining the CCE data, as previously shown in Fig. 2, we can see that as soon as the pressure drops below the P_d, liquid saturation immediately reaches a maximum value (Max_S_{oCCE}) around the P_d, then it falls gradually as a function of pressure. Our idea of utilizing CCE data in generating the IPR curves is really to account for this phenomenon of liquid re-vaporization as pressure drops below the P_d[9]. We have found that using a fixed value of k_{rg} (S_{or}) or k_{rg} (Max_S_{oCCE}) will underestimate the gas productivity for cases where initial reservoir pressure is below the P_d.

Therefore, for any reservoir pressure below P_d, k_{rg} needs to be estimated at the corresponding pressure and oil saturation from the CCE data according to Eqn. 17:

$$\frac{J^*}{J}(P_r) = \text{Productivity Ratio Ratio} = K_{rg}(S_{occe}) \quad (17)$$

Estimate the Gas Rate

Finally, the gas rate can be directly estimated from Eqn. 18:

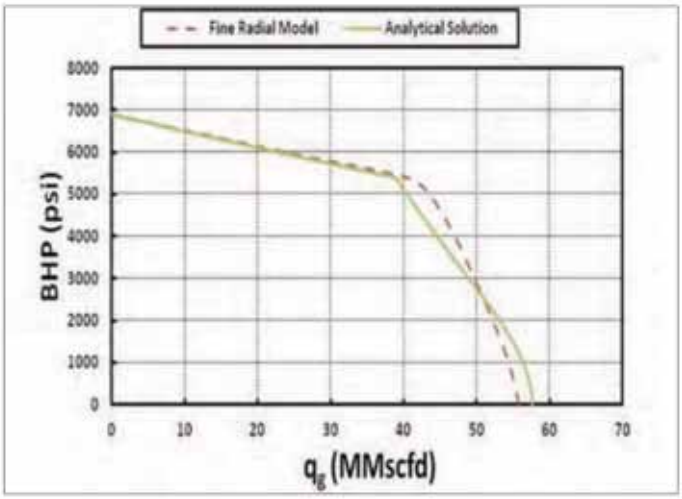

Fig. 16. IPR curve for Pr of 6,900 psi.

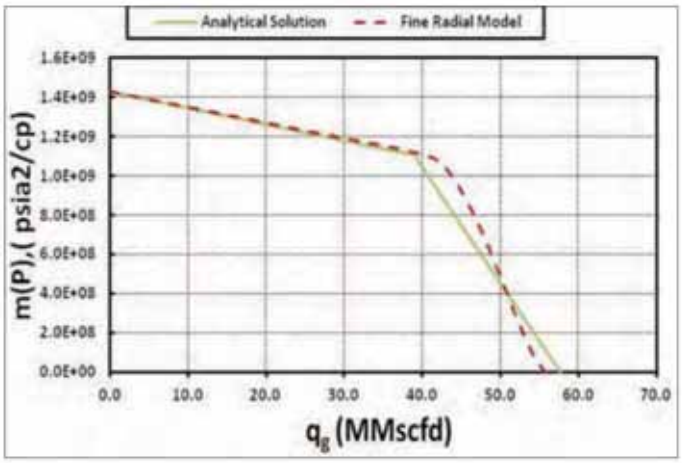

Fig. 17. Pseudo-pressure vs. gas rate plot for Pr of 6,900 psi.

$$q = [m(P_r) - m(P_{wf})]\, J^* \qquad (18)$$

The above outlined procedure for generating IPR curves assumes that S_{or} = Max_S_{oCCE}, but that is not always the case in real field applications. Since S_{or} is a rock property while Max_S_{oCCE} is a fluid property, we expect them to be different in most of the field application cases.

For that reason, we have analyzed several cases where S_{or} could be equal to, less than, or greater than Max_S_{oCCE}. Based on our evaluation, we believe that the maximum of the two values should be used to correctly capture the fluid behavior around the wellbore and thereby accurately estimate the gas productivity.

The procedure to estimate PI (J^*) here is exactly the same as the procedure outlined above for the case where S_{or} = Max_S_{oCCE}, but with some modifications as given by Table 3. This procedure is used for flowing pressure that is less than the dew point. In effect, what we are saying in this table is that, if we have reservoir

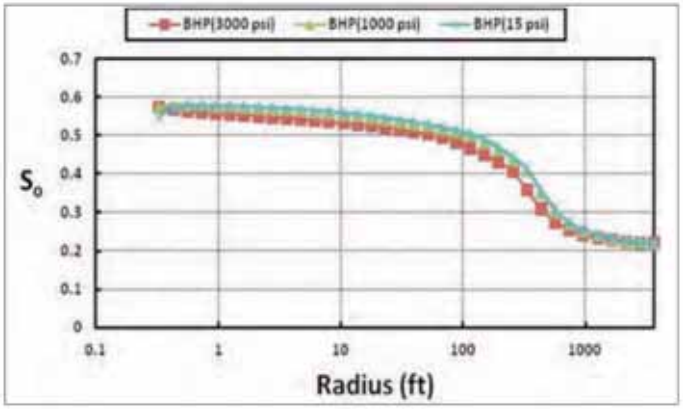

Fig. 18. Oil saturation distribution as a function of BHP for Pr of 5,000 psi.

pressure above the dew point, then to calculate the IPR curve for the BHP below the dew point, we can use a constant slope (J^*) based on the k_{rg} estimate as stated in Table 3. Subsequently, once the reservoir pressure drops below the dew point, we will need to use k_{rg} as a function of average reservoir pressure.

Importance of Threshold Oil Saturation (S_o*)

We have found that accurate estimation of gas productivity depends not only on S_{or} but also on the threshold oil saturation (S_o*) for reservoirs having tight oil relative permeability curves. Figure 14 shows an oil relative permeability curve that was generated based on S_{or} = 0.20 and a high value for the oil exponent (m=4). This higher value for the oil relative permeability exponent makes the oil relative permeability very low and eventually makes oil practically immobile until its saturation exceeds the threshold value (S_o*), which is in this case 0.48. After testing several tight oil relative permeability curves, we found that for practical applications, we can determine the threshold (S_o*) as corresponding to k_{ro} = 1% of the maximum value of oil relative permeability.

Therefore, in generating IPR curves, it is more important to know S_o* than S_{or}. We define S_o* as a minimum saturation needed to make oil mobile (i.e., k_{ro} is at least 1% of the end point value). It is a strong function of the curvature of the relative permeability curve. Therefore, all we need to do is to just to use Table 3 as it is, but replace S_{or} with S_o*, Table 4.

Cases where S_o* > Max_S_{oCCE}

This is probably the most common case in the field. Even for rich condensates, it is not unusual to find that the minimum saturation for oil mobility is greater than the maximum oil sat- uration in the CCE experiment. The rich condensate fluid with maximum liquid

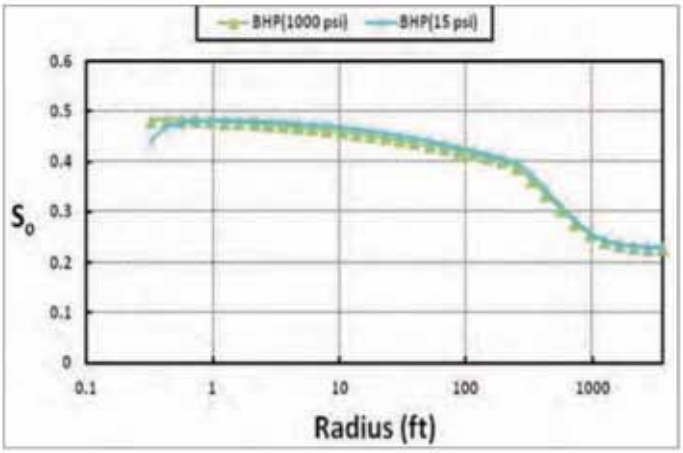

Fig. 19. Oil saturation distribution as a function of BHP for Pr of 3,000 psi.

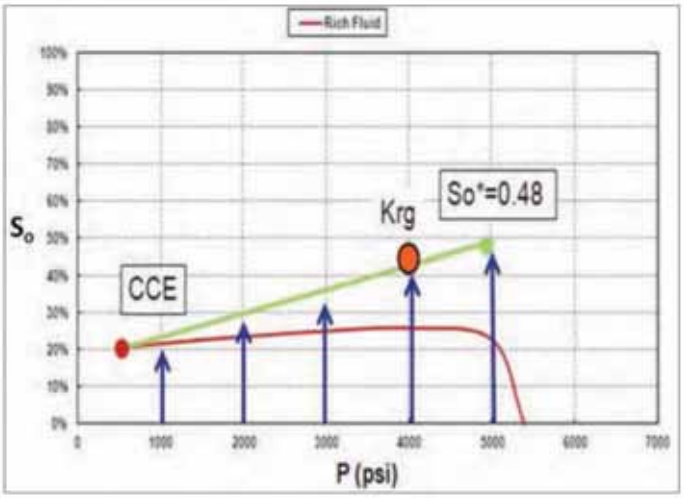

Fig. 21. Developing linear relation between So* and CCE data.

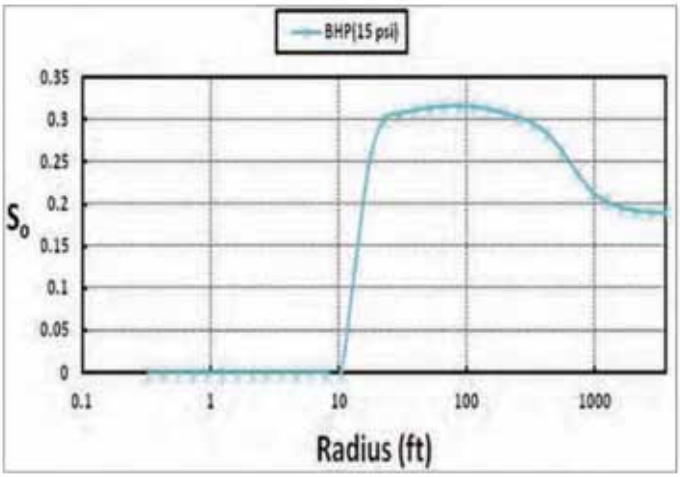

Fig. 20. Oil saturation distribution as a function of BHP for Pr of 1,000 psi.

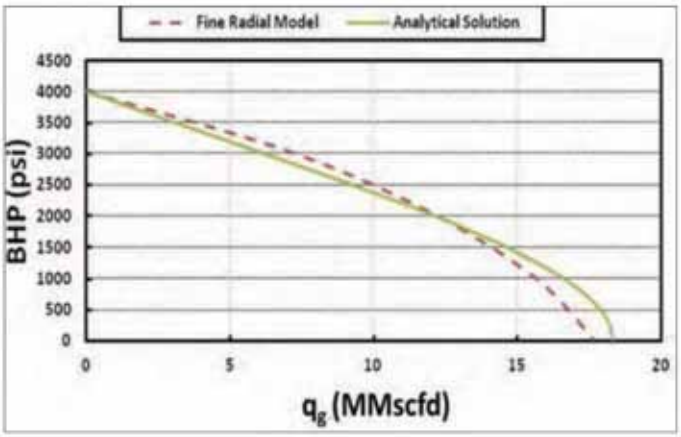

Fig. 22. IPR curve for Pr of 4,000 psi.

dropout (26%) is being used for this case where it is less than $S_o^* = 0.48$, as shown previously in Fig. 14. Referring back to Table 4, we can see that in this case the PI ratio is determined by $k_{rg}(S_o^*)$.

Initial Reservoir Pressure is Above the Pd

Figure 15 shows the S_o distribution around the wellbore as a function of the BHP. We would like to examine this figure carefully. As soon as the BHP drops below P_d, which is 5,400 psi for this fluid, liquid starts dropping out close to the wellbore first. The radius of oil banking expands inside the reservoir, and oil saturation away from the wellbore increases as the BHP decreases. We can see that at a BHP of 3,000 psi, S_o reaches a maximum value of about 0.62, and this value almost stays constant even though the BHP drops to 1,000 psi and then to atmospheric conditions.

What we want to highlight here is that as long as reservoir pressure is above the P_d, the oil saturation near the wellbore remains reasonably constant irrespective of the BHP. Since in this case the threshold (S_o^*) is higher than Max_S_{oCCE}, the value of S_o^* should be used to get the corresponding k_{rg} and therefore estimate the well productivity for the cases where reservoir pressure is above P_d. By following the general procedure outlined above for the case where initial reservoir pressure is above the P_d, we can generate the IPR curve as shown in Figs. 16 and 17. Just keep in mind that the only change you would make for this case where the threshold (S_o^*) > Max_S_{oCCE} is to use the larger value of (S_o^*) or Max_S_{oCCE}, which is in this case the S_o^*.

$$\frac{J^*}{J} = \text{PI Ratio} = K_{rg}(S_o^*) \qquad (19)$$

Initial Reservoir Pressure is Below the P_d

Now, we will illustrate an example where the IPR is below the P_d. To correctly generate the slope of the IPR curve on the pseudopressure plot, we need to account for re-vaporization. Again we need to utilize the fine

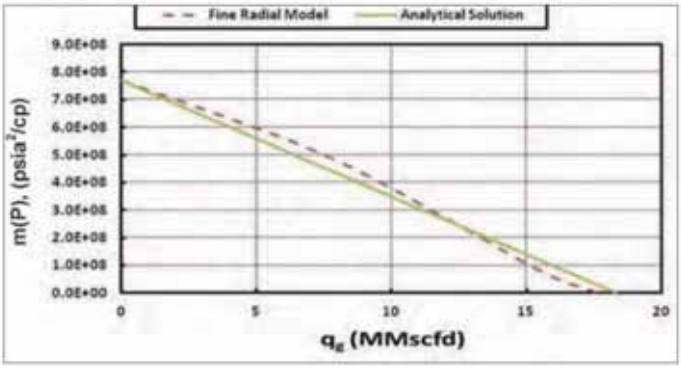

Fig. 23. Pseudo-pressure vs. gas rate plot for Pr of 4,000 psi.

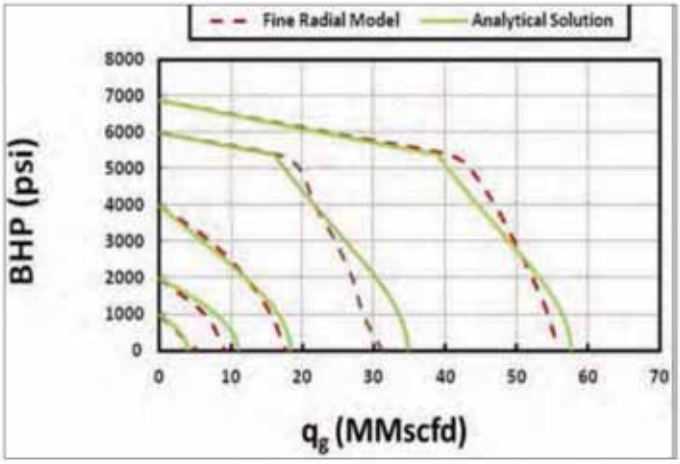

Fig. 24. IPR curves for rich gas (Corey-14).

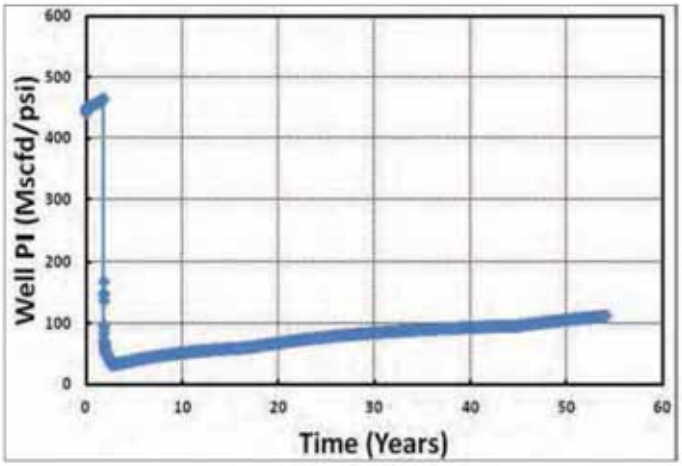

Fig. 25. Well PI as a function of time

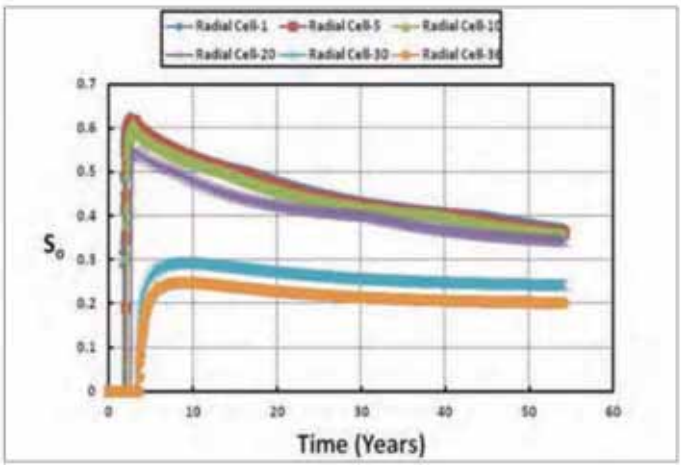

Fig. 26. Oil saturation profiles around the well as a function of time.

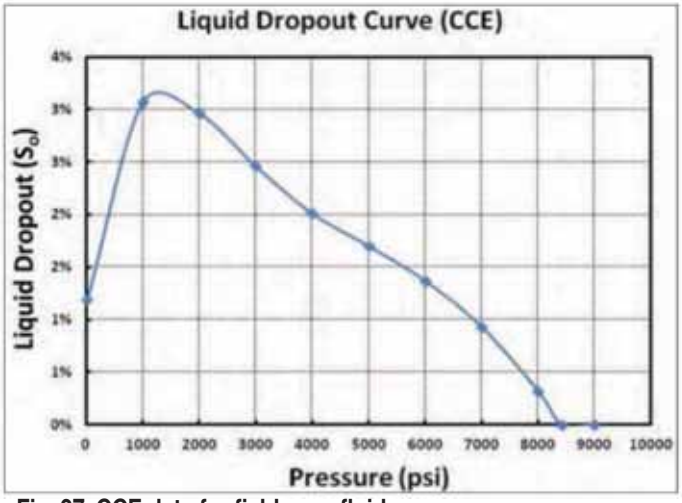

Fig. 27. CCE data for field case fluid.

grid model to capture the condensate behavior near the wellbore.

By examining the three figures, Figs. 18 to 20, which show the So distribution for saturated reservoirs, one will notice that So is decreasing gradually as a function of reservoir pressure, from about 0.62 when P_r = 6,900 psi, Fig. 15, to almost 0.30 when P_r = 1,000 psi, Fig. 20. We conclude from this that oil re-vaporization close to the wellbore is a strong function of decreasing reservoir pressure.

For each saturated reservoir pressure, we can see that S_o builds up to a uniform value close to the wellbore. This uniform S_o remains almost constant as BHP decreases. Therefore, a valid assumption for the application of our method is to assume a uniform So for every saturated pressure under consideration. Figure 20 shows an example of an extreme case where all the oil evaporates at a very low flowing pressure.

Once we have understood gas condensate behavior around the wellbore, we see that we really need to use a method that can mimic condensate re-vaporization as reservoir pressure depletes. The best tool to use is the CCE or CVD data for each condensate fluid being used[9]. The CCE data of the rich fluid was previously shown in Fig. 2. Following Fevang and Whitson (1995)[2], we will assume that the CCE experiment provides the best description of fluid near the wellbore. That is, we can use CCE data to predict the re-vaporization of oil. The reason we choose the CCE data is because

Initial Reservoir Pressure (psia)	9,000
Dew Point Pressure (psia)	8,424
Reservoir Temperature (°F)	305
Maximum Liquid Dropout (%)	3

Table 5. Fluid properties for the field case

Component	Composition (Fraction)
H_2S	0
CO_2	0.0279
N_2	0.0345
C1	0.7798
C2-C3	0.1172
C4-C6	0.0215
C7-C9	0.0132
C10-C19	0.00445
C20+	0.00145

Table 6. Fluid composition for the field case

the accumulation near the wellbore is minimal, which means that near the wellbore region whatever flows from the reservoir will flow into the wellbore without any change in its composition.

Since in this case the threshold (S_o*) is greater than Max_S_{oCCE}, our approach is to develop a linear relationship between the S_o* and the CCE data, Fig. 21. Careful examination of Fig. 15 and Figs. 18 to 20 tells us that actual liquid dropout around the wellbore is much greater than Max_S_{oCCE} and is closer to the threshold S_o*. We have seen from testing several cases under this category that using k_{rg} (Max_S_{oCCE}) will overestimate the gas rate since it will not account for the relative permeability of the oil phase; however, we can use CCE data to account for changes in oil saturation as the reservoir pressure declines.

It is very clear that condensate banking (accumulation) is tied up with two factors. The first factor is fluid properties (Maximum S_o from CCE), and the second factor is rock properties (Immobile S_o). Accordingly, we have asked ourselves this question: Although we know that the actual liquid dropout around the wellbore is much greater than Max_S_{oCCE}, how can we still utilize the CCE data along with relative permeability curves to come up with a robust analytical procedure that is accurate enough to estimate the well productivity?

Other researchers have shown that relative permeability has a first order effect on condensate banking, greater

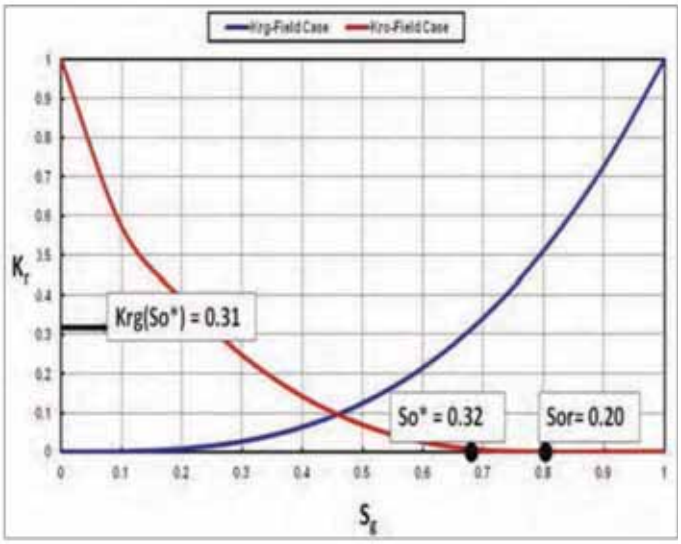

Fig. 28. Relative permeability set of the field case.

than the PVT properties[3]. As we have concluded from the results of the sensitivity study, different fluids will have a similar productivity loss for the same relative permeability curve used, confirming to us that it is the relative permeability that is the most important factor in determining the productivity loss.

We used engineering approximation to model the behavior below the dew point pressure. As we have stated before, we are going to assume that the area around the wellbore behaves like the CCE data for every designated saturated pressure. Following the general procedure previously outlined for the case where IPR is below the P_d, we are going to explain our approach at P_r = 4,000 psi. After estimating the PI (J) as shown in Step 1 of the procedure, we can estimate PI (J*) as:

$$\frac{J^*}{J(P_r)} = K_{rg}(S^*_{oCCE}) \qquad (20)$$

At P_r = 4,000 psi, we should estimate S_o from the linear relation between the S_o* and CCE data, Fig. 21. The next step is to go back to the relative permeability curves to estimate k_{rg} at the corresponding S_o from this linear relation. After that, J* can be calculated directly from Eqn. 20. The last step before generating the IPR curve is to estimate the gas rate directly from Eqn. 18. Just keep in mind that in this case the pseudopressure vs. rate plot will have only one straight line as this is what we expect to see in saturated reservoirs. The IPR curve is shown in Fig. 22 along with the pseudopressure plot in Fig. 23. The complete IPR curves of this case are shown in Fig. 24.

Figure 25 shows the well PI producing at a constant

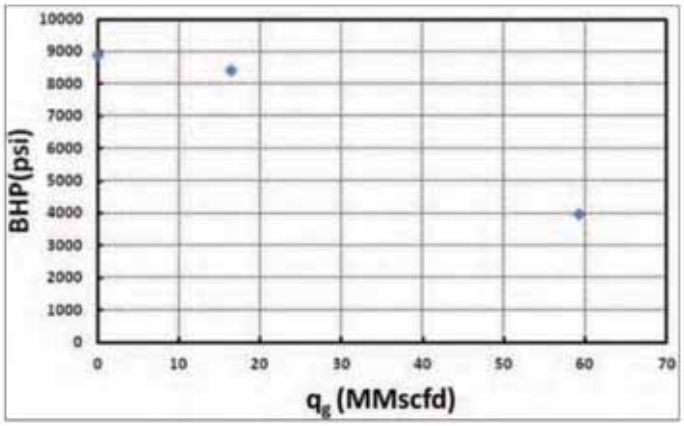

Fig. 29. Production data from two tests.

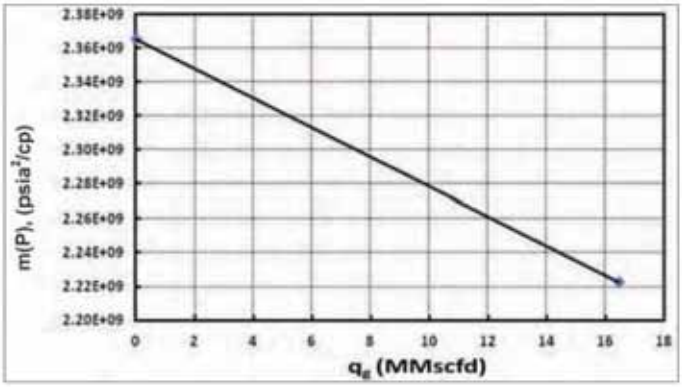

Fig. 30. Pseudo-pressure vs. gas rate plot for points above P_d.

rate. As expected, we found that the PI ratio is very close to k_{rg} (S_o*) as follows:

$$\frac{Min\ Well\ PI}{Max\ Well\ PI} \approx K_{rg}(S_o^*) = 0.11 \qquad (21)$$

Based on the PI ratio, we can define the productivity loss as:

$$\frac{Min\ Well\ PI}{Max\ Well\ PI} \qquad (22)$$

Therefore, in this example, the productivity loss is 0.89. This means that this well will experience an 89% productivity loss as soon as the BHP reaches the P_d. Looking back at Fig. 25, we can see that the well restores some of its productivity after about 5 years of production. Figure 26 shows the saturation profiles as a function of time, which shows the re-vaporization process.

Field Applications

In this section we will show the application of our method to a field case. Both compositional model data and relative permeability curves were provided. A nine-component compositional model was used with the PR3 to simulate phase behavior and the CCE laboratory experiment, Fig. 27. Tables 5 and 6 show fluid properties and composition for the field case, respectively.

Figure 28 shows the relative permeability curves. As is common in field applications, what matters here is the threshold S_o*. Although S_{or} = 0.20, the threshold S_o* = 0.32, which corresponds to about k_{ro} = 1% as a practical value. As we have stated before, accurate estimation of gas productivity in this case depends on the value of krg estimated at the threshold S_o*, which equals 0.32 in this case.

Moving to the production operations view in the field, we will show that our method can be used to generate IPR curves based on production test data in the same way as Vogel's, Fetkovich's, and other IPR correlations.

Assume that we are working in a production environment in a field where we have no knowledge about its relative permeability curves. The only thing that we have is some production data. Since initial reservoir pressure is above the P_d, we know that the pseudopressure vs. gas rate plot will have two straight lines, as explained earlier. Therefore, to generate the IPR curve for a given reservoir pressure, all we need is two test points. One point should be above the P_d and the other point should be below the P_d.

Figure 29 shows an example of data from two production tests. To explain how our method will work, we have designated one of the test data to be at the P_d. Otherwise, any available test data above the P_d will fit the procedure. Our method uses the following procedure:

1. Estimate the PI (J) by utilizing P_r and the test data at the P_d using Eqn. 7:

$$J = \frac{q_{sc}}{[m(P_r) - m(P_{wf})]} \qquad (7)$$

Or another way to estimate J is to plot the test points above the P_d on the pseudopressure plot, Fig. 30. J can then be calculated from Eqn. 8:

$$slope = -\frac{1}{J} \qquad (8)$$

2. Using J, you should be able to generate the first portion of the IPR curve using Eqn. 7.

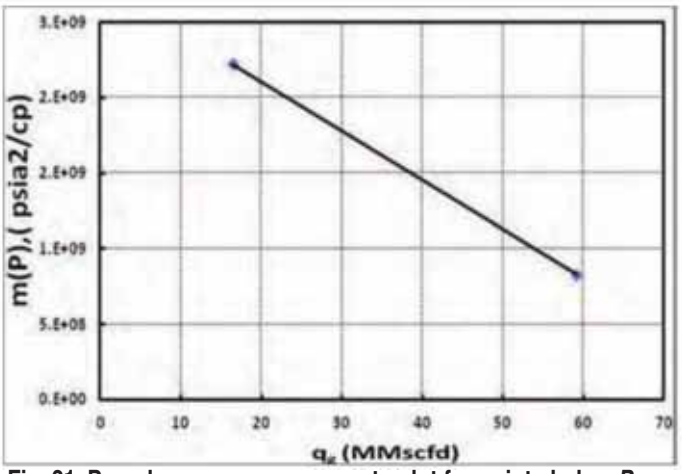

Fig. 31. Pseudo-pressure vs. gas rate plot for points below P_d.

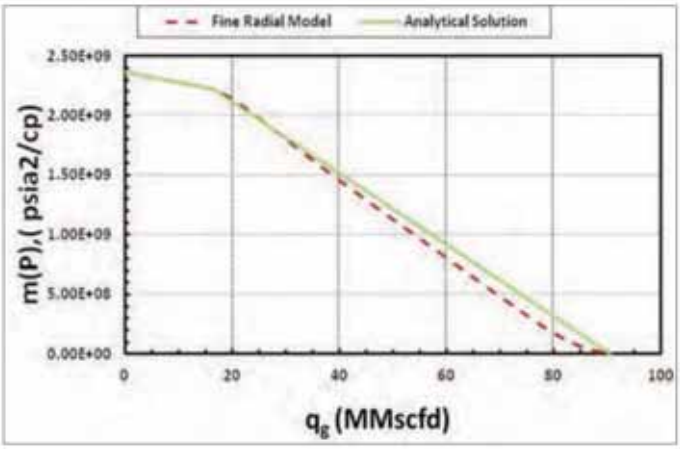

Fig. 33. Pseudo-pressure vs. gas rate plot for P_r of 8,900 psi.

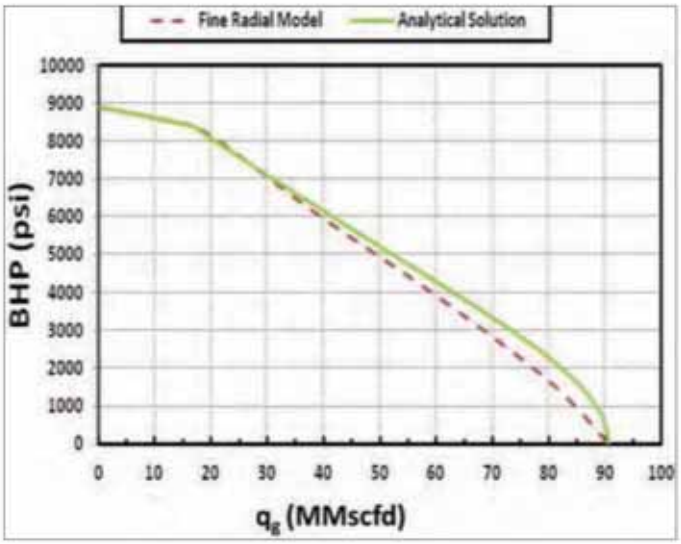

Fig. 32. IPR curve for P_r of 8,900 psi.

3. The same way as we did in Step 1, we need to plot the test points below the P_d on the pseudopressure plot, Fig. 31. Then J^* can be calculated from the slope as:

$$slope = -\frac{1}{J^*} \tag{9}$$

4. The intercept of the straight line (b) should be estimated by using Eqn. 14 as follows:

$$b = m(P_d) + \frac{q_d}{J^*} \tag{14}$$

5. Finally, we can estimate the gas rate for any BHP less than the P_d using Eqn. 15 as follows:

$$q = [b - m(P_{wf})].\, J^* \tag{15}$$

The generated IPR curve and the pseudopressure plot are shown in Fig. 32 and Fig. 33, respectively.

We have shown that our method can be used to generate IPR curves based on available test data without any basic knowledge about the relative permeability curves. Before we proceed to an example where initial reservoir pressure is below the P_d, we would like to highlight one important thing. We found that the PI ratio equals 0.30 by using Eqn. 10:

$$\frac{\text{Slope of the line above Pd}}{\text{Slope of the line above Pd}} = \frac{\left(\frac{1}{J}\right)}{\left(\frac{1}{J^*}\right)} = \text{Productivity Ratio} = 0.30 \tag{10}$$

We would have expected this value to be equal to krg (So*), or 0.31, as previously shown in Fig. 28. We can easily quantify the productivity loss once we have an idea about the PI ratio or k_{rg} (S_o*) using Eqn. 22 as follows:

$$Productivity\ loss = 1 - Productivity\ Ratio \tag{22}$$

Therefore, in this example, we can conclude that once the FBHP drops below the P_d, the well will lose 70% of its productivity. We would like to highlight two major points here:

1. Having two test points of production data clearly helped us to characterize one value of relative permeability, which is k_{rg} at (S_o*). By knowing k_{rg} (S_o*), one can easily utilize relative permeability curves (if available) to estimate (S_o*) or maximum oil saturation around the well.

2. Although this field case has very lean gas with maximum liquid dropout of only 3%, as previously shown in Fig. 27, the loss in productivity is significant (70%). This clearly tells us that the most important parameter in determining productivity loss is the gas-oil relative permeability curves, expressed in terms of krg estimated at residual (or threshold) oil saturation.

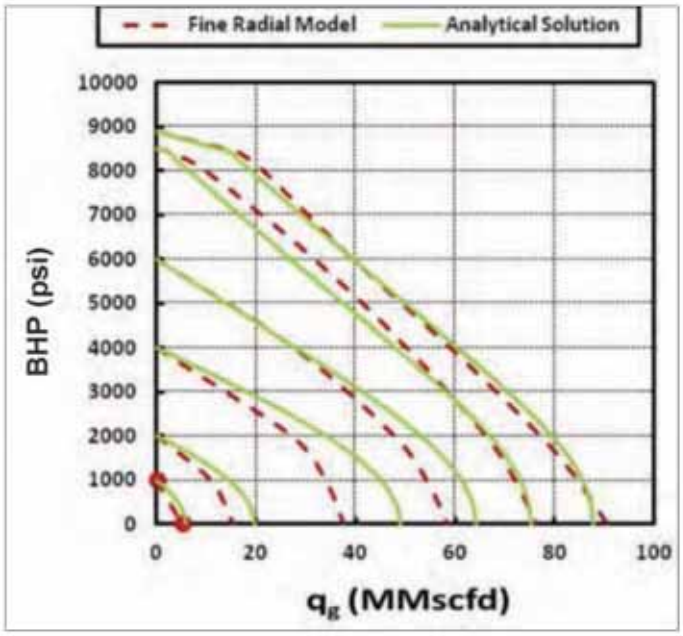

Fig. 34. IPR curves for the field case

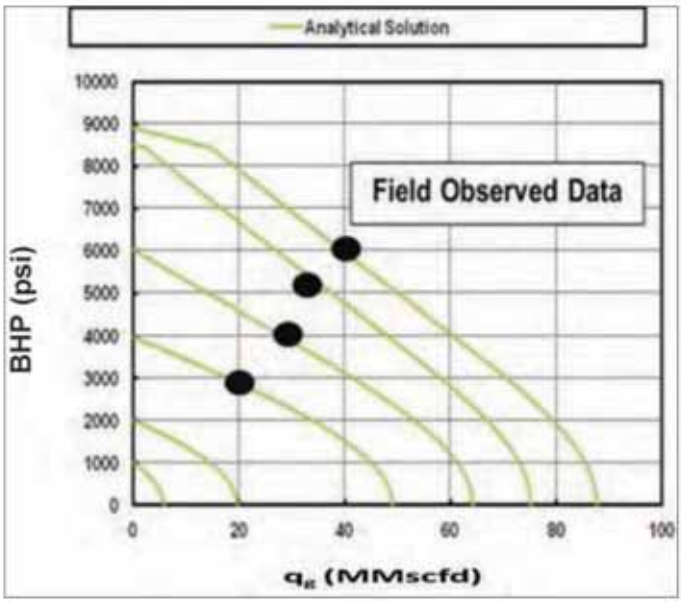

Fig. 35. Validation of the new method with field data.

We can easily generate the IPR curves for reservoir pressure above the dew point pressure. The slope of the IPR curves above and below the dew point will remain the same, except that the curve will shift downwards as the reservoir pressure declines. If the reservoir pressure is below the dew point, to generate the entire IPR curve, we will just need one observation.

The PI (J^*) can be calculated directly based on the test data and reservoir pressure using Eqn. 16.

$$J^* = \frac{q_{sc}}{[m(P_r) - m(P_{wf})]} \quad (16)$$

After that, the gas rate can be directly estimated from Eqn. 18.

$$q = [m(P_r) - m(P_{wf})].\, J^* \quad (18)$$

If we want to predict the future IPR based on the current IPR curve, we will need to have information about relative permeability and CCE data. The complete IPR curves for this case are shown in Fig. 34 where the generated IPR curves are validated with the results of the fine radial compositional model.

Using our methodology, we examined 10 years of the production history of a gas condensate well with known CCE and relative permeability data. We used the initial production data and calculated the future IPR curves using our methodology. Figure 35 shows the future IPR curves. Superimposed on those curves, we also show the actual production data as a function of time as the reservoir pressure has declined. The match between predicted rates and observed rates is quite good, validating our procedure.

Conclusions

In this article, a new analytical procedure has been proposed to estimate the well deliverability of gas condensate reservoirs. Our new method analytically generates the IPR curves of gas condensate wells by incorporating the effect of condensate banking as the pressure near the wellbore drops below the dew point. Other than basic reservoir properties, the only information needed to generate the IPR is the rock relative permeability data and CCE experiment results. In addition to predicting the IPR curve under current conditions, our method can also predict future IPR curves if the CCE data are available.

We found that the most important parameter in determining productivity loss is the gas relative permeability at immobile oil saturation. We observed that at low reservoir pressures some of the accumulated liquid near the wellbore re-vaporizes. This re-vaporization can be captured by using CCE data. In our method, we propose two ways of predicting the IPR curves:

- Forward Approach: By using the basic reservoir properties, relative permeability data, and CCE information, we can predict the IPR curves for the entire pressure range. Comparison with simulation results validates our approach.

- Backward Approach: By using field data, we can predict the IPR curves for the entire pressure range. This method does not require reservoir data; instead, similar to Vogel's approach, it uses point information from the IPR curve and then predicts the IPR curve for the entire BHP range. Both synthetic and field data validate our second approach.

Acknowledgements

The authors would like to thank Saudi Aramco management for permission to present and publish this article. The authors would also like to acknowledge the support from the Reservoir Description and Simulation Department at Saudi Aramco and extend thanks to the Tulsa University Center of Reservoir Studies for their support.

This article was presented at the SPE International Petro- leum Exhibition and Conference (ADIPEC), Abu Dhabi, U.A.E., November 11-14, 2012.

Nomenclature

J = productivity index, (Mscfd/psia^2/cp)
K = absolute rock permeability, md
k_{rg} = gas relative permeability
k_{ro} = oil relative permeability
m(p) = pseudopressure function, (psi^2/cp)
P_d = dew point pressure, psia
P_r = average reservoir pressure, psia
P_{wf} = flowing bottom-hole pressure, psia
q_{sc} = gas flow rate at standard conditions, Mscfd
r_e = external reservoir radius, ft
r_w = wellbore radius, ft
R_p = producing GOR, Scf/STB
S_g = gas saturation, fraction So = oil saturation, fraction
S_o* = threshold oil saturation, fraction
S_{or} = residual oil saturation, fraction
S_{wi} = connate water saturation

References

1. Afidick, D., Kaczorowski, N.J. and Bette, S.: "Production Performance of a Retrograde Gas Reservoir: A Case Study of the Arun Field," SPE paper 28749, presented at the SPE Asia Pacific Oil and Gas Conference, Melbourne, Australia, November 7-10, 1994.

2. Fevang, O. and Whitson, C.H.: "Modeling Gas Condensate Well Deliverability," SPE paper 30714, presented at the SPE Annual Technical Conference and Exhibition, Dallas, Texas, October 22-25, 1995.

3. Mott, R.: "Calculating Well Deliverability in Gas Condensate Reservoirs," paper 104, presented at the 10th European Symposium on Improved Oil Recovery, Brighton, U.K., August 18-20, 1999.

4. Mott, R.: "Engineering Calculations of Gas Condensate Well Productivity," SPE paper 77551, presented at the SPE Annual Technical Conference and Exhibition, San Antonio, Texas, September 29 - October 2, 2002.

5. Xiao, J.J. and Al-Muraikhi, A.J.: "A New Method for the Determination of Gas Condensate Well Production

Performance," SPE paper 90290, presented at the SPE Annual Technical Conference and Exhibition, Houston, Texas, September 26-29, 2004.

6. Guehria, F.M.: "Inflow Performance Relationships for Gas Condensates," SPE paper 63158, presented at the SPE Annual Technical Conference and Exhibition, Dallas, Texas, October 1-4, 2000.

7. Evinger, H.H. and Muskat, M.: "Calculation of Theoretical Productivity Factor," Transaction of the AIME, Vol. 146, No. 1, December 1942, pp. 126-139.

8. Kelkar, M.: Natural Gas Production Engineering, Tulsa, Oklahoma: PennWell Books, 2008, p. 584.

9. Vo, D.T., Jones, J.R. and Raghavan, R.: "Performance Prediction for Gas Condensate Reservoir," SPE Formation Evaluation, Vol. 4, No. 4, December 1989, pp. 576-584.

Biographies

Ali M. Al-Shawaf is the Lead Simulation Engineer for offshore gas fields in Saudi Aramco's Reservoir Description and Simulation Department. He joined the company in 2006 and began working for the Southern Area Gas Production Engineering Division as a Production Field Engineer in the Haradh Engineering Unit.

In May 2008, Ali joined the Southern Area Reservoir Simulation Division where he conducted several full field simulation models in onshore and offshore development and increment fields. His major responsibilities include working with a multidisciplinary team in a full Integrated Reservoir Study, which ranges from building static geological models to history matching and ends with forecasting full field development plans.

In 2006, Ali received his B.S. degree in Petroleum Engineering from King Fahd University of Petroleum and Minerals (KFUPM), Dhahran, Saudi Arabia. In 2012, he received his M.S. degree in Petroleum Engineering from the University of Tulsa, OK, where he developed a new method to predict the performance of gas condensate wells.

Ali is the author and coauthor of several technical papers. He has participated in several regional and international technical conferences and symposiums.

Ali is an active member of the Society of Petroleum Engineers (SPE) where he serves on several committees for SPE technical conferences and workshops.

Dr. Mohan Kelkar is the Director of the Tulsa University Center for Reservoir Studies (TUCRS). He is currently working with several medium- and small-sized oil and gas companies in relation to reservoir characterization and optimization of tight gas reservoirs.

Mohan has published over 50 refereed publications and has made over 100 technical presentations. He is a coauthor of a bestseller titled Applied Geostatistics for Reservoir Characterization, published by the Society of Petroleum Engineers (SPE) in 2002, and Gas Production Engineering, published in 2008 by PennWell Books.

In 1979, Mohan received his B.S. degree in Chemical Engineering from the University of Bombay, Mumbai, Maharashtra, India. He received his M.S. and Ph.D. degrees in Petroleum Engineering and Chemical Engineering, respectively, from the University of Pittsburgh, Pittsburgh, PA, in 1982.

Dr. Mohammad Sharifi is a Reservoir Simulation Engineer. His main research is in the area of bridging static to dynamic models through efficient upgrading and upscaling techniques. Mohammad is currently working on developing a fast dynamic method for ranking multiple reservoir realization models.

He received his B.S., M.Eng., and M.S. degrees from the Petroleum University of Technology (PUT), the University of Calgary, and PUT, respectively, all in Reservoir Engineering. Mohammad received his Ph.D. degree in Petroleum Engineering from the University of Tulsa, Tulsa, OK.

MASTERGEAR UK

The **Stainless Steel** Gearbox Range.

Built to withstand the World's most **extreme environments.**

www.mastergearworldwide.com

Experience with Fiberglass (GRE) Lined Carbon Steel Tubulars for Corrosion Protection for Oil Production Applications

By Dr. Qamar J. Sharif, Dr. Omar J. Esmail, Gokulnath Radhakrishnan, John A. Simpson and Martin R. Bremner.

Reprinted with kind permission from Saudi Aramco Journal of Technology.

Abstract

Saudi Aramco experienced serious corrosion problems in an oil production tubing in one offshore field – attributed to the presence of carbon dioxide (CO_2), hydrogen sulfide (H_2S) and varying levels of water cut.

In early 2002, the company installed, on a trial test basis, glass reinforced epoxy (GRE), commonly known as fiberglass, lined carbon steel tubing in three wells. The fiberglass lining was installed to provide a corrosion barrier to protect the steel tubing from internal corrosion. As for the technology, the fiberglass lining or sleeve is carried out joint by joint by inserting a solid fiberglass tube into the low cost carbon steel tubing and cement is pumped into the narrow annulus between the fiberglass liner and the carbon steel tubing. The connection area is protected by the combination of end flares and a corrosion barrier ring.

The company examined various methods to evaluate the performance of the fiberglass lined tubing, without having to pull out the tubing from the well as these wells are oil producers. After review of the evaluation options, it was decided to run a multifinger caliper to evaluate the condition of the fiberglass lining and check for any internal corrosion in the steel tubing. The log showed the fiberglass lining to be in good condition with no damage, indicating that the steel tubing was protected from corrosion. The other two wells had no tubing leaks, indicating the GRE lining is providing corrosion protection.

Based on successful trial test results, the company adopted the technology to protect tubing strings deployed in corrosive environments in oil producers, water injectors and water supply wells.

Field experience has shown that the use of fiberglass lined tubing is a low "life cycle cost" solution compared to other options. There has been no workover in these wells since installation. Today, fiberglass lined tubing is applied in Saudi Aramco in high water cut oil producers, water injectors and combined water source and injection wells.

This article shares the history of corrosion, challenges and lessons learned during the implementation of the solution, various performance assessment methods evaluated and the results and interpretation of the caliper log.

Introduction

Five oil producers were worked over during 2001-2002. These offshore wells had been completed with carbon steel J55 tubing with API connections. The failures of tubing were attributed to corrosion related problems. These wells were based offshore and the wellbore fluids had combinations of various levels of carbon dioxide (CO_2), hydrogen sulfide (H_2S) and with water cuts ranging from zero to a maximum of 10%. The corrosion was so severe that four out of the five oil wells required multiple milling/fishing runs to retrieve the tubing string, resulting in high workover

Fig. 1. Corroded tubing pulled out from one of the wells in the subject field.

costs. Figure 1 shows the condition of the tubing pulled out from one of the wells in the subject field.

Three wells were selected for the trial test of glass reinforced epoxy (GRE) lined tubing to evaluate the effectiveness of the fiberglass lining in protecting the steel tubing from corrosion. The flow rates of the wells ranged from 2,000 to 6,000 barrels of oil per day (bopd). The CO_2 and H_2S levels were about 1% and 2%, respectively. The static bottom-hole temperature (SBHT) was 220 °F. With water-wet conditions in the presence of CO_2, the corrosion potential of the wells was high for low alloy carbon steel exposed to the low pH well fluids. But the co-existence of CO_2 and H_2S brings in a certain level of unpredictability to the expected corrosion rates and the corrosion mechanisms.

Bijan et al.[1], presents an extensive discourse on the effects of CO_2 and H_2S coexisting in the production stream with water. The prevalence of H_2S can either increase CO_2 corrosion by acting as a promoter of anodic dissolution through sulfide adsorption and affecting the pH or decrease sweet corrosion through the formation of a protective sulfide scale. The exact interaction of H_2S on the anodic dissolution reactions in the presence of CO_2 is not fully understood. Both CO_2 and H_2S gases lower the solution pH and potentially increase the corrosion rate. With a CO_2 and H_2S ratio of less than 1:5 (1% and 2%, respectively), the corrosion is dominated by H_2S with FeS as the main corrosion product[2]. The in-situ pH is also a key parameter governing corrosion in wet hydrocarbon production conditions affecting the formation and retaining a protective layer. Apart from the CO_2 and H_2S ratio, corrosion is dependent on multiple yet interacting factors such as temperature, fluid chemistry (water chemistry, pH, organic acids, water cut, oil wetability, phase ratios, etc.), the hydrocarbon phase, flow characteristics and fluid velocity, including corrosion products, scales, wax and asphaltene and steel chemistry[1].

While the investigations were in process to identify the causes of the corrosion in the tubing, the company decided to trial test the GRE lined tubing. A total of 17,873 ft of 3½", J55, 9.3 ppf, external upset end (EUE) tubing was lined with a GRE lining at Saudi Aramco's pipe yard. Well-2, (callipered in 2008) was completed with 237 joints of GRE lined tubing and 288 ft of 4½" J55, 11.6 ppf, new Vallourec and Mannesmann (VAM), internally plastic coated (IPC) tubing at the top of the completion string.

GRE Lined Tubing

The technology of lining the tubing with GRE has been used by the industry as a method for corrosion protection of downhole tubing. Over 30,000 wells have been installed in water handling, oil and gas producing and gas injection and disposal wells. GRE lining acts as a barrier between the corrosive fluids and the base metal.

Fiberglass reinforced plastic (FRP) or GRE pipe is a composite material formed from thermosetting epoxy resins with continuous fiberglass filament reinforcements. The GRE liner tube is manufactured in a filament winding process, which applies continuous lengths of fiberglass filaments that are wetted with epoxy to a steel mandrel in helical angles. The epoxy resin is heat cured at temperatures above the recommended operating ranges for the product. The

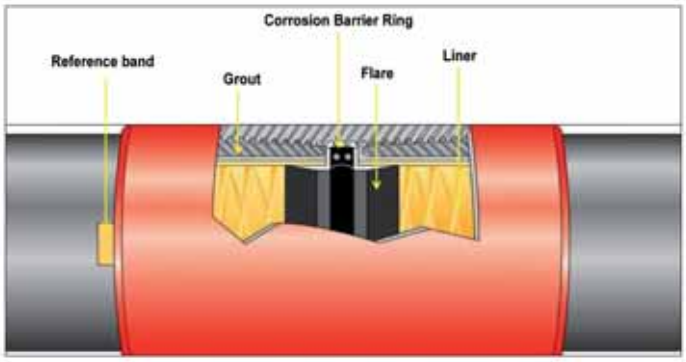

Fig. 2. GRE lining inside API connection.

resulting GRE pipe exhibits high strength combined with excellent chemical resistance. GRE or "fiberglass" pipe is used extensively in the oil, gas and chemical industry for low-pressure oil and gas transmission, salt water disposal, chemical piping system, etc. It is resistant to corrosion and prone to other deterioration generally caused by crude oil and other common oil field chemicals.

The GRE lining is a joint-by-joint process carried out on a pumping rack with specialized pumping equipment and qualified personnel. The corrosion protection barrier is achieved by inserting a rigid GRE lined tube into the steel pipe and filling the annular space with a special mortar/cement. The cement is a closely regulated mixture of oil well cement and oil well cement additives mixed with water to a controlled slurry viscosity. The purpose of the cement is to support the GRE lined tube in the steel tubing and not to provide a pressure seal between the two tubes. After the GRE liner is placed inside the pipe, mortar is pumped through special end fittings into the annulus. The mortar slurry is pumped under pressure from the lower end of the tubing. The other end of the tubing is raised to ensure a complete filling of the annulus with no possible air bubbles. The pressure is raised to affect a squeeze and cause partial dehydration of the mortar.

The liner is centralized at each end by the threaded fixtures used for injection of the mortar. More impor- tantly, the end fixtures centralize the liner to the thread profile, providing for improved joint to joint centerline alignment within the couplings, an important consideration in wireline or other through tubing interventions. There are no centralizers along the length of the joint, but this is not important since the outside diameter of the GRE liner is slightly larger than the drift diameter of the pipe, providing little room for deviation. Any deviation from concentricity in the body area of the pipe is minimal and unimportant.

On both ends of the tubing, the GRE liner is protected by a precisely molded fiberglass flange, commonly known as the "flare." A specially designed reinforced elastomeric corrosion barrier ring (CBR) is compressed in the coupling by the opposing flares. For API con- nections, the CBR is an oil resistant nitrile rubber ring with spring steel wire reinforcements, which hold the ring in place during pressure cycles. For premium or proprietary threaded connections, a glass reinforced PTFE CBR is installed, which is designed exclusively for the system with specifications from the premium thread manufacturing companies. Figure 2 presents details of the API lining system.

Completion Considerations

Tubing details from top to bottom after the workover are:

- 4½" J55, 11.6 ppf, new VAM, IPC tubing to 288 ft.
- Subsurface safety valve.
- Crossover 4½" new VAM x 3½" 9.3 ppf EUE at around 310 ft.
- 3½" 9.3 ppf J55 GRE lined tubing (2¾" internal diameter (ID)) to 7,835 ft.
- 9⅝" packer.
- Crossover 3½" J55, 9.3 ppf EUE x 2⅞" J55, 6.5 ppf EUE.
- 2⅞" nipple (2.313" ID) at 7,888 ft.

For a standard 3½" API unlined completion, the nipple profile sizes would be 2.813", whereas with a GRE lining, the ID of 3½" tubing is reduced to 2¾". This requires the nipple profiles to be re-sized to 2.313". Table 1 provides the dimensional changes and reprofiling requirements for the commonly applied tubing sizes for reference purposes.

API Connections	Standard Unlined Completion				Lined Tubing				
Size, inch	Tubing ID	Drift	X Nipple Profile	XN Nipple No-Go ID	Tubing ID	Flare ID (Lowest)	Drift	X Nipple Profile	XN Nipple No-Go ID
2⅞" 6.5 ppf	2.441	2.347	2.313	2.205	2.251	2.195	**1.945**	1.875	1.791
3½" 9.3 ppf	2.992	2.867	2.813	2.666	2.750	2.670	**2.420**	2.313	2.250
4½" 11.6 ppf	4.000	3.875	3.813	3.725	3.691	3.600	**3.350**	2.813	2.666
4½" 11.6 ppf	4.000	3.875	3.813	3.725	3.691	3.600	**3.350**	3.313	3.135
4½" 12.6 ppf (Opt)	3.958	3.833	3.813	3.725	3.691	3.600	**3.350**	2.813 3.313	2.666 3.135
5½" 17 and 20 ppf (R Nipple Opt)	4.892	4.767	4.562	4.455	4.520	4.400	**4.150**	4.125	3.912
5½" 17 and 20 ppf (X Nipple Opt)	4.892	4.767	4.562	4.455	4.520	4.400	**4.150**	3.813	3.725
7" 23 ppf (R Nipple)	6.366	6.241	5.963	5.770	6.091	5.976	**5.726**	5.625	5.500
7" 26 ppf (R Nipple)	6.276	6.151	5.963	5.770	5.900	5.785	**5.535**	5.250	5.018
7" 29 ppf (R Nipple)	6.184	6.059	5.963	5.770	5.800	5.685	**5.435**	5.250	5.018
7" 32 ppf (R Nipple)	6.094	5.969	5.963	5.770	5.800	5.685	**5.435**	5.250	5.018

Table 1. API completions: Reference table for dimensional changes while applying GRE lining

Depth, Pressure / Corrosive Fluids H_2S/CO_2	Low	High
Low	Quadrant 1: Low alloy carbon steel API connections	Quadrant 2: Low alloy carbon steel Premium connections
High	*Quadrant 3:* *Corrosion resistant alloy* *Premium connections*	Quadrant 4: Corrosion resistant alloy Premium connections

Table 2. Basic connection and material selection matrix

Depth, Pressure / Corrosive Fluids H_2S/CO_2	Low	High
Low	Quadrant 1: Low alloy carbon steel API connections	Quadrant 2: Low alloy carbon steel Premium connections
High	*Quadrant 3:* *GRE lined tubing* *API connections*	Quadrant 4: GRE lined tubing options Premium connections

Table 3. Reflecting the option GRE lined tubing brings in (Quadrant 3)

Material and Connection Considerations

Completion accessories in a GRE lined completion should follow the same metallurgy as the GRE lined carbon steel tubing. The GRE lined completion provides the cost savings, while the accessories that cannot be lined are installed in the CRA suitable for the process conditions[3].

Generally, the "material and connection selection" for production wells can be compartmentalized based on the mechanical demands (pressure, depth, onshore vs. offshore) and the corrosive nature of the well fluids, as presented in Table 2. Quadrants 1 and 2, with little or no corrosion impact would rightfully adopt low alloy carbon steel solutions with a corrosion management program. Quadrants 3 and 4 are worthwhile applications for GRE lined tubing.

Specific attention is required to Quadrant 3 — one

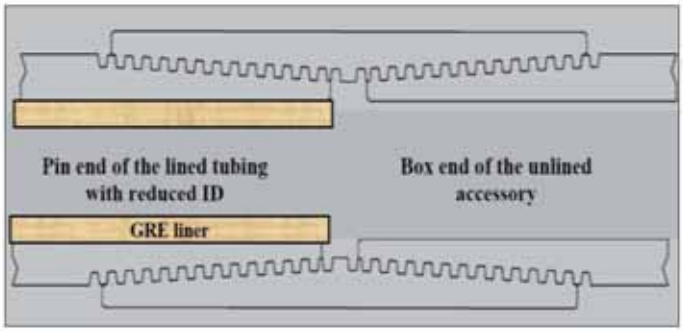

Fig. 3. Illustration of step change in ID when making up a lined pin to an unlined box of an accessory.

Fig. 4. AR for API completions (also referred as a packer AR).

would notice that to address the corrosion issue by going for CRA material for the tubing in a mechanically not so demanding condition, the connections need to be in premium as CRA tubing is rarely delivered in API connections. The same application can be served by a GRE lined API completion resulting in more than 50% cost savings on the completion. The GRE lining takes care of the corrosion issues and the API connections serve the mechanical need of these wells. For Quadrant 3, Table 2 can be revised to reflect the above concept as shown in Table 3.

Transition Between Lined Tubing and Unlined Accessories

The transition between the GRE lined tubing and unlined accessories is achieved by the combination of an adapter ring (AR) and CBR. The AR is used to crossover from unlined accessories to lined tubing with an API EUE 8 round/long thread and coupling (LTC)/ short thread and coupling (STC) or buttress thread and coupling (BTC) threads.

When making up a joint of GRE lined EUE tubing to an unlined accessory, such as a packer, on/off tool, gas lift mandrel, hanger, etc., the most important consideration is that a CBR must be compressed against the GRE lined tubing joint to protect the lined joint and the connection area from corrosion[4].

There are two possible combinations to connect the GRE lined tubing connection with the unlined tubing or completion components. Option 1, to make up a GRE lined tubing pin, mating into an unlined accessory coupling or box, or option 2, to make up an unlined pin mating into a GRE lined tubing box or coupling. When a GRE lined tubing pin mates into an unlined accessory box/coupling, a CBR and possibly an AR must be placed into the unlined accessory box.

Figure 3 presents the illustration of the step change in the ID when GRE lined tubing is made up to an unlined box of an accessory. Figure 4 is the schematic and the actual photo of the AR. The AR is a nitrile butadiene rubber beveled ring designed to help provide a shoulder with an ID consistent with the CBR ID. This provides full support for the compressed CBR. The AR should be used with a CBR in the case where the shoulder in the unlined box may not provide a full mating surface for the CBR. The AR design may vary depending on the configuration inside the box.

API GRE LINED COMPLETION	DESCRIPTION	ID	MATERIAL
	Tubing hanger 3 1/2" x 11" Box down - NU/EUE	2.992"	CRA
	Adapter ring	2.992"x 2.750"	GRE
	3-1/2" 9.3# EUE Pup - Pin Up x Pin Down.	2.750"	L 80 + GRE
	Duoline 20 lined 3-1/2" 9.3# joints	2.750"	L 80 + GRE
	Adapter ring	2.750" x 2.992"	GRE
	Expansion joint EUE Box x Pin	2.992"	CRA

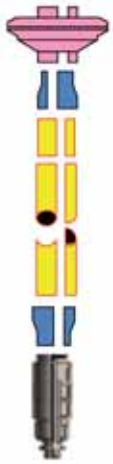

PREMIUM GRE LINED COMPLETION	DESCRIPTION	ID	MATERIAL
	Tubing hanger 3 1/2" x 11"; ABC Box down	2.990"	CRA
	ABC Pin x Crossover accessory Box for ABC down	2.990"x 2.75"	CRA
	Duoline 20 lined ABC Pup joint 3 1/2 9.2 ppf Pin x Pin	2.750"	L80 + GRE
	Duoline 20 lined Tubing joints 3 1/2 9.2 ppf ABC Box xPin	2.750"	L 80 + GRE
	Crossover accessory Box for ABC x ABC Pin	2.750"	CRA
	Expansion joint ABC Box x Pin	2.750"	CRA

Fig. 5. Crossovers configuration to connect GRE lined tubing to unlined accessories in API and premium connection (ABC is a generic name given to represent a premium connection) completed wells.

The smaller beveled end of the AR should be placed into the box first, the thicker end of the AR supports the CBR. The CBR is always compressed against the mating GRE lined tubing pin end flare.

For an unlined pin end to be made into a GRE lined tubing box, a CBR will be installed in the GRE lined tubing box as usual. Because the unlined pin ID is not consistent with the CBR ID, a "half" or "sh" CBR (different heights of the ring) needs to be installed in the box with an AR on top of the CBR to mate against the unlined pin. The unlined pin end must contact against the AR and CBR to protect the GRE lined tubing connection. It is recommended that the manufacturer authorized service technician is on location when GRE lined tubing is run in a well. Figure 5 shows the cross-over configuration from GRE lined tubing to unlined completion accessories for a new VAM connection. A profile is cut in the base of the box connection to seat the CBR, referred to as the Duoline accessory box profile.

Intervention History

During the evaluation period of the GRE lined tubing performance, from June 2002 to December 2008, the three wells were subjected to various types of well interventions such as wireline SBHP/T surveys and cased hole logs without any incidents. The intervention history of Well-2 is summarized in Table 4. No material interference has been encountered and there were no issues with the driftability.

Discussion on the Performance of GRE Lined Tubing

Industry evaluation criteria for plastic reinforced steel are to look for failures within the first 6 to 12 months. If the plastic had to fail because of any incompatibility issues from chemicals and water, it shall fail within

Date	Remarks
May 2002	Workover: Recompleted the well with permanent downhole monitoring system (PDHMS) and GRE lined 3.5" EUE tubing. Acidized the well with 8,500 gallons of 20% HCl acid. The PDHMS was tested with surface readout successfully.
June 2002	Placed the well on production after workover.
Sep 2002	Trap test, water cut: 0%.
Nov 2004	Annuli survey was conducted and showed zero psig.
Feb 2005	Trap test, water cut: 0%.
Apr 2005	Flow meter survey. Drifted the tubing to TD.
Aug 2006	Well went wet. Wireline work.
Oct 2006	Jack up separator tests.
Mar 2007	Trap test.
April 2007	Wireline work. Drift the well to TD. Increased water cut.
July 2007	Trap test.
Dec 2008	Drifted the well. Shut in the well and run log: MIT/PMIT logs for corrosion evaluation of the tubing.

Table 4. Summary of intervention history for Well #2

the first year. The three wells installed with the GRE lining had passed about 7 years of service with no evidences of corrosion or annulus pressure buildup and no driftability issues. The failure mode for GRE lined tubing is breakage of the fiberglass liner into pieces rather than wall thickness losses and if any failures had to occur, pieces of the GRE liner would have shown up in the choke. No such events were recorded in any of the three trial wells. The wells were acidized after completion in 2002 followed by multiple wireline runs and drifting to ensure that the well is free of any obstructions. The production rates were consistent with the expectations of the Operations teams.

The company had plans to run the trial test for more than 5 years to qualify the technology. The goal was to have a long-term evaluation to arrive at a more realistic "life cycle cost" estimate and compare it with alternate solutions. After successful qualification of the product for an extended period of time, it is relatively easy to prove and make a business case for the implementation of the GRE lined tubing as an alternative to other corrosion barrier solutions. The company plans to go for a large scale implementation, therefore a longer and more definitive evaluation was necessary. The company also saw the opportunity for the potential application of the product as a cost-effective alternative to chrome tubing. Notwithstanding the above observations, which were interpreted as inferences, the company decided to go further to do a detailed intrusive investigation on the GRE liner integrity inside the tubing.

Evaluation of the GRE Liner Integrity

The company considered three options to assess the condition of the GRE lining inside the tubing.

1. Run a downhole video camera.
2. Run a caliper log.
3. Pull out and inspect the tubing.

The downhole camera requires the presence of a clear fluid in the tubing string to provide pictures. It was considered to displace the tubing with clear water/brine, but it was ruled out because of multiple reasons, such as the need for unnecessarily killing the producing well and loss of production. The possibility of pulling out the tubing for investigation was also ruled out because of costly workover and loss of production. It was against common sense to lose revenue from a producing well just for tubing evaluation.

The company decided to log the well using a caliper Multifinger Imaging Tool (MIT), but getting the $1^{11}/_{16}$" outer diameter (OD) 24 finger MIT tool was a challenge in itself. There are not very many "small" tools available and there needs to be enough business volume for the logging companies to bring the tool in Saudi Arabia. The company tried to line up a few more jobs to justify the import of the tool in the country and the reason for delays in evaluation. About 2 years were lost because of delays in the commissioning of the caliper log into the well. Multiple attempts were made from 2007 until the end of 2008 to carry out the caliper log in Well-2, and finally it was run in December 2008.

In the meantime, the service provider of the GRE lining services continue to make the case with Saudi Aramco by presenting GRE lined tubing evaluation data from another regional oil company. Trials were carried out on the surface with tools from two service

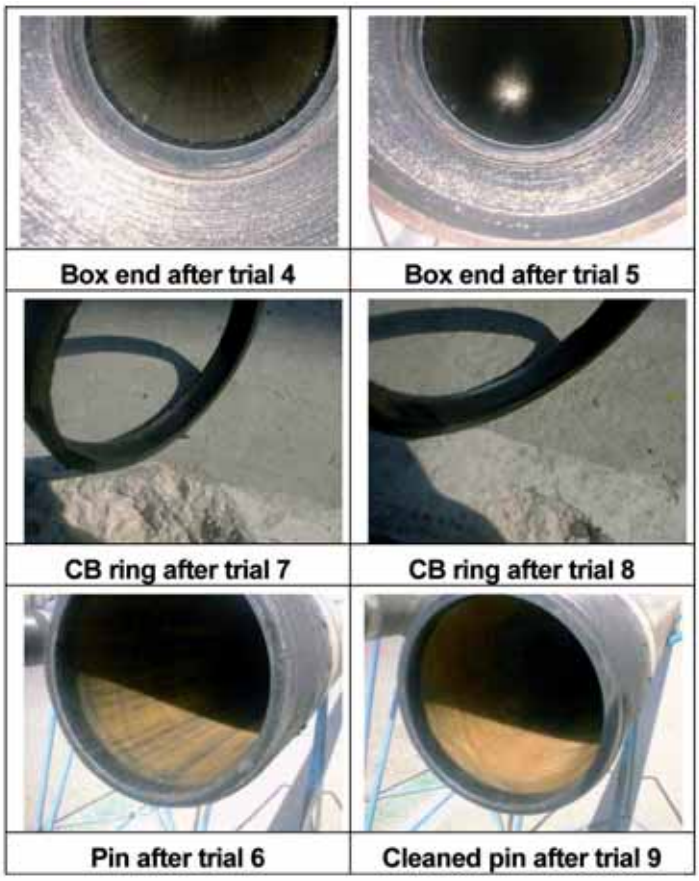

Fig. 6. Pictures showing condition of GRE lined tubing and CBR after multiple caliper runs.

companies. Service Company 1 applied a 2¾" 40 finger Sondex tool with a production roller centralizer. The oil company machine shop cut longitudinal sections of the tubing to allow close examination of the GRE lining, which showed no adverse effect on the lining material; in fact there were no evident marks on the ID of the GRE liner at all.

Service Company 2 applied a similar 2¾" 40 finger Sondex caliper tool with a motorized centralizer. Marks and scratches were observed on the surface of the GRE liner; however, they were not significant enough to affect the performance of the liner. The marks were not caused by the caliper finger itself but by the motorized centralizing system deployed with the caliper tool.

Based on the data from the above two trials, the recommendation was made to use non-motorized production roller centralizers whenever caliper runs are conducted on the GRE lining system. Pictures of lined tubing and corrosion barrier rings taken after the caliper runs are presented in Fig. 6.

The caliper log gives more meaningful results if the well has a base log. The well under consideration did not have a caliper log run at the time of installation but given that the well had been in service for about 7 years and the GRE lined tubing had a fixed ID of 2¾" with a maximum ovality of 0.01", the caliper log was expected to highlight it in any case, all changes in the ID of the GRE liner. It was also taken into consideration that after about 7 years, if the GRE lined tubing had maintained its wall thickness and smoothness the results could be compared with IPC tubing installed in the same well.

Experience with MIT Caliper Log

In December 2008, a 24 finger caliper log was run in Well-2 to check the condition of the tubing after about 7 years of service. The caliper tool allows three dimensional imaging and the calculation of rates of corrosion or scale deposition by collecting continuous signals from 24 spring loaded, hardened tip fingers, which push against the ID of the tubing with low force and provide an independent reading on the movement of each finger corresponding to the irregularities in the ID or the wall thickness. Data from each finger is recorded and plotted independently.

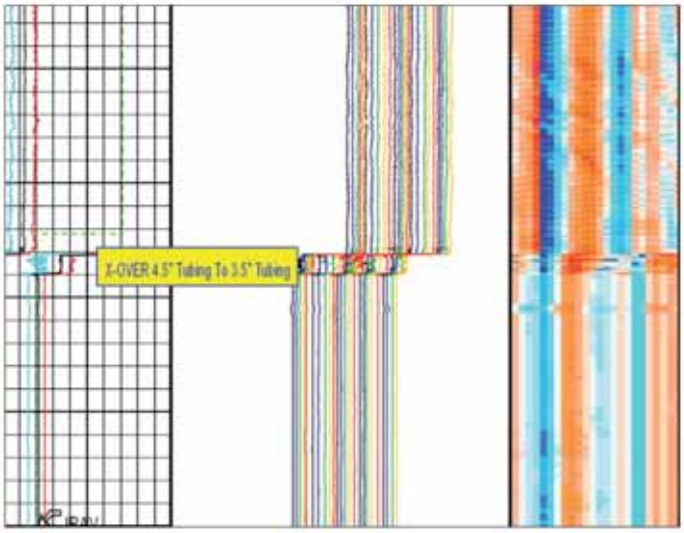

Fig. 7. Caliper readings across the crossover between 4½" IPC and 3½" GRE lined tubing.

The log recorded the interval from surface to tailpipe. At the time of the log, the wellhead temperature was 89 °F, log speed was up to 1,000 ft/hr; the logging cable tension was recorded up to 5,000 lbf through the system, which is again a test of the endurance of the GRE lined tubing to typical loads encountered during slick line runs. A detailed analysis of the MIT caliper log indicated that the fiberglass was in good condition with no internal pitting.

Caliper Log Interpretation

The liner is not guaranteed to be a perfect circle. During the cement pumping process in the narrow annulus between carbon steel tubing and the GRE liner, there is a possibility of ovality of up to 0.01" in the ID of the GRE lined tubing.

The caliper readings across the lined tubing do not exhibit any abrupt changes but exhibit wavy patterns, which represent the flowing diameter change and not missing or broken parts of the liner. The increase in the ID is an indication of the eroded or missing liner while the decrease in the ID is an indication of a scale or corrosion by product buildup. The caliper readings showed that there was neither wall loss nor scale/deposits buildup. The spikes in the caliper readings at about every 31 ft are the reading from the caliper fingers passing over the CBR and the flares installed at each connection. The consistent shape of the spikes shows that all CBRs and flares are intact after about 7 years of service with frequent interventions carried out in the well.

The caliper readings from the 4½" IPC tubing in the upper section of the well can be compared with the readings from the 3½" GRE lined tubing in Fig. 7. The caliper readings smoothened immediately after passing from the 4½" IPC tubing to the 3½" GRE lined tubing. There was a reduced disturbance on the caliper fingers providing clear evidence that the smooth surface of the GRE liner still remained intact. It is worth noting that the variation in the average, minimum and maximum radii readings is a lot less in the GRE liner compared to the IPC tubing.

Figure 8 is a snapshot of the interpreted caliper/corrosion monitoring log. The metal loss graph shows that the first 288 ft of the 4½" IPC tubing is in the red zone. Figure 9 is a zoomed out image of the same caliper log to present the comparison between the 3½" GRE lined tubing section, green color, (lowest or no wall loss) and the 4½" IPC tubing. The data between 550 ft and 650 ft is not available as the tool was reported to have a failure. The GRE lined 3½" tubing below the crossover shows no evidence of wall corrosion or erosion loss. Figure 10 shows the 24 finger MIT Sondex tool that was run for the evaluation.

Lessons Learned

1. The GRE lined API 8 round EUE tubing exhibited a greater resistance to corrosion than the premium IPC tubing over the 7 years of continuous service in production.
2. Caliper results showed that majority of the tubing remained intact with no wall losses and scale buildup

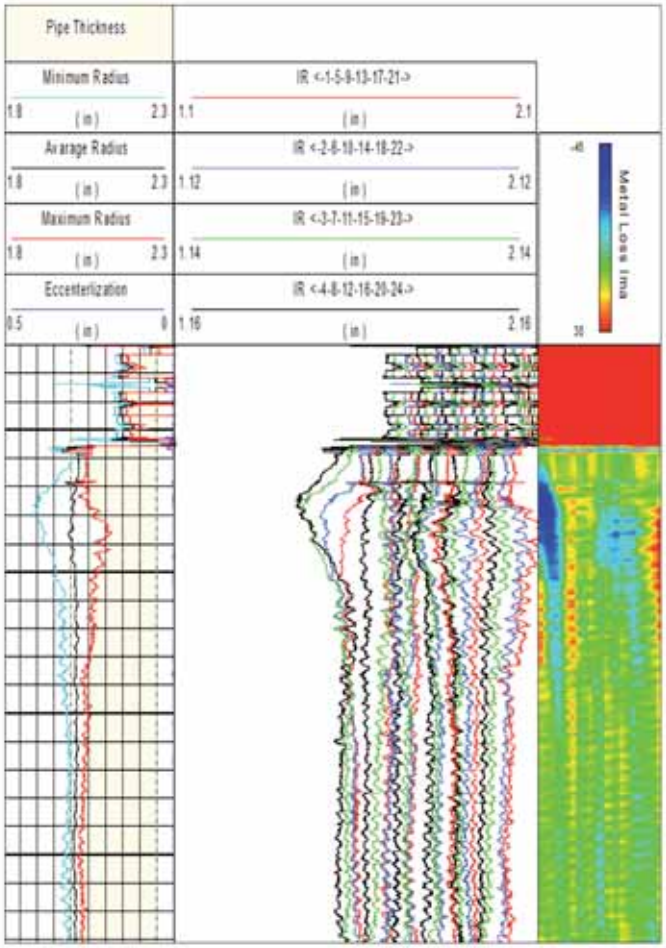

Fig. 8. 24 finger caliper, corrosion monitoring log across 4½" IPC tubing and GRE lined 3½" tubing.

as direct benefits of being inert to corrosive fluids and being smoother compared to carbon steel.

3. Repetitive interventions over the 7 year period and the satisfactory status of the tubing showed that the GRE lined tubing is tolerant to wireline intervention without compromising its integrity.

4. We could establish that 20% hydrochloric (HCl) acid pumped through the GRE tubing did not cause any appreciable damage to the ID and it is acceptable to bullhead 20% HCl acid through the GRE lined tubing.

5. It is advisable to run non-motorized production roller centralizers whenever caliper runs are conducted on the GRE lining system.

6. GRE lined API connection tubing can be a cost-effective alternative to CRA tubing with premium connections in low mechanical demand (lower depth and pressures, but with high corrosion potential) wells.

Benefits/Features of GRE Lined Tubulars

1. Extended well life and avoidance of frequent workover operations because of corrosion related problems.

2. Continuity of production/injection operations.

3. Positive business impact with less frequency of workover jobs and improved allocation of rigs and resources.

4. The connection area is better protected with GRE lined tubing compared to IPC tubing.

5. Within the allowed temperature limits, the application of this product in sour gas wells as an alternative to expensive chrome alloys that can offer substantial savings in completion costs.

Operational Considerations and Limitation of GRE Lined Technology

1. Reduction in the ID of the tubing and restrictions to run production logging tools. With GRE lined tubing the sizes of X-nipples need to be stepped down.

2. Hydrofluoric acid (commonly known as mud acid) cannot be pumped through the GRE lined tubing. It is recommended to use coiled tubing to spot the acid, if required.

3. The key limitation of this nonmetallic GRE lining

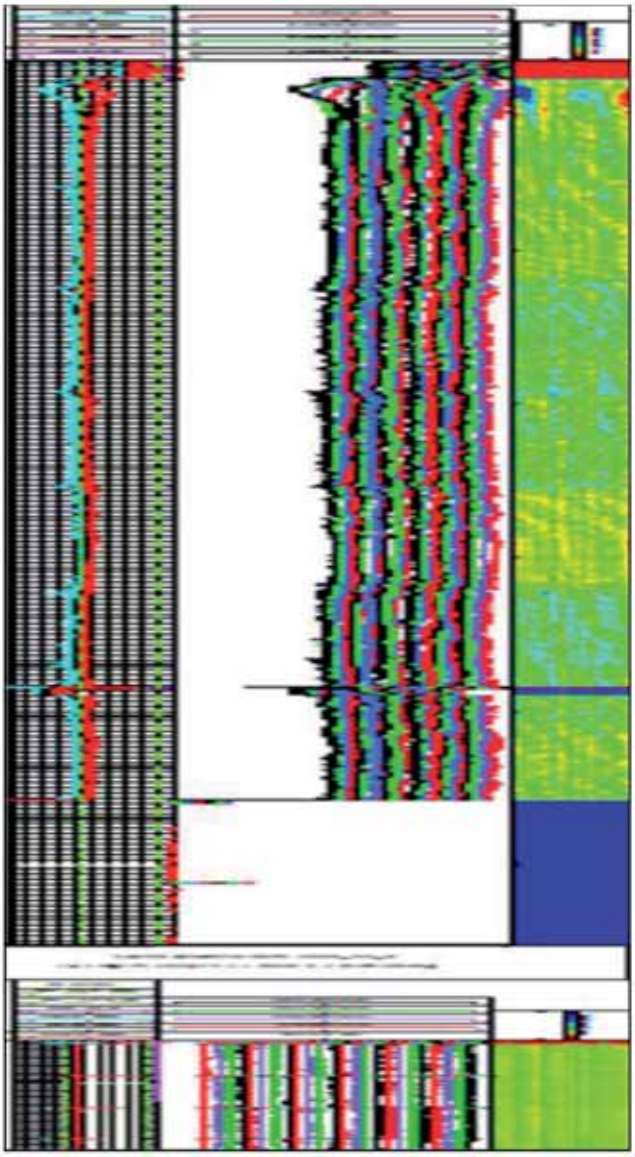

Fig. 9. CML (zoomed out).

technology is the maximum temperature limit of 130 °C (266 °F).

4. GRE lined tubing does not protect the tubing against scale formation from $BaSO_4$ and $SrSO_4$, however, there are successful case studies in the prevention of $CaSO_4$ and $CaCO_3$ and $Fe2CO_3$ scales, paraffin and asphaltene deposition.

5. GRE lining is not steel but it has better mechanical wear and resistance properties than plastic or epoxy coatings. The wireline operations require simple procedures and precautionary measures to get prolonged life.

Future Outlook

The product has been adopted for use in oil producers, power water injectors and water source wells. At the time of writing this article, more than 50 wells have been installed with GRE lining between 2008 and 2014. This excludes the three wells where the GRE lined flush joint tubing was installed with an electrical submersed pump in 2002; none of these wells have reported any failures.

Further product development is in progress by the manufacturers to develop a high temperature (up to 350 °F) product capable of handling sour gas conditions

Potential applications exist within Saudi Aramco to apply the product in flow lines and in sour gas production/injection wells (subject to further evaluation).

Fig. 10. 1 11/16" OD 24 finger MIT tool.

Acknowledgements

The authors wish to thank Saudi Aramco management for permission to publish this article. The authors also express their gratitude to the Drilling Technical Department and the Northern Area Production Department for their support in implementation and evaluation of the technology.

References

1. Kermani, B., Martin, J.W. and Esaklul, K.A.: "Materials Design Strategy: Effects of H2S/CO2 Corrosion on Material Selection," paper 06121, presented at the Corrosion NACE Exposition, San Diego, California, March 12-16, 2006.

2. Radhakrishnan, G., Bremner, M. and Simpson, J.: "Downhole Completion Considerations while Applying GRE Lining Barriers to Downhole Tubing for Corrosion Protection," paper 10126, presented at the 13th Middle East Corrosion Conference and Exhibition, Bahrain, February 14-17, 2010.

3. Pots, B.F.M., Kapusta, S.D., John, R.C., Simon Thomas, M.J.J., Rippon, I.J., Whitman, T.S., et al.: "Improvements on de Waard-Milliams Corrosion Prediction and Applications to Corrosion Management," paper 02235, presented at NACE Annual Corrosion Conference, Denver, Colorado, April 7-11, 2002.

4. Duoline Technologies Inc.: Best Practices for Duoline Tubular Goods, Rev. 16, July 2007.

Biographies

Dr. Qamar J. Sharif is a Petroleum Engineering Specialist with Saudi Aramco's Drilling and Workover (D&WO) Department. He has more than 30 years of diversified experience in the oil and gas industry, including academics. Qamar joined Saudi Aramco in 2005, working in the Drilling Engineering Department. During this period, his responsibilities included conducting trial tests for the application of new technologies and services in drilling operations, such as drilling with casing. Qamar has also conducted failure investigations of downhole tools and performed root causes analysis, making recommendations to establish new procedures to prevent reoccurrence, along with other technical and commercial studies, including analyzing drilling operations and making recommendations for performance improvement.

In 2012 he moved to the D&WO Training and Competency Development Division and developed a stuck pipe prevention course, specific to Saudi Aramco's needs and has been teaching the course.

Qamar has worked in drilling, workover and completion operations, research, business planning, operations management, technology development and implementation and competencies development.

His expertise is in the development of novel ideas and transforming them into robust and practical solutions. One example includes the development of innovative Multistring (Quad) Steam Injection Well Design for Aera Energy, Bakersfield, CA, which included a novel concept for a thermal packer and a ninefold increase in the length of oriented perforation per run.

Qamar has contributed to the professional development of individuals in the oil and gas industry as an instructor and a mentor, and currently teaches undergraduate and graduate courses in the Petroleum Engineering Department at King Fahd University of Petroleum and Minerals (KFUPM), Dhahran. He served as Curriculum Advisor for Well Construction, representing Saudi Aramco with PetroSkills.

Previously, Qamar worked with Shell International Exploration and Production for about 9 years at the Bellaire Technology Center, Houston, TX. He worked on multi-string steam injection well design in Bakersfield, CA, the development of expandable tubular technology for Enventure from initial surface tests to the first downhole application for the BAHA deep-water project in the Gulf of Mexico, and dual string completions in Nigeria. Qamar also worked with Shell Deepwater Services as senior drilling engineer.

He started his career on a steam-powered rig in 1980 with Pakistan Oilfields Ltd. and worked in drilling/workover operations for about 10 years, which included about 7 years on jack-up rigs, offshore Abu Dhabi with the National Drilling Company, working as assistant driller, driller and tool pusher.

Qamar received his B.S. degree in Mining Engineering from the University of Engineering and Technology, Lahore, Pakistan, and his M.S. and Ph.D. degrees, both in Petroleum Engineering, from Texas A&M University, College Station, TX.

He is a member of the Society of Petroleum Engineers (SPE) and is the author of more than 10 papers.

Qamar is the recipient of the Shell President Award for premier performance for 1997.

Dr. Omar J. Esmail retired from Saudi Aramco after working for the company for more than 38 years. He worked in the areas of reservoir, production, workover and drilling engineering and held various supervisory and managerial positions in both of these departments prior to retiring in 2011.

In 2009 Omar joined the Upstream Professional Development Career (UPDC) as a subject matter expert where he wrote drilling engineering courses for training young Saudi Aramco drilling engineers. He continues to teach drilling engineering courses in the UPDC as a Consultant.

He received his B.S. degree in Chemical Engineering and his M.S. degree in Petroleum Engineering, both

from Louisiana State University, Baton Rouge, LA, and then received his Ph.D. degree in Petroleum Engineering from the University of Texas at Austin, Austin, TX.

Gokul Radhakrishnan is a Process Engineer by training with 20 years of work experience in various upstream domains, such as control systems, surface facilities, multiphase flow metering, Oil Country Tubular Goods (OCTG) material selection and nonmetallics. He works for MaxTube

Limited as Regional Manager — Middle East and North Africa and Southeast Asia — promoting his company's fiberglass (GRE) lining services for downhole tubing for corrosion protection. Gokul's expertise involves making recommendations to his customers when to use nonmetallics based on technical suitability and commercial attractiveness, along with helping to modify completions to suit the GRE lining. He has been actively involved in the testing of the GRE liners for Saudi Aramco for sweet and sour gas production applications.

Gokul is an active member of the Society of Petroleum Engineers (SPE) and the National Association of Corrosion Engineers (NACE) and has coauthored several papers on multiphase metering and GRE lined completions for production and injection applications.

He received his B.Eng. degree (with honors) in chemical Engineering from Birla Institute of Technology and Science, Pilani, Rajasthan, India, and his Post- Graduate Diploma in International Trade, from the Indian Institute of Foreign Trade, Mehruli, New Delhi, India.

John Simpson is the General Manager of MaxTube, which provides fiberglass (GRE) lined completions for corrosion protection in oil/gas producers and water injection well systems. He has over 25 years of experience in upstream oil and gas commercial operations, with extensive experience

in drilling and completion operations as well as pressure control and drill through equipment. John has been a resident in the Middle East since 1997 and has wide exposure to drilling and completion practices throughout the Arabian Gulf, Middle East and North Africa and Asian oil fields. He has also been actively involved in the testing of the GRE liners for Saudi Aramco for sweet and sour gas production applications.

John has coauthored several papers for both the National Association of Corrosion Engineers (NACE) and Society of Petroleum Engineers (SPE) on GRE lined completions.

He received his B.S. degree in Chemistry from the University of Aberdeen, Aberdeen, Scotland, U.K.

Martin Bremner has been the Operations Director of MaxTube since 2006 and also previously served as Technical Sales Support Manager, Quality Manager and Operations Manager. He has been with MaxTube since 2002. Martin has a background in Oil Country Tubular Goods (OCTG) inspection and quality assurance.

He has coauthored several papers for both the National Association of Corrosion Engineers (NACE) and Society of Petroleum Engineers (SPE) on GRE lined completions and has been involved in the design and delivery of GRE lining systems for a wide range of premium OCTG connections.

Martin received his MBA degree in Oil and Gas Management from the Robert Gordon's University School of Business, Aberdeen, Scotland, U.K.

Exits from the Hydrocarbon Highway

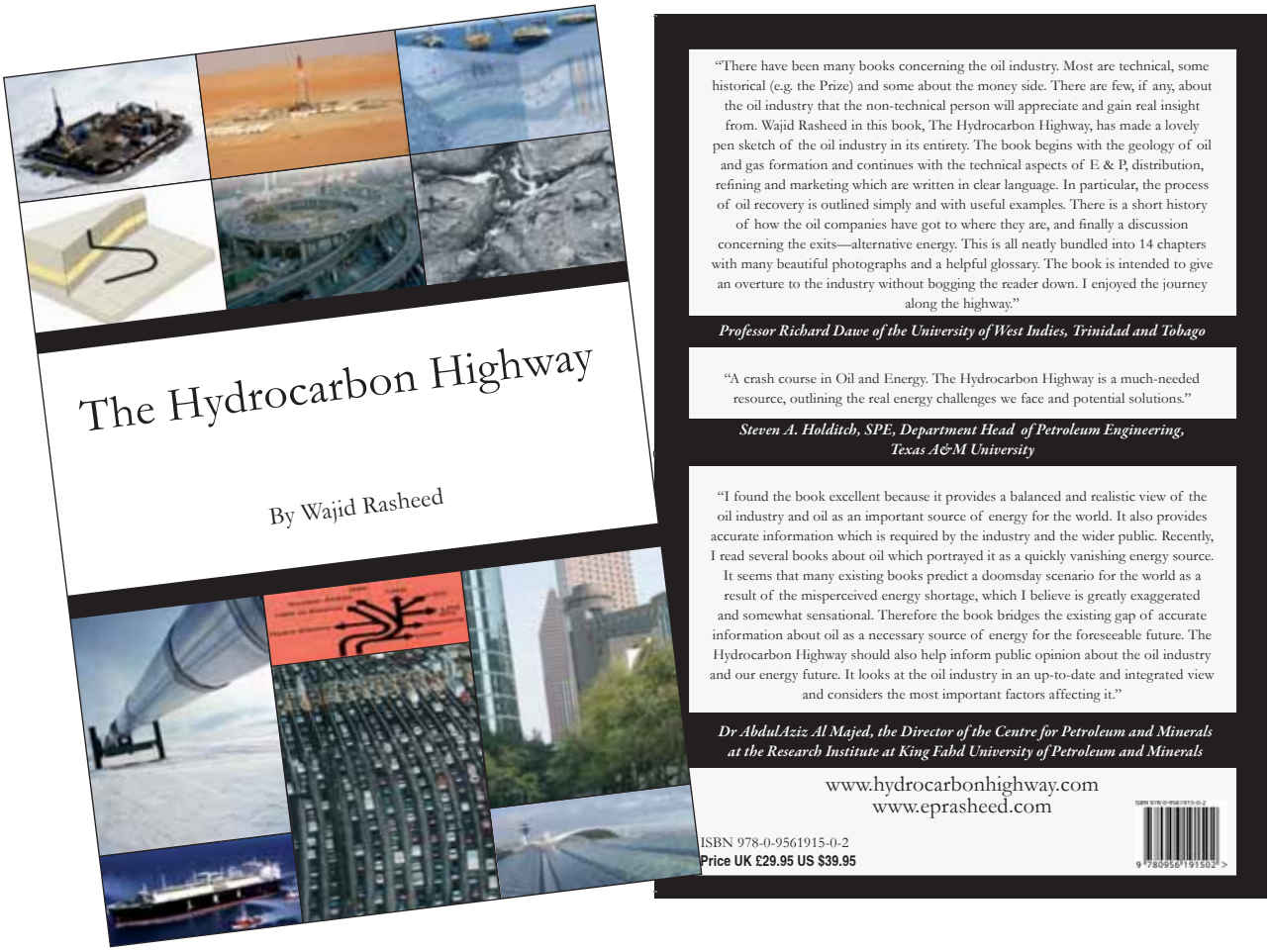

'Sometimes the best exit is the way we came in.'

Wajid Rasheed

Picture this: primeval man struggling to move a big kill or a great log. Carcasses of meat were no doubt hard to drag, but logs could be rolled and the invention of the wheel was not far off. Fast forward to the 21st century and witness the evolution of the wheel which is now entirely mechanised, powered by the internal combustion engine and fueled by petroleum. While petroleum is not a 'perfect' fuel (it is finite and pollutes), the high density energy that is packed into every litre and the convenience with which it can be moved make it hard to beat. That is why it is not going away. Together, this triple combo – wheel, engine and petroleum – ranks

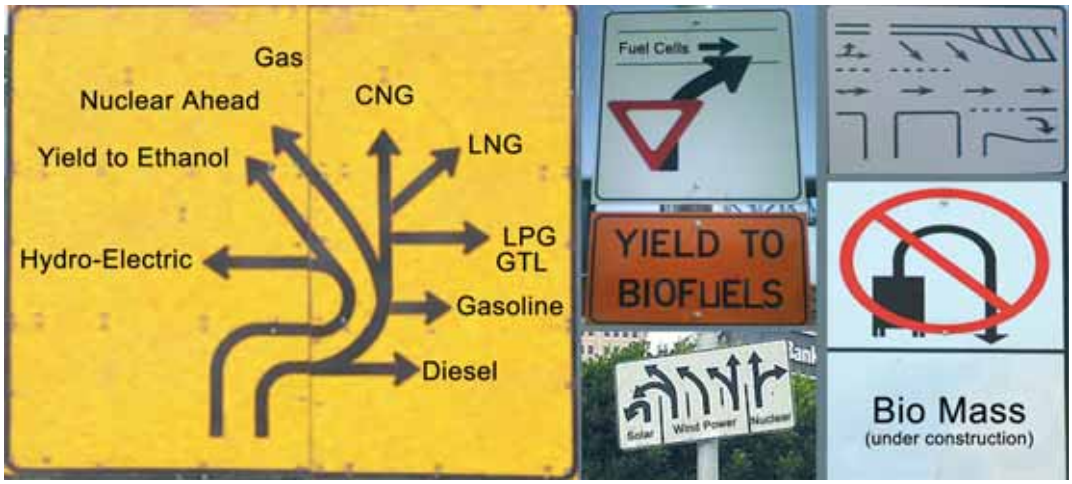

Our Energy Future Images 1- Plenty of Signs Beckon But Where Do They Lead?

among mankind's greatest inventions and has rolled-out mankind's greatest infrastructure endeavour, the Hydrocarbon Highway.

Our route along the Hydrocarbon Highway has shown that peak oil is not a physical shortage; there is plenty of untapped and unmapped oil. Moreover, technology is continually improving recovery.Consequently, peak oil is more of a psychological shortage. Our route has taken us behind the 'Oil Curtain' revealing the causes and effects of oil nationalism. We have seen how valuable oil leases are acquired, developed and how 'Extreme EP' and intelligent wells are the future of production. Not least, we have considered renewable energy sources against the backdrop of carbon emissions and climate change. Before we reach our final destination, 'beyond petroleum', we have to define those scenarios and 'exits' to the highway where oil and gas can be practically replaced.

Plenty of signs jostle for our attention and some seem easy to take – do nothing, business as usual. Others require complex questions to be considered: should more gas infrastructure be developed?; where should we build nuclear plants?; where should we dispose of nuclear waste?; what will compensate for shortfalls in renewable power?; how should we store electricity effectively?; and, are biofuels causing food poverty? Tackling such difficult questions provides some insight into why there is so much dependence on hydrocarbons. We need to identify exits that are genuine and not those that just detour back to the hydrocarbon highway. This means fully thinking through where energy is supplied from and its end-use consumption (see Our Energy Future Images 1, above).

In order to move beyond petroleum, we need to understand that there are no easy exits to hydrocarbon dependence; there is no silver bullet. Many so-called exits are still early prototypes 'under construction' requiring extensive research and development, political will, investment and time. It will take at least a generation before they become widely used. Still, each exit is applicable in certain scenarios only. Not all countries wish to build or handle spent nuclear waste. Cold temperate climates do not lend themselves to solar power and wind power may not always be consistent. Not all countries can grow biofuels. The pivotal point is that no single energy source fits all needs.

All energy sources suffer from limitations related to fit-for-purpose technicalities, start-up costs, output efficiency or societal trade-offs (see Our Energy Future Images 2). Any practical future energy scenario must include each and every one of these energy sources. Consequently, the answer lies in researching all options. That means experimenting and developing all

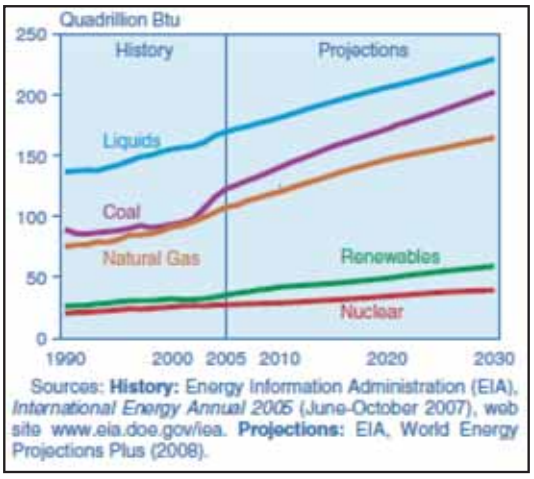

Figure 2 - World Energy Demand and Supply Use By Fuel Type 1990-2030 (Source US EIA)

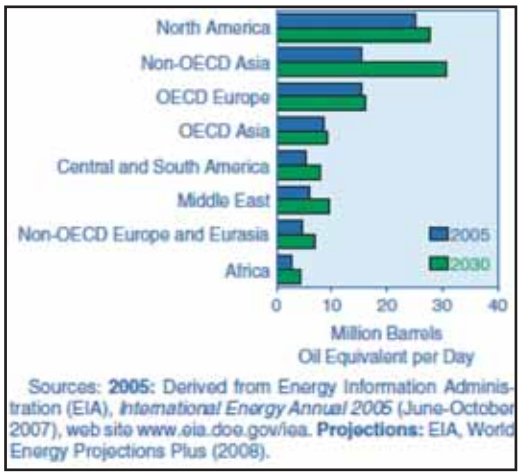

Figure 3 - World Liquids Consumption by Region 2005-2030 (Source US EIA)

applications until we find what works. The bottom line is that the Hydrocarbon Highway just got longer.

Gas Is the 'New' Oil

From all perspectives, gas emerges as one of the best potential exits from the Hydrocarbon Highway. If gas is a hydrocarbon though, how can it be an exit? Isn't it just the same as oil being a finite fossil fuel? Gas is the best choice that we have as a bridge to the truly 'renewable energy' scenario as it can be man-made or naturally produced and has low carbon emissions when burnt. The role of gas becomes clear in the energy models from the present period to the year 2030 which show that gas re-directs and eases off considerable demand for a broad number of oil applications[1]. The foundations for a 'gas' future have already been built using a broad set of advanced gas[2] technologies. Exemplifying this are Liquefied Natural Gas (LNG) which mobilises and commercialises stranded reserves. Additional examples are Compressed Natural Gas (CNG) and Liquefied Petroleum Gas (LPG) which provides fuel for the transport and power-generation sectors through to Gas to Liquids (GTL) technology which offers high quality gasoline fuel but at a high cost. Capping it all is renewable methane or man-made 'bio-gas' which is biologically produced. Gas is not a panacea though; it has limitations too.

So how much of a choice does gas or any other energy source really provide? That depends on whether the fuel can actually replace oil and how well it fits into future energy scenarios. In a major oil application such as aviation fuel, for example, gas in any form cannot replace oil due to engine design. Further complications exist as gas is not as easily transported as oil. It needs a specialised infrastructure to be developed which may be cost-effective at a high oil price but not at a low one (see Figure 1).

The reason for considering all possible energy sources, and evaluating their strengths and weaknesses objectively, is to create a logic-based demand and supply equation for oil – one that qualifies, future energy sources so that replacements can be identified.

By asking whether oil can be replaced and whether the resulting carbon emissions are lower than those of oil, we can see just how far each energy source can really take us. Once they pass this qualification stage, they can then be fitted into future energy trends allowing us to glimpse the future.

Summary: The Masses

Most of today's hydrocarbon dependence can theoretically be 'phased-out' over the long term with renewable resources theoretically 'phased in' by 2050. This cannot happen in the short or medium term because replacements for oil do not offer straight oil swaps in

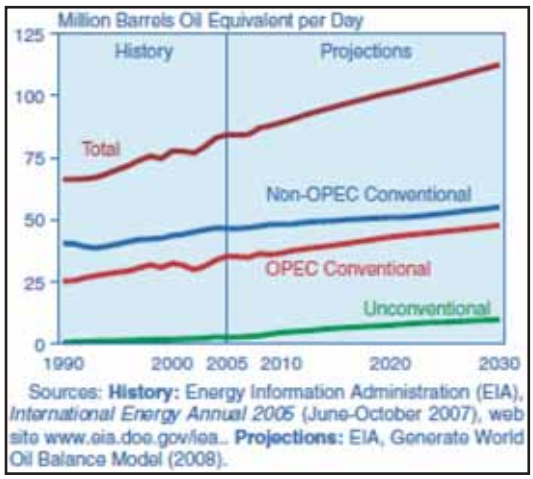

Figure 4 - World Liquids Production 1990-2030 (Source US EIA)

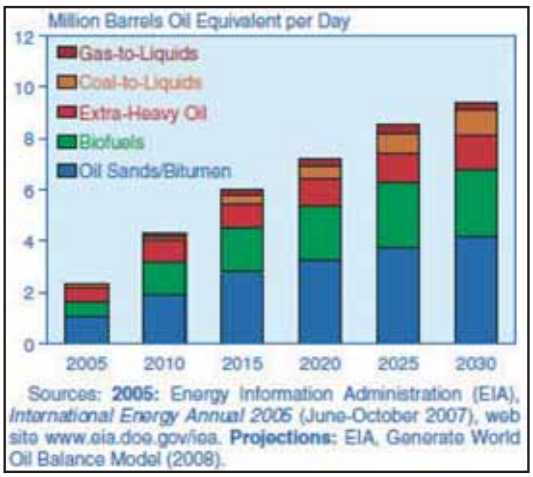

Figure 5 - World Production of Unconventional Liquids 2005-2030 (Source US EIA)

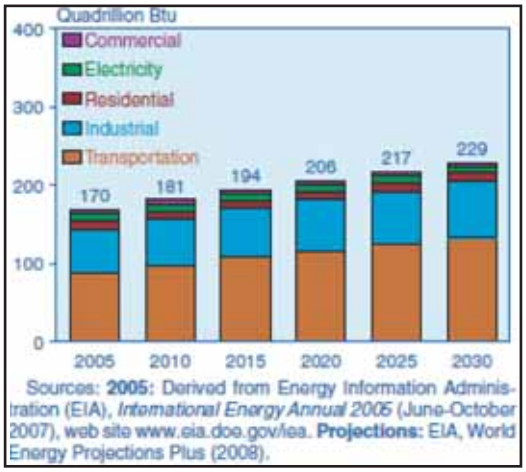

Figure 6 - World Liquids Consumption by Sector 2005-2030 (Source US EIA)

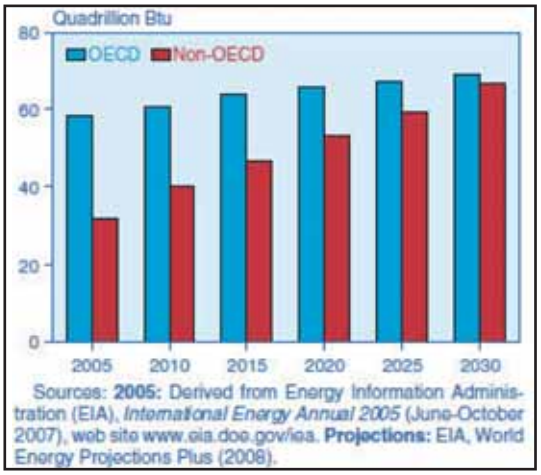

Figure 7 - Transportation Liquids Consumption 2005-2030 (Source US EIA)

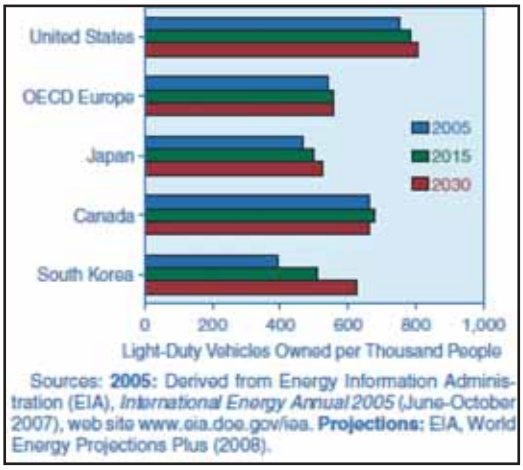

Figure 8 - Motor Vehicle Ownership in OECD Countries 2005, 2015 and 2030 (Source US EIA)

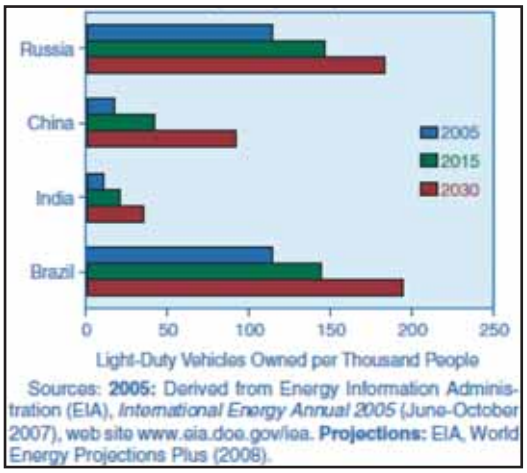

Figure 9 - Motor Vehicle Ownership in Non-OECD Countries 2005, 2015 and 2030 (Source US EIA)

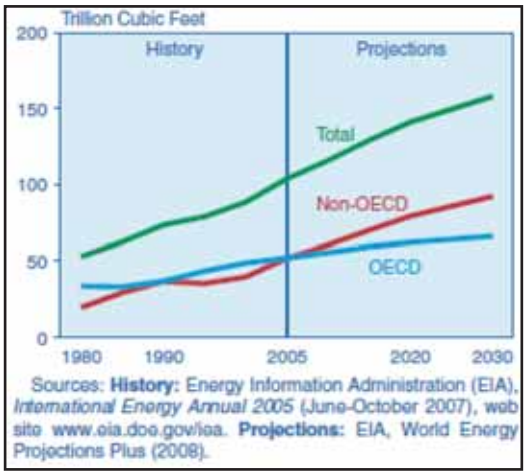

Figure 10 - World Natural Gas Consumption 1980-2030 (Source US EIA)

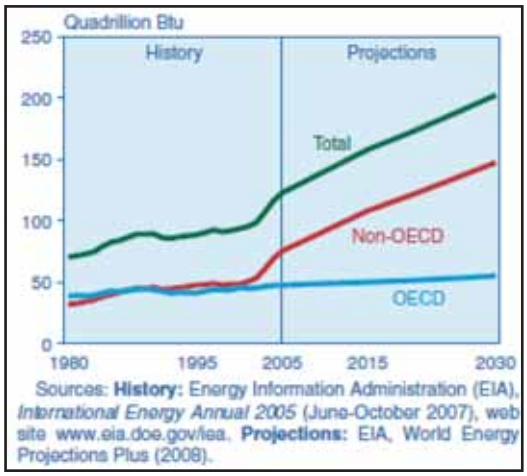

Figure 11 - World Coal Consumption (Source US EIA)

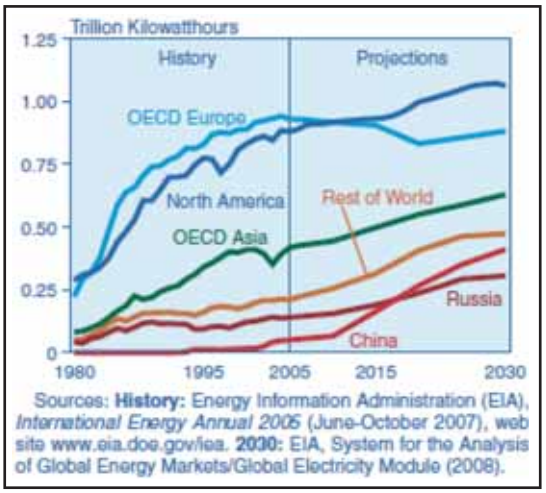

Figure 12 - Nuclear Power Generation 1980-2030 (Source US EIA)

mass; they are only usable in minute niches contributing to less than 5% of total oil energy demand worldwide. In contrast, 90% of oil and natural gas consumption is concentrated in trillions of transactions[3]. This vast consumption is most visibly spread worldwide among fleets of cars, planes, trains and specialised machinery and equipment.

In order to appreciate the vast scale involved, imagine reconfiguring every gasoline station in your home town or city, in the state itself, the country, the continent and the world. Then think about the network of distribution and storage behind the retail outlets. That would represent half the equation – supply side only. The consumption side consisting of the engines that power the world's fleet of cars, trucks and buses would need to be reconfigured too. Imagine doing the same for aviation, maritime and rail transport. There is demand in other components that would need to be considered too. Imagine reconfiguring existing power generation and industrial processes. The mass automotive and aviation products and mass processes such as power-generation plants and petrochemical feedstock are configured for oil and natural gas usage; they are extremely difficult to change. In the short run, not much changes because of the demand inelasticity; however, in the medium term, a growing number of gas-based technologies, as well as growing volumes of ethanol and biodiesel can replace oil in mass products and mass processes*. Not only does this strengthen investment in the infrastructure and usage of gas, ethanol and biodiesel but this also acts as a safety valve to dampen the demand for oil, redirect the excess demand from oil to gas and ultimately to the development of renewable resources.

> The mass automotive and aviation products and mass processes such as power-generation plants and petrochemical feedstock are configured for oil and natural gas usage; they are extremely difficult to change.

This allows the next generation of new mass products and mass processes to be designed using gas, GTL, biodiesel, ethanol or co-generation while allowing the existing infrastructure to be reconfigured. In the long run, this acts as an exit as greater oil and gas demand elasticity is achieved overall [4].

Energy Consumption Models

Principally developed by governments, energy companies and universities, energy models seek to map out trends in future energy consumption. Many variants exist, but essentially models are geared to low, medium and high levels of population, economic and demand growth. Salient trends are identified and drawn up as scenarios allowing organisations to better handle potential future risk and opportunity. Corporate models are generally kept confidential due to their commercial nature, while certain state and academic models are publicly available[5].

US EIA/IEO Reference Case to 2030

For our purposes, the US Energy Information Administration (EIA) or International Energy Outlook (IEO) reference case was selected as a global model for future energy consumption*. Considered by the US EIA to be the 'business as usual' future scenario, the IEO2008 reference case estimates world energy demand and supply to the period ending 2030. It attributes principal energy supply from oil, gas, coal, nuclear and hydroelectric sources and separates the consumption of energy into the categories of transport, industrial, residential and commercial usage. Total global energy demand is estimated to increase by 50% from 462 quadrillion Btu to 695 quadrillion Btu in 2030 (see Figure 2). This is mostly driven by sustained consumer demand in the Organisation for Economic Co-operation and Development (OECD) and industrial growth in Brazil, Russia, India and China (the 'BRIC's) (see Figure

> To 2015, demand is concentrated most heavily in Western countries such as the US and UK which have high numbers of vehicles per capita and respectively the largest worldwide fleets and numbers of private, commercial and industrial vehicles.

3). World Gross Domestic Product (GDP) and primary energy consumption also grows more rapidly in the first half than in the second half of the projections, reflecting a gradual slowdown of economic growth in non-OECD Asia. The model envisages sustained high per capita energy consumption in western countries and growth in consumption in certain non-OECD countries such as Asia, China and India. This reflects the trend that western populations continue to grow and consume a disproportionate amount of energy as compared with the rest of the world[6,7].

Values for the principal sources of energy demand and supply have been plotted for convenience (see Figure 2 World Energy Demand). In the case of oil demand growth, this is predicted to increase from 83.6 million barrels per day (MMbbl/d) in 2005 to 95.7 MMbbl/d in 2015 and 112.5 MMbbl/d in 2030. At first sight, when one looks at these figures, it is hard to imagine 16 MMbbl/d coming onto the market. When one considers the new frontiers of extreme E & P and mature fields, however, the figure seems plausible[8].

To meet world liquids demand in the IEO2008 reference case, total liquids supply in 2030 is projected to be 28.2 MMbbl/d higher than the 2005 level of 83.6 MMbbl/d. The reference case assumes that the Organisation of the Petroleum Exporting Countries (OPEC) maintain its market share of world liquids supply, and that OPEC member countries invest in additional production capacity for conventional oil leading to approximately 40% of total global liquids production throughout the projection. Increasing volumes of conventional liquids (crude oil and lease condensate, natural gas plant liquids and refinery gain) from OPEC contribute 12.4 MMbbl/d to the total increase in world liquids production, and conventional liquids supplies from non-OPEC countries add another 8.6 MMbbl/d (see Figure 4 World Liquids Production) . Unconventional resources (including oil sands, extra heavy oil, biofuels, coal-to-liquids and GTLs [see Figure 5 World Production of Unconventional Liquids]) from both OPEC and non-OPEC sources are expected to become increasingly competitive as indicated in the reference case.

Energy Source	MMBtu/bbl	Energy Source	MMBtu/bbl
Crude Oil	5.800	Natural Gasoline	4.620
Natural Gas Plant Liquids	3.735	Pentanes Plus	4.620
Asphalt	6.636	Petrochemical Feedstocks:	
Aviation Gasoline	5.048	Naphtha < 401° F	5.248
Butane	4.326	Other oils >= 401° F	5.825
Butane-Propane (60/40) Mixture	4.130	Still Gas	6.000
Distillate Fuel Oil	5.825	Petroleum Coke	6.024
Ethane	3.082	Plant Condensate	5.418
Ethane-Propane (70/30) Mixture	3.308	Propane	3.836
Isobutane	3.974	Residual Fuel Oil	6.287
Jet Fuel, Kerosene-type	5.670	Road Oil	6.636
Jet Fuel, Naphtha-type	5.355	Special Naphthas	5.248
Kerosene	5.670	Still Gas	6.000
Lubricants	6.065	Unfinished Oils	5.825
Motor Gasoline - Conventional	5.253	Unfractionated Stream	5.418
Motor Gasoline - Oxygenated or Reformulated	5.150	Waxes	5.537
Motor Gasoline - Fuel Ethanol	3.539	Miscellaneous	5.796
Source: U.S. Department of Energy, Energy Information Administration (2001)			

Table 1 - Approximate Heat Content of Petroleum Products Million Btu (MMBtu) per Barrel

The following serves as a breakdown of the categories of demand and supply.

Transportation

To the year 2030, transportation emerges as the strongest component of future oil and gas demand contributing 74% of all increased future oil demand (see Figure 6 Consumption by Sector). To 2015, demand is concentrated most heavily in Western countries such as the US and UK which have high numbers of vehicles per capita and respectively the largest worldwide fleets and numbers of private, commercial and industrial vehicles. After 2015, transport demand in the BRICs and eastern countries is of a magnitude higher with the Indian and Chinese numbers of vehicles per capita showing only strong growth in demand for transportation fuel (see Figures 7, 8 and 9)[9]. Energy consumption in transportation increases from 93.2 quadrillion Btu in the present period to 135.4 quadrillion btu in 2030. In barrel terms, the increase results in the following consumptions: North America (28 MMbbl/d); China and India combined (31 MMbbl/d); and, Europe (15 MMbl/d). In this model, oil is one of the most important fuels for transportation because there are few alternatives that can compete widely with liquid fuels. With world oil prices remaining relatively high through 2030, the increasing cost-competitiveness of non-liquid fuels reduces many stationary uses of liquids (that is, for electric power generation and for end uses in the industrial and building sectors). These replacements based on alternative energy sources, increase the transportation share of liquids consumption. Gas consumption for transportation purposes increases from 1 quadrillion Btu from 2005 to 1.6 quadrillion Btu in 2030.

Industrial

The second largest demand component is created by industry which increases from 57 quadrillion Btu in 2007 to 72% quadrillion Btu in 2030 (see Figure 6 World Liquids Consumption by Sector). Industrial demand is concentrated in the eastern hemisphere in countries such as China and India. This reflects the cost-driven migration of industrial and manufacturing processes to China and India from western hemisphere

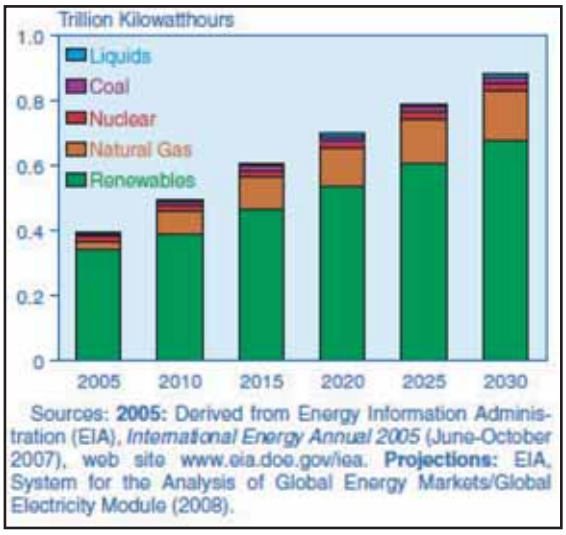

Figure 13 - Electricity Generation in Brazil by Fuel (Source US EIA)

countries. The industrial sector including manufacturing, agriculture, mining, and construction accounts for a 39% share of hydrocarbon demand comprising mainly petrochemical feedstock[10]. Industrial consumption of gas increases from 45.2 quadrillion Btu in 2005 to 70.2 quadrillion Btu in 2030.

Commercial

The commercial sector – often referred to as the services sector or the institutional sector – consists of businesses, institutions, and organisations that provide intangible services, as opposed to those in manufacturing or agriculture. Demand for commercial energy increases from the present 5.1 quadrillion Btu to 5.3 quadrillion Btu in 2030. Demand for commercial energy grows more acutely in OECD countries rather than India and China. This is interesting as it appears that the latent demand in India and China do not materialise as strongly as widely reported by other energy models with growth only averaging 2.2% per annum[10]. Commercial consumption of gas increases from 7.3 quadrillion Btu to 9.6 quadrillion Btu.

Residential

Residential demand for energy increases from the current 10.4 quadrillion Btu to 11.1 quadrillion Btu in 2030. Demand for energy consumption grows most in non-OECD countries in the residential sector at an average of 2.7%. Residential gas consumption increases from 19.1 quadrillion Btu to 25.2 quadrillion Btu[11].

Gas

Consumption of natural gas worldwide almost doubles from 104 trillion cubic feet (tcf) in 2005 to 158 tcf in 2030 as per the IEO2008 reference case (see Figure 10). Although natural gas is expected to be an important fuel source in the electric power and industrial sectors, the annual growth rate for natural gas consumption is slightly lower than the projected growth rate for coal consumption. Higher world oil prices in the IEO2008 increase the demand for and price of natural gas, making coal a more economical fuel source in the projections. Industry accounts for the largest component of natural gas demand worldwide, generating 52% of the total growth in natural gas use in IEO projections. Natural gas also provides the power generation sector with increasing supply and accounts for 39% of the increase in global natural gas demand to 2030[12].

Coal

In the IEO2008 reference case, world coal consumption increases by 65 percent over the projection period, from 122.5 quadrillion Btu in 2005 to 202.2 quadrillion Btu in 2030 (see Figure 11). The increase in coal consumption averages 2.6 percent per year from 2005 to 2015, then slows to an average of 1.7 percent per year from 2015 to 2030[13].

> To 2015, demand is concentrated most heavily in Western countries such as the US and UK which have high numbers of vehicles per capita and respectively the largest worldwide fleets and numbers of private, commercial and industrial vehicles.

Nuclear Power

Electricity generation from nuclear power is projected to increase from about 2.6 trillion kilowatthours in 2005 to 3.8 trillion kilowatthours in 2030, (see Figure 12). This is based on rising fossil fuel prices, concerns regarding energy security and greenhouse gas emissions which tend to support new and existing nuclear power generation[14].

Renewables

Renewables including hydroelectric power (and other generating capacities fueled by renewable energy resources) are projected to increase by 352 billion kilowatt hours from 2007 to 728 billion kilowatt hours in 2030, at an average annual rate of 3.2%[15].

Hydrocarbon Demand Supply Equation

The IEO reference case is a very useful map to understand the direction of future energy. It still requires systematic treatment and evaluation of specific renewable energy sources as well as oil-price dynamics which are non-linear. Its approach, however, is a very good basis from which to consider global energy markets, oil and gas segments and how mass transactions fit in the overall picture. The oil and gas demand supply equation serves this purpose by outlining the six major oil and gas applications and the twenty-one uses (mass products/mass processes) that result in mass transactions. This serves to pinpoint exit scenarios where oil and gas demand can be phased using an energy resource that is renewable. The value of the exercise lies in qualifying what is technically replaceable given an economic framework, i.e. high oil prices or government subsidies rather than calculating the economic or market value of each replacement.

What emerges from the analysis is an extremely broad and complex set of oil and gas applications and ultimate uses or transactions. These range from transportation, to power generation, heating, petrochemicals, lubricants and surfacing. It was necessary to detail each specific end usage in order to determine whether oil and gas were replaceable commodities.

This is a key step in achieving higher elasticity of demand by satisfying end usage with replacement options. We assume that the production of petroleum will peak and then plateau, but that the broad range of petroleum applications that we see today will narrow down to a few that cannot be substituted by gas or other renewables.

Today, the only oil application that cannot be substituted

Figure 14 - Brazilian Options at the Pump 2009 shows Ethanol, Gasoline, Diesel and Natural Gas (EPRasheed)

given the necessary economic framework, i.e. high oil prices or government subsidies, is aviation fuel which generates 5.7 million Btu per barrel compared to ethanol which generates 3.5 million Btu. Aviation fuel then takes up approximately 0.61 times the volume of jet kero or it has 0.61 of the Btu[17].

Firstly, there are six major categories of petroleum applications which are split into a further 21 sub-categories all of which have been kept as broad as possible, i.e. derivatives are split into Alkanes, Alkenes and Arenes which cover demand for derivatives such as plastics and pharmaceuticals.

Secondly, successfully substituting oil and gas depends on several unpredictable factors. These include global economic stability in order to maintain oil prices above certain levels. Each alternative energy source has a corresponding oil price threshold at which it becomes profitable – or not – to pursue R & D. That threshold is not simple to calculate; for example, in the case of bioethanol, it may be considered that an oil price of US $40 to US $60 per barrel makes ethanol production viable, but this does not take into consideration government intervention in the form of subsidies or incentives that are hidden away from ethanol or biofuel production. It is worth remembering that all biofuels are subject to seasonal conditions required for harvest. Unpredictable events such as inclement weather, hurricanes or market speculation can distort the acceptance curve of renewables, accelerating or delaying the overall uptake[18].

Thirdly, on a macro level there are no consensual figures on global consumption versus production data from major authorities. Much credit should go to BP for putting the statistical review together. Regarding country and global data, the issue is that ultimately all collating organisations must rely on country export data as they have no way of verifying that data. The statistics therefore incorporate OPEC/OGJ (Oil and Gas Journal)/non-OPEC data and so on. The approach has been to use regional or local data sources wherever possible.

Further discrepancies between consumption and production data exist from the same source; for example, the BP statistical review 2008 places global oil production at 81.53 MMbbl/d and consumption

> The US EIA sees real resource limits to vegetable seed oil conversion to diesel, however, gasification of biomass and then conversion to diesel should have much more promise in terms of available volumes.

at 85.22 MMbbl/d. According to the BP statistical review, there is a deficit of oil and a surplus of gas. The standard and fundamentally sound explanation for this discrepancy is explained by fuel additives, refinery gains, measurement and rounding up differences, inventories, etc. The discrepancy may also be partially explained due to illicit production not reported at the well-head, GTL production of liquids, gasification and liquids from coal[19]. Another challenge with the data is conversion between physical volumes and oil equivalent volumes. The US EIA includes volume adjustments to the production side so that production and consumption balance. The implicit assumption is that stocks don't change.

Beyond Petroleum

As we look through the demand/supply equation it is apparent that it will take many years to provide other choices beyond petroleum. Indeed, oil may not be completely replaced; rather, other choices will be offered that have their own set of costs, trade-offs and limitations. Natural gas has emerged as an energy bridge to nascent renewables. Liquefaction commercialises stranded reserves, while biologically produced methane offers renewability. Capping it all, GTL offers high quality gasoline. Others such as oil-fired power generation can be replaced by gas, nuclear, hydroelectric, or other renewables. Co-generation and biomass production processes that create methane or ethanol also offer effective renewable solutions. Last but not least, bio-diesels can be created from vegetable seed oil via trans-esterification to provide replacements for diesel usage[20].

The US EIA sees real resource limits to vegetable seed oil conversion to diesel, however, gasification of biomass and then conversion to diesel should have much more promise in terms of available volumes.

The early trend here, and that which accompanies other oil and gas applications, is that until a new broadly applicable fuel is found, oil and gas will remain the preferred source for global energy, against a backdrop of a myriad of developing energy sources. This diverse scenario – the energy inclusive model – exists in Brazil, India and Pakistan, albeit in a nascent form (see Figure 13 Electricity Generation in Brazil by Fuel and 14 overleaf Brazilian Fuel Options at the Pump). These countries are already using advanced gas technologies

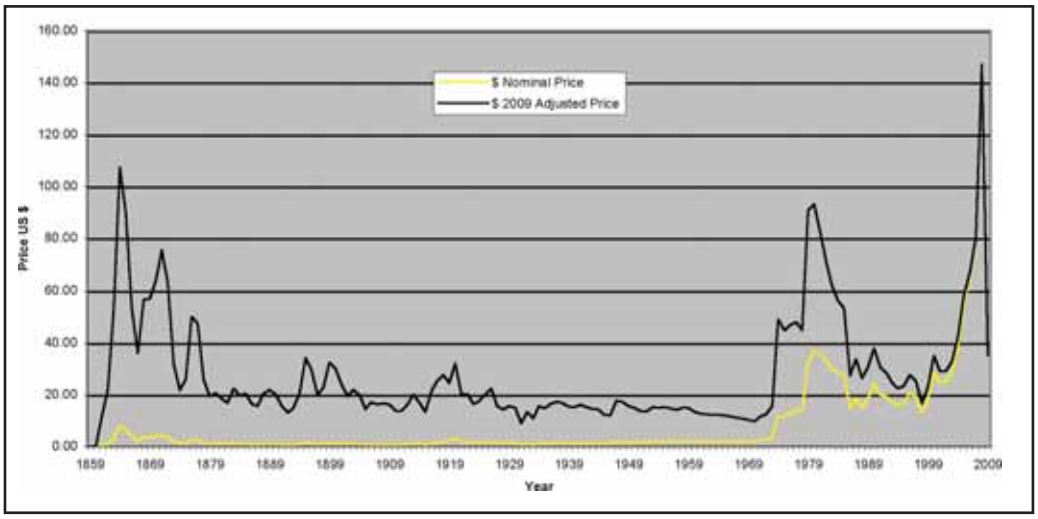

Figure 15 - Oil price 1861-2009. Source BP and EPRasheed (US, Arab Light and Brent Prices)

and ethanol. Most countries worldwide are at different points of energy development, with emphasis on hydro-electric, nuclear or other renewables varying from country to country[21].

2008 World Demand (Consumption)

1. Gas 2921.9 Bm^3. This figure is based on storage facilities, liquefaction, the disparities with production are due to definition, measurement or conversion, proposed additional sources, flaring and GTL[22].

2. Oil 85.22 MMbbl/d. The difference in consumption and production is due to inventories, additives such as ethanol, stock changes, substitutes, measurement/ conversion, proposed additional sources, illicit production and GTL[23].

2007 World Supply (Production)

1. Gas: 2940 Bm^3 which excludes GTL, Coal to Gas)[24].

2. Oil 81.53 MMbbl/d which includes NGL and GTL production[25].

For detail on the individual demand or supply components, refer to the Notes at the end of the book. The major categories are: transportation, heating, petrochemicals, lubricants, surfacing and power generation. Now let us look at the demand components and what choices we have for oil replacement.

Transportation (Aviation, Automotive, Marine and Rail)

Replacements in high-demand areas of aviation, automotive and marine usage are limited. Choices exist, but they are tempered by engine type, fuel tank size*, upgrading retail outlets and upgrading existing automotive and marine fleets. From the outset, the thermodynamic cycle and engine type – Otto or Diesel – dictates application suitability. Otto cycle engines use gasoline which can be replaced by ethanol. Diesel cycle engines use diesel which can be replaced by biodiesel. Both are ideal for spark-ignition and compression-ignition engines.

Ethanol, the much vaunted 'flex-fuel', offers only a partial exit scenario by substituting gasoline in the Otto cycle applications only. It is also fair to note that Brazil's adoption of ethanol (and LPG) technologies took at least 30 years to achieve, with car manufacturers and oil companies creating the required infrastructure. Government legislation required 25% of all gasoline to be mixed with ethanol. Today, that percentage has

> The US EIA sees real resource limits to vegetable seed oil conversion to diesel, however, gasification of biomass and then conversion to diesel should have much more promise in terms of available volumes.

fallen to 20% as demand (and exports) of ethanol rises. Ethanol does have its own supply volatility and liquidity limitations[26].

Successful usage in one country, however, does not mean that global roll-out can occur. As Brazil is one of the most advanced in energy diversification, what lessons can be drawn from its experience? First, government support was not enough; intervention was required. It was Brazil's dictatorship in the 1970s that issued the directives that led to today's usage. More than 30 years of government intervention, manufacturing incentives, infrastructure and retail outlets were needed to reach the current 'flex-fuel' conditions of 5% of all fuel consumed and 100% of all nationally manufactured cars. The main obstacle to worldwide roll-out is that the existing fleet of cars, buses, and boats around the world are configured for petroleum and diesel. This requires a phasing out or phasing in approach. Meanwhile, incentives or directives for new build vehicles should ensure that they are configured for flex-fuel renewables[27].

The Brazilian government has now applied the 5% minimum usage target to bio-diesel. This requirement has a number of transport fuel implications. First, it is likely to create more demand for petroleum replacements or 'unconventional fuels' as long as prices stay high. Second, more unconventional liquid fuels (GTLs, ethanol and biodiesel produced from alcohol or seeds) and natural gas (compressed or liquid) are likely to come onto the market and take up a larger share of overall demand for transportation petroleum liquids to 2030. Over the short run, this can be considered as a safety valve that eases off demand for traditional oil fuels (gasoline and diesel) in the transport demand component. In the long run, it can be considered as a partial exit scenario[28]. The major part of demand, however, resides within transportation and is highest in OECD countries such as the US, Canada and Western Europe. It is these countries that can help reduce demand by using more efficient vehicles as well as sharing transportation. A good idea would be to provide tax incentives for fuel efficient vehicles as well as car pooling.

Heating

Similar obstacles face the stock of domestic dwellings in that they cannot easily be configured to use oil or replacement gas. Greater acceptance of renewable energy sources (nuclear, solar, wind) can be expected in new-build residential usage. Natural gas (compressed or liquid) is also likely to take up a greater portion of total residential demand for petroleum. Over time, this can

Figure 16 - Future Options at the Pump; The Energy Express (EPRasheed)

be considered another safety valve that eases off demand for traditional residential oil fuels (gas and diesel) in residential demand. Localised burning of any carbon-based fuel for residential heating creates considerable difficulties. Firstly, establishing an efficient distribution infrastructure to transport the fuel to the homes can be expensive, time-consuming and problematic. Secondly, the control and capture of CO_2 (or other GHGs) is virtually impossible at the house-to-house level. Better to provide 100% electrification of communities, whereby carbon-based fuels are converted to electric energy at a few, centrally-located and controlled power stations where emissions can be controlled and GHGs sequestered. Electric power grids are relatively easy to establish, expand and maintain. Electric energy is a much more versatile form of energy, capable of providing many more services from heating to cooling, to illumination, to cooking and to powering appliances of all sizes. It is truly the world's cleanest and most easily-assimilated energy resource. Localised or dispersed burning sites would therefore be dramatically reduced, thus reducing the carbon footprint. More unconventional liquid fuels (GTLs, ethanol and biodiesel produced from alcohol or seeds respectively) and natural gas (compressed or liquid) are likely to come onto the market and take up a larger share of overall demand for commercial heating petroleum liquids to 2030. Over time, this can be considered a partial exit for traditional heating oil fuels (kerosene, diesel, heavy oil) in the commercial demand component[29].

Power Generation

What is important here is that each country's energy needs and resource profiles differ, and this affects how advanced (or not) their renewables uptake is and what size contribution it makes. It is clear to see that renewables offer a broad band of applications, concentrated in low-scale power generation, large scale gas turbine power generation or biomass co-generation applications. Choices exist, but they are tempered by the power generation facility type. Gas turbine or combustion turbines use natural gas, light fuel oil, diesel or biologically produced gas.

Still, many limitations exist; for example, power generating conditions for renewables do not always coincide with peak demands. Specific levels of sunshine or wind speed must exist at a given time to generate energy which must then be stored, creating a further challenge that must be resolved.

In the reference case, however, natural gas and renewable

> More unconventional liquid fuels (GTLs, ethanol and biodiesel produced from alcohol or seeds respectively) and natural gas (compressed or liquid) are likely to come onto the market and take up a larger share of overall demand for commercial heating petroleum liquids to 2030.

energy sources are predicted to increase in power generation markets. The natural gas share of world electricity markets increases from 19% in 2003 to 22% in 2030, and the renewable share rises from 18% in 2003 to 20% in 2010 before declining slightly to 19% in 2030. The relative environmental benefits and efficiency of natural gas make the fuel an attractive alternative to oil and coal-fired generation. Higher oil and gas prices enable renewable energy sources to compete more effectively in the electric power sector[30].

Petrochemical

High petrochemical feedstock demand is likely to create more demand for reformulated or 'synthetically' produced feedstocks. More synthetically produced alkenes and arenes will be created from gas, GTL and ethanol. As these products come onto the market, they will contribute to meeting higher levels of demand from the petrochemical sector. Over time, this will tend to a partial exit scenario with petrochemical-based hydrocarbon demand taking up to a 60% share of industrial demand up to 2030.

Lubricants and Surfacing

More synthetic lubricants (reformulated or vegetable seed based) and surfacing products (cement type) are likely to come onto the market and take up a larger share of overall demand for lubricants and surfacing. Over time, this can be considered an exit for traditional lubricants and surfacing (heavy oils, asphaltene) in the commercial demand component.

Price and Alternate Scenario

At any given point, the oil price is the closest, albeit imperfect indicator, due to delay of how the demand/supply equation is balanced. High oil and gas prices tend to indicate high demand and tight supply and vice versa. There is a complex inter-play, but clearly high oil and gas prices have three major implications. First, energy attracts investment. This is because high oil prices awaken demand for all types of energy sources, not just oil. This is double edged as not only does oil attract investment so do renewables. Exemplifying this is coal and ethanol which reached record prices during 2008. In the case of agriculturally produced ethanol,

the price of other agricultural crops can also increase as arable land is used for ethanol production. Given that the uptake of renewables is very sensitive to oil and gas prices, a 1.5% increase per annum in renewables uptake can help stabilise energy demand with oil production staying constant. Second, large reserve holders do increase E & P but not relative to the oil price. As the absolute value of oil increases, these countries reduce domestic consumption, encourage substitutes and focus on maximising recovery from existing assets rather than producing from new finds. Third, high oil prices depress demand. Over time, all of this happens almost imperceptibly; pent up consumption for oil dissipates and demand for goods and services falls due to higher costs. It was incorrect thinking that suggested that high oil prices could be borne by economies without greatly affecting growth. This has been proven time and again to be the downfall of high oil prices and the precursor to a bust cycle[31].

It is difficult to predict oil prices because oil price cycles tend to perform in a complex almost chaotic manner. Oil, however, is a commodity and obeys market rules or fundamentals despite the distortions. Research focused on commodities and, although not specifically designed for oil, shows how commodity cycles are affected by inventory, immediate production capacity and long-term production capacity. The combination of different timescales, time delays, different operators and human fallibility only adds to the complexity of the system. Although cycles (peaks and troughs) are not entirely random, we know that they will occur. The length of each cycle (say from peak to peak) is not entirely predictable as some last three years while others can last as long as ten years. There are, however, some telltale signs: economic conditions worldwide; extreme swings from a low to a high price or vice versa within a six month period; and, major geo-political tension. Prolonged periods of tightness in acquiring supply or services (or vice versa) also provide a good indication of where we are in the cycle.

The much touted increase in demand from China and India occurred in 2008 and is now slowing down. The growth in demand for energy is a much more gradual and long-term event linked to positive economic growth and consumption in developed countries. Combined demand from China and India exceeds North America by 2030, but not on a per capita energy usage basis. The bulk of Chinese and Indian industry and services are produced for end consumption by foreign customers mostly in Western countries and North America. Consumption has been transferred to China and India to reflect the industrial activity and production there. Endogenous demand for petroleum would be much lower without the energy consumption from traditionally high energy per capita users. The bulk of energy consumption, therefore, arises from the traditional users, i.e. in the US and Western Europe.

How long will the present recession last? Not even the world's best economists can say. Without getting too much into economic theory, we can say that there will be a market correction: a collapse or a period of depressed demand and lower oil and gas prices. We know that is certain because oil and gas are cyclical commodities that periodically experience peaks and troughs[32]. The problem is nobody knows when these will occur because the cycles are not entirely predictable; however, current market situations clearly seem to herald a low price cycle.

From a market perspective (putting government intervention aside), the troughs mean diminished demand for oil and gas and its applications, less cash for exploration and even less cash for renewable resources. Put simply, the return forecasts are lowered and the principal flow of capital from investors and speculators is diverted into markets other than energy and oil.

Nobody wants to talk about a collapse in prices. It frightens investors. Nobody wants to talk about a collapse when growth is strong, but ignoring a low price scenario is asking for trouble. This perhaps explains why oil companies want to stay cash rich. They have lived through the low price scenario—low revenues, poor utilisation and even lower returns. This is what some say keeps the cycle of under investment alive—fear of price collapse[33] (see Figure 15).

Our Legacy?

Our task is to lobby for investment, both in oil and gas and R & D in renewables and to understand there is no easy way out. We will all have to work to find an exit. What about an energy revolution? It may happen, but my money is on the evolution: experimenting and tinkering with all energy sources. And what of global warming and energy? Simply put, we must reduce carbon emissions. There are new kids on the block (e.g. ethanol and wind farms) and there are some old-timers back as well (e.g. nuclear and coal). I believe that in the future, energy will become a new engineering discipline, along with mining, civil, mechanical, petroleum and nuclear and one that encompasses wind, solar and all other forms of energy.

Think legacy. Think future generations. Do we want to

> Renewables increase over time but do not displace petroleum entirely creating an inclusive energy model. Petroleum remains a permanent feature, its demand increasing from time to time as ethanol crops fall short or rainfalls fall below hydro-electric dam requirements.

leave a mess of energy waste and environmental damage as a legacy for future generations? What does that say about us? Together, we need to apply our minds to exit the Hydrocarbon Highway without leaving a mess behind us. So how will things look in the future?

The narrowing base of opportunities for IOCs due to a changing E & P landscape means their activities will tend toward gas (GTL, LNG) and renewables. Here IOCs take a leadership position by differentiating themselves and adopting the 'Inclusive Energy Model' with project management, the know-how and capital. Gas becomes the fuel of choice from renewable streams, i.e. biomass as well as fossil fuel streams. Other applications are replaced, effectively relieving the major part of demand pressure on petroleum. Due to unreplaced applications, seasonal events and die-hards, the Hydrocarbon Highway runs on. Renewables increase over time but do not displace petroleum entirely creating an inclusive energy model. Petroleum remains a permanent feature, its demand increasing from time to time as ethanol crops fall short or rainfalls fall below hydro-electric dam requirements (and just as people still warm to a log-fire, people will always enjoy the thrill of gasoline powered revs).

Nuclear energy becomes a leading renewable energy source. Electricity prices rise, noticeably driven by the global rise in gas prices. As more nuclear energy plants come onstream, nuclear energy becomes more competitive and gas prices fall. Hydrocarbon demand is reduced by other factors too. Increasing GHGs and global warming becomes a reality. Companies are sued for producing emissions. The cases are defended, but companies become the champions of levying carbon taxes on the generation of GHGs. This is similar to the relationship between obesity and fast food chains. The fast food chains avoided direct responsibility in lawsuits and learned the lesson to offer 'healthy' alternatives. Aviation prices rise; the industry is thrown into disarray. Cheap airlines are forced to consolidate and stress on petroleum aviation demand is lowered further. Oil prices continue to fluctuate, yet a balance of residual demand keeps oil companies in business. A flourishing trade in carbon miles exist at the state, corporate and individual level. Worldwide, those who do not use their allowances sell the difference to high users. Electrically charged cars run globally.

Gasoline stations are still affectionately known as petrol

or gas stations as a throwback to when petroleum spirit was the dominant fuel, but they now offer biofuels, electricity, hydrogen and gasoline. The Hydrocarbon Highway has become the Energy Express. We have more choices than ever – the highway is still endless, but now there are many branching intersections one can take.

References

1. These are:
a) Power Generation [PGOil +PGGasTurbine (Non Ethanol/Brighton cycle) +PGGasSteam (Combustion)] (Gasoil/Fueloil) Gas & Oil (Methane, Heavy Oil)

b) Heating [H Industrial Process + H Construction +H Domestic Premises +H Commercial Premises] (Gas, Kerosene, Gasoil)

c) Transport [T Light Automotive Cars + T Aviation + T Marine Light T Marine T Military T Industrial + T Heavy Automotive Truck/Construction/Mining T Heavy Automotive Bus +T Train] (Gasoline, Diesel, Heavy Oil)

d) Petrochemicals [D Alkane Feedstocks (Naphthas) + D Arene Feedstocks (Pharmaceuticals) + D Alkene Feedstocks Plastics + D Foods + Resins & Waxes]

e) Lubricants [L GearOil + L IndustrialGrease], and

f) Surfacing [S Road+S Roof] Roofs, Cement.

2. Especially considering man-made Gas.

3. That make up the Oil and Gas Demand Equation: [PGGT+PGGS+PGO]+[HIP++HCon+HDP+HCP] +[TLAC+ TA + T M+ THAT+THAB+TT]+ [PCArF (Pharmaceuticals) + PC AlF PC AlkeneF + PC RW] + [LGO + LIG] + [SRd+SRf] 2007 World Demand (Consumption) Gas 2921.9 BCM and Oil 85.22 million bopd 2007 World Supply (Production) Gas: 2940 BCM and Oil 81.53 million.

Supply = [PGMethaneGT +PG MethaneGS+LPG,LNGGS + PG Oil] + [HGasOilIP+HGasDP Diesel, CNG,LPG] +[TLAC Gasoline+ Diesel + TA Compressed Natural Gas, Liquid Petroleum Gas + TM Diesel+ THAT Diesel+THAB Diesel+TT Heavy Oil] + [PCArF Naphtha (Pharmaceuticals) + PC AlF Naphtha PC AlkeneFNaphtha + PC RW Heavy Oil] +[LGOHeavy Oil + LIGHeavy Oil] + [SRdAsphalt+SRfBitumen].

4. This is our goal.

5. See EIA IEO 2008 Outlook.

6. See EIA IEO 2008 Outlook.

7. Idem.

8. Idem.

9. Certainly the EIA IEO 2008 Outlook thinks so.

10. EIA.

11. EIA.

12. EIA.

13. Idem.

14. Idem.

15. EIA.

16. EIA Footnote.

17. Increasing Feedstock Production for Biofuels: Economic Drivers, Environmental Implications, and the Role of Research. See also Options for Alternative Fuels and Advanced Vehicles in Greensburg, Kansas Harrow, G.

18. Further is the intrinsic volatility of the oil markets which complicates investment in renewables.

19. Exchange with EIA.

20. Exchange with EIA.

21. Brazil is a case in point hence why it was chosen.

22. BP Statistical Review 2008.

23. Idem.

24. Idem.

25. Gasoline and Ethanol Prices Fall" (in Portuguese). Folha Online 18 09 2008.

26. US DOE Flexible Fuel Vehicles: Providing a Renewable Fuel Choice. Again no single source of energy is universally applicable.

27. See also The Methanol Story: A Sustainable Fuel for the Future Roberta J Nichols.

28. US DOE Flexible Fuel Vehicles: Providing a Renewable Fuel Choice.

29. In many ways this is more elastic than transportation demand.

30. It is the backdrop of high oil prices that makes renewables viable.

31. The trends for continued economic and population growth will create further demand on oil and gas in the medium and long term.

32. The problem is that not even the world's foremost thinkers can satisfactorily predict the cycles.

33. Due to the vicious cycle involved it is likely that change will be slow and steady.

Saudi Arabia oil & gas

www.saudiarabiaoilandgas.com

Contribute to Saudi Arabia Oil & Gas during 2014

EPRasheed is looking for editorial submissions on the topics outlined in the editorial calendar. This can provide your company with the opportunity to communicate EP technology to the wider oil and gas community.

Please send abstracts or ideas for editorial to **wajid.rasheed@eprasheed.com**

Preference is given to articles that are Oil Company co-authored, peer reviewed or those based on Academic research.

Editorial 2014 Calendar

Jan/Feb	Mar/Apr	May/Jun	Jul/Aug	Sep/Oct	Nov/Dec
Ad Closing: 1 Jan 2014 **Materials Closing:** 8 Jan 204	**Ad Closing:** 15 Feb 2014 **Materials Closing:** 8 Feb 2014	**Ad Closing:** 15 April 2014 **Materials Closing:** 8 April 2014	**Ad Closing:** 3 July 2014 **Materials Closing:** 10 July 2014	**Ad Closing:** 29 August 2014 **Materials Closing:** 30 August 2014	**Ad Closing:** 5 October 2014 **Materials Closing:** 12 October 2014
• New Stimulation Technology • Advances in Drilling Technology • Smart Reservoirs • Deep Diagnostics & Reservoir Mapping • Geosciences • E&P Software Solutions for Asset, Field and Well Management	• Intelligent Fields • Oil Field Automation and Optimization • Extreme Reservoir Contact • Wide Azimuth • Near Surface Resolution • Technology Innovation to Secure Future of Energy Supply Middle East	• Successful Innovation from Paper to Prototype • Accelerating and De-risking New Technologies • Real Time Operations • I Field • Drilling Automation • KSA Upstream Research & Development • KFUPM Techno Valley	• Deep Water Red Sea Challenges • Assessment of KSA & IOCs Gas Exploration Initiatives • Shale Gas • Tight Gas Developments • Tight Gas Technology Development	• KSA Offshore Gas Development Projects (Karan, Wasit, Arabia, etc....) • Smart Water Chemistry in Carbonate Recovery • Development of Unconventional Gas	• Maximizing Sweep Efficiency in Heterogeneous Carbonate Reservoir Using Advanced Intelligent Completion Technology • Red Sea Salt Challenges
Issue 36 *'Deep Diagnostics'*	**Issue 37** *'Transforming the Energy Future'*	**Issue 38** *'The Upstream Innovation Spark, Lighting Our Way To A Better Tomorrow'*	**Issue 39** *'Red Sea Challenges'*	**Issue 40** *'Offshore Gas'*	**Issue 41** *'Maximising Sweep Efficiency'*
BONUS CIRCULATION					
International Petroleum Technology Conference 19-22 January 2014 Doha Qatar	**SPE/IADC Drilling Conference & Exhibition** 4-6 March 2014 Texas USA **11th Middle East Geosciences Conference & Exhibition** 9-12 March 2014 Bahrain **SPE-SAS Annual Technial Symposium & Exhibition** 21-24 April 2014 Al-Khobar Saudi Arabia	**Offshore Technology Conference** 5-8 May 2014 Houston Texas USA **76th EAGE Conference & Exhibition** 16-19 June 2014 Amsterdam Netherlands **Middle East Petrotech** 18-21 May 2014 Bahrain		**SPE Annual Technical Conference and Exhibition** 27-29 October 2014 Amsterdam Netherlands	
SPECIAL PUBLICATIONS					
	** Official Saudi Magazine	* Official Technical Magazine			* Media Partner